

NORTHWESTERN UNIVERSITY

**The Role of Contralateral and Ipsilateral Descending Motor Pathways in the Expression of  
Abnormal Coordination Patterns in Hemiparetic Stroke Subjects**

A DISSERTATION

SUBMITTED TO THE GRADUATE SCHOOL

IN PARTIAL FULFILLMENT OF THE REQUIREMENTS

for the degree

DOCTOR OF PHILOSOPHY

Neuroscience Institute Graduate Program

By

Susan Caroline Schwerin

EVANSTON, ILLINOIS

December 2006

© Copyright by Susan C. Schwerin 2006

All Rights Reserved

## ABSTRACT

### The Role of Contralateral and Ipsilateral Descending Motor Pathways in the Expression of Abnormal Coordination Patterns in Hemiparetic Stroke Subjects

Susan C. Schwerin

The objective of this study was to determine the relationship between descending motor pathway reorganization and abnormal coordination, defined as a reduced set of muscle coactivation patterns between shoulder and elbow muscles in hemiparetic chronic stroke subjects, using transcranial magnetic stimulation (TMS). Specifically, we wanted to 1) determine the relationship between the ipsilateral and contralateral projections to the paretic arm and strength, clinical impairment level, and degree of abnormal coordination; 2) determine an optimal paired pulse TMS interstimulus interval (ISI) to cause facilitation in both healthy and paretic distal and proximal upper limb muscles at rest; 3) quantify the relative strength of the contralateral and ipsilateral projections to distal and proximal upper limb muscles in the paretic arm using paired pulse TMS; 4) estimate the possible contribution of corticobulbospinal systems in the expression of abnormal coordination in the paretic limb using asymmetric tonic neck reflexes (ATNRs) and TMS.

Our results indicate that the relative magnitude of the ipsilateral and contralateral responses in a paretic proximal limb muscle was correlated with the Fugl-Meyer score as well as with the degree abnormal coordination, but not with strength. In addition, we identified the ISIs of 25-40 ms as the optimal ISI. Using 30 ms ISI, we found that all the paretic muscles studied had a greater ipsilateral than contralateral input than in the control subjects, and that muscles involved in the pathological flexor synergy had significantly greater ipsilateral input than the muscles in the pathological extensor synergy. In addition, the onset of flexor synergy was delayed compared to extensor synergy muscles, suggesting a more indirect route to the flexor muscles. Interestingly, we only observed ATNR modulation of the ipsilateral and contralateral responses in the biceps and triceps.

The results presented in this dissertation demonstrate the preferential input of the ipsilateral projections to the pathological flexor synergy muscles of the upper limb of stroke subjects. The delayed onset, and similarity of responses to those observed with reticular formation stimulation in the monkey suggest that a corticobulbospinal pathway may be upregulated following stroke and may be involved in the expression of abnormal coordination.

## DEDICATION

This thesis is dedicated to the stroke and control volunteers who participated in the studies herein. Each of you nobly gave of your time, volunteered the use of your body, and offered your friendship. These experiments were not always easy and they were always long. I professionally and personally thank you for your generosity.

The items below will make me think of each of you:

- Wrigley gum
- Turkey calls
- Sick kittens
- Dry/wet sponges
- Cold Coronas
- Recycled vitamin rich urine
- Italy
- Homemade wine and Swedish pastries
- Documentaries
- Women's hips
- Belgian beer
- Drums
- Klondike bars

## ACKNOWLEDGEMENTS

I would like to thank my advisor and friend, Dr. Jules Dewald, for his unlimited enthusiasm for science and especially for his approach to advising a graduate student. I always felt as if I was a partner in scientific discovery and not a student, and for that I am grateful. I would also like to thank my committee members: Dr. W. Zev Rymer, Dr. James Baker, Dr. Sandro Mussa-Ivaldi, and Dr. Colum MacKinnon. Their assistance and suggestions along the way were invaluable.

I would like to express my love and gratitude to my parents, George and Penny, for their continuous support and encouragement in everything I do. I also extend my appreciation to my family - Jeannette, Mike, Patti, Jason, George and Carolyn - who were always there if I needed them. And, a special thanks goes to Richelle, Michaela, Brandon, Amber, Robbie, Emmitt and Garrett who were always able to lift my spirits and make me laugh.

Thanks to my friends and colleagues - Drs., Ana Maria Acosta, Jun Yao, and Yasin Dhaher - without whom this project would not have been completed. Thanks also to Dr. Leah Solberg, Dr. David Lorber, Erin Thomas, Carren Loreda, and Dr. Annette Weiss-McNulty for their friendship and advice. Finally, I would like to express my love and gratitude to Michael Barrett for his unlimited and creative ways to add color to my days and for his willingness to do anything I needed in finishing this thesis.

## LIST OF ABBREVIATIONS

ADL	anterior deltoid	LAT	latissimus dorsi
ATNR	asymmetric tonic neck reflex	LI	laterality index
AW	away	MEG	magneto encephalography
BIC	biceps	MEP	motor evoked potential
BRD	brachioradialis	MRI	magnetic resonance imaging
cMEP	contralateral motor evoked potential	PET	positron emission tomography
CMSA	Chedoke McMaster Stroke Assessment	PDL	posterior deltoid
DF	distal limb flexors	PLIC	posterior limb of internal capsule
DE	distal limb extensors	PMJ	pectoralis major
ECR	extensor carpi radialis	ST	straight forward
EEG	electroencephalography	TMS	transcranial magnetic stimulation
EMG	electromyography	TO	toward
FCR	flexor carpi radialis	TPS	superior trapezius
FDI	first dorsal interosseus	TRI	triceps
FMA	Fugl-Meyer Assessment	TRILA	triceps lateral head
fMRI	functional magnetic resonance imaging	TRILO	triceps long head
IDL	intermediate deltoid		
iMEP	ipsilateral motor evoked potential		
ISI	interstimulus interval		

## TABLE OF CONTENTS

ABSTRACT.....	3
DEDICATION.....	4
ACKNOWLEDGEMENTS.....	5
LIST OF ABBREVIATIONS.....	6
LIST OF FIGURES.....	11
LIST OF TABLES.....	13
INTRODUCTION.....	14
1.1    Specific Aims and Hypothesis.....	16
2    BACKGROUND.....	20
2.1    Motor Performance Following Stroke.....	20
2.2    Motor System Anatomy.....	23
2.2.1 <i>Primary Motor Cortex: Cortical Layers</i> .....	23
2.2.2 <i>Major Motor Cortices</i> .....	23
2.2.3 <i>Gross Somatotopy</i> .....	25
2.2.4 <i>Fine Somatotopy in the Primary Motor Cortex</i> .....	26
2.3    Descending Motor Tracts.....	27
2.3.1 <i>Corticospinal Motor Pathway</i> .....	27
2.3.2 <i>Bulbospinal Motor Pathways</i> .....	28
2.3.2.1    Rubrospinal.....	28
2.3.2.2    Vestibulospinal.....	29
2.3.2.3    Reticulospinal.....	30
2.3.3 <i>Propriospinal System</i> .....	31
2.4    Possible Recovery Methods.....	33
2.4.1 <i>Reorganization Within the Motor Cortex</i> .....	33
2.4.2 <i>Non-Primary Motor Region Takeover</i> .....	34
2.4.3 <i>Descending Pathway Reorganization</i> .....	35
2.4.4 <i>Ipsilateral Motor Region Takeover</i> .....	36
2.4.5 <i>Spinal Interneuron Excitability Alteration</i> .....	37
2.5    Transcranial Magnetic Stimulation.....	38
2.5.1 <i>Activation of the Motor Cortex by TMS</i> .....	38
2.5.2 <i>TMS in Studying Motor Recovery Following Stroke</i> .....	40
3    SIGNIFICANCE.....	42
4    IPSI- VERSUS CONTRA-LATERAL CORTICAL MOTOR PROJECTIONS TO A SHOULDER ADDUCTOR IN CHRONIC HEMIPARETIC STROKE: IMPLICATIONS FOR THE EXPRESSION OF ARM SYNERGIES.....	44
4.1    Introduction.....	44
4.2    Materials and Methods.....	46
4.2.1 <i>Subject Selection</i> .....	46
4.2.2 <i>Experimental Set-Up</i> .....	47
4.2.3 <i>Transcranial Magnetic Stimulation</i> .....	48

4.3	Analysis.....	49
4.3.1	<i>MEP prevalence</i> .....	50
4.3.2	<i>Relative Size of Responses in Paretic Limb</i> .....	50
4.3.3	<i>Hemispheric Laterality</i> .....	50
4.3.4	<i>Strength</i> .....	51
4.3.5	<i>Secondary Elbow Torque</i> .....	51
4.3.6	<i>Spatial Analysis</i> .....	51
4.3.7	<i>Latency Analysis</i> .....	52
4.4	Results.....	52
4.4.1	<i>Raw Data</i> .....	52
4.4.2	<i>Prevalence of cMEPs and iMEPs</i> .....	53
4.4.3	<i>Relative Size of MEPs in the Paretic Limb</i> .....	54
4.4.4	<i>Laterality</i> .....	55
4.4.5	<i>Correlation of Laterality Index with Impairment</i> .....	56
4.4.6	<i>Correlation of Paretic cMEP and iMEP Magnitude with Clinical Score</i> .....	57
4.4.7	<i>Relative Spatial Location of Optimal cMEPs and iMEPs</i> .....	57
4.4.8	<i>Onset Latency</i> .....	57
4.5	Discussion.....	58
4.5.1	<i>Ipsilateral MEP Prevalence</i> .....	58
4.5.2	<i>Evidence for an Increased Reliance on Indirect Descending Motor Pathways Following Stroke</i> .....	59
4.5.3	<i>Clinical Correlates</i> .....	60
4.6	Conclusion.....	61
5	FACILITATION OF CONTRA- AND IPSI-LATERAL MEPS IN UPPER EXTREMITY MUSCLES IN CHRONIC HEMIPARETIC STROKE USING PAIRED PULSE TMS ...	63
5.1	Introduction.....	63
5.2	Materials and Methods.....	66
5.2.1	<i>Subject Selection</i> .....	66
5.2.2	<i>Experimental Set-Up</i> .....	67
5.2.3	<i>Electromyography</i> .....	67
5.2.4	<i>Transcranial Magnetic Stimulation</i> .....	68
5.2.5	<i>Optimal Stimulation Site Exploration</i> .....	68
5.2.6	<i>ISI Investigation</i> .....	69
5.2.7	<i>Experimental Sessions</i> .....	69
5.3	Analysis.....	70
5.3.1	<i>Motor Evoked Potential Occurrence</i> .....	70
5.3.2	<i>MEP Magnitude</i> .....	71
5.3.3	<i>Muscle Groups</i> .....	72
5.3.4	<i>MEP Latency</i> .....	72
5.4	Results.....	72
5.4.1	<i>Optimal Stimulation Site</i> .....	72
5.4.2	<i>Raw Data</i> .....	74



5.4.3	<i>Occurrence</i> .....	75
5.4.4	<i>Magnitude</i> .....	77
5.4.5	<i>Muscle Groups</i> .....	79
5.4.6	<i>Onset Latency</i> .....	80
5.5	Discussion.....	81
5.5.1	<i>Possible Mechanisms of Facilitation at Medium Interval ISIs</i> .....	82
5.5.2	<i>Muscle Group ISI Curves</i> .....	83
5.5.3	<i>Possible Mechanisms for Delayed Onsets of iMEPs Following Stroke</i> .....	85
5.6	Scientific Implications.....	86
6	IPSILATERAL AND CONTRALATERAL CORTICOBULBOSPINAL PROJECTIONS INVOLVED IN THE EXPRESSION OF ABNORMAL COORDINATION PATTERNS IN MODERATE TO SEVERE HEMIPARETIC STROKE SUBJECTS.....	87
6.1	Introduction.....	87
6.2	Materials and Methods.....	89
6.2.1	<i>Subject Selection</i> .....	89
6.2.2	<i>Experimental Set-Up</i> .....	90
6.2.3	<i>Electromyography</i> .....	91
6.2.4	<i>Transcranial Magnetic Stimulation</i> .....	93
6.2.5	<i>TMS Stimulation Grid Generation and MRI Co-Registration</i> .....	93
6.2.6	<i>Grid Testing</i> .....	96
6.2.7	<i>Laterality and ATNR Testing</i> .....	96
6.3	Analysis.....	97
6.3.1	<i>Laterality</i> .....	97
6.3.2	<i>Correlation with Recovery Level in Stroke Subjects</i> .....	98
6.3.3	<i>MEP Onset Latency and Duration</i> .....	98
6.3.4	<i>Asymmetric Tonic Neck Reflex</i> .....	98
6.4	Results.....	99
6.4.1	<i>Raw Data</i> .....	99
6.4.2	<i>Laterality</i> .....	100
6.4.3	<i>Correlation with Recovery Level in Stroke Subjects</i> .....	101
6.4.4	<i>Latency</i> .....	101
6.4.5	<i>Duration</i> .....	102
6.4.6	<i>Spatial Location</i> .....	102
6.4.7	<i>ATNR</i> .....	103
6.5	Discussion.....	106
6.5.1	<i>Bias Towards Pathological Flexor Synergy Muscles in Ipsilateral Takeover</i> ...	106
6.5.2	<i>Delayed Onset Latency in Flexor Synergy Muscles of the Ipsilateral Projection</i>	108
6.5.3	<i>Effects of Head Rotation</i> .....	108
6.5.4	<i>Cortical Origin of Ipsilateral Responses</i> .....	109
6.6	Clinical Implications.....	110
7	SUMMARY.....	111

8	FUTURE WORK.....	114
9	REFERENCES .....	116
10	APPENDIX.....	129
10.1	Stimulation Grid Generation.....	129
10.1.1	<i>MRI Utilization</i> .....	129
10.1.1.1	Segmentation.....	129
10.1.1.2	Landmarks.....	131
10.1.1.3	Anatomical Plane Identification .....	132
10.1.1.4	Triangulation of Head Surface.....	133
10.1.2	<i>Stimulation Grid Generation</i> .....	134
10.1.2.1	Headsurfgrid.m .....	135
10.1.2.2	The m-files used follow. ....	141
10.1.3	<i>Coregistration of Stimulation Grid with MRI</i> .....	171

## LIST OF FIGURES

Figure 2-1 Motor cortices and motor homunculus.....	25
Figure 2-2 Mechanism of TMS neural excitation.....	39
Figure 4-4 Correlation results.....	56
Figure 5-1 Stimulation sites.....	73
Figure 5-2 Raw data.....	74
Figure 5-3 Occurrence.....	76
Figure 5-4 Magnitude.....	78
Figure 5-5 Muscle groups.....	80
Figure 5-6 Latency.....	81
Figure 6-1 Experimental setup.....	91
Figure 6-2 Planes used to generate stimulation grid.....	95
Figure 6-4 Laterality index.....	101
Figure 6-5 Onset latency.....	102
Figure 6-7 ATNR raw data results.....	105
Figure 6-8 ATNR results.....	105
Figure 10-1 Cortex Segmentation.....	130
Figure 10-2 Skin Segmentation.....	131
Figure 10-3 Anatomical Landmarks.....	132
Figure 10-4 Anatomical Planes.....	133

Figure 10-5 Triangulation Mesh.....	134
Figure 10-6 Headsurfgrid Window.....	135
Figure 10-7 Headsurfgrid start results.....	136
Figure 10-8 Headsurfgrid midway results.....	137
Figure 10-9 Headsurfgrid final results.....	138
Figure 10-10 Stimulation Sites on Skin Segmentation of MRI.....	177
Figure 10-11 Stimulation Sites above Sensorimotor Cortices.....	178
Figure 10-12 TMS_dialog Coordinate Transformations Performed .....	179
Figure 10-13 Ired plate on the wand.....	180
Figure 10-14 Stimulation point on the wand.....	180
Figure 10-15 Facial rigid body.....	181
Figure 10-16 Nasion coordinate frame using landmarks digitized on the subject's head.....	182
Figure 10-17 Four midsagittal plane points for .pln file.....	183
Figure 10-18 Scalp points coregistered with MRI.....	184
Figure 10-19 Mannequin actual stimulation sites.....	192
Figure 10-20 Hotspots found at the scalp surface projected onto the cortical surface.....	193

**LIST OF TABLES**

Table 2-1 Flexor and Extensor Upper Limb Synergies (Based on Brunnstrom, 1970).....	21
Table 4-1 Clinical data for hemiparetic stroke participants.....	47
Table 4-2 Summary of results.....	54
Table 5-1 Clinical data for hemiparetic stroke participants.....	66
Table 6-1 Clinical data for hemiparetic stroke participants.....	90

## INTRODUCTION

The objective of this study was to determine the relationship between descending motor pathway reorganization and abnormal coordination following hemiparetic stroke. Abnormal coordination has proven to be one of the most debilitating aspects of movement impairment following stroke. Abnormal muscle coordination in the paretic arm is expressed in the form of stereotypic movement patterns characterized by a reduced set of coactivation patterns between shoulder and elbow muscles that severely limits the functional usage of the paretic upper limb. The physiological mechanisms involved in the expression of abnormal coordination are unknown. Following stroke, reorganization in the motor cortices occurs and recently it was determined that the ipsilateral cortex to the paretic limb becomes active. In longitudinal studies, activity in the ipsilateral cortex has been recorded soon after the stroke, but as recovery progresses, ipsilateral activity decreases while activity in the lesioned cortex returns. In cases where poor recovery occurs, the ipsilateral activity remains. Patients with moderate to severe impairment express abnormal muscle coordination during voluntary movement. To date, the link between these phenomena has not been studied. Corticobulbospinal pathways have been implicated as the ipsilateral pathway used following stroke, however, data in support of this theory is cursory. This theory is supported by anatomical evidence revealing extensive branching within the spine in these pathways which could provide the infrastructure for the abnormal coordination patterns.

This dissertation was designed to examine the relationship between the ipsilateral and contralateral motor projections and the expression of abnormal coordination. Specifically, this

work examined the relative strength of the contralateral and ipsilateral projections to muscles of the paretic limb as measured by the peak-to-peak amplitude of the motor evoked potential (MEP). Several hypotheses were studied. First, it was hypothesized that the degree of ipsilateral takeover would be correlated with the degree of abnormal coordination. Second, it was hypothesized that the muscles with greater ipsilateral takeover would be the muscles involved in the stereotypic muscle coordination patterns observed in abnormal coordination following stroke. Thirdly, we postulated that the ipsilateral and contralateral projections we were tapping into with transcranial magnetic stimulation (TMS) following stroke were corticobulbospinal pathways.

To achieve the objective of measuring the relative strength of the ipsilateral and contralateral projections in paretic muscles of stroke subjects, a secondary goal was to test the technique of paired pulse TMS as a method to facilitate the muscle responses such that responses could be observed and measured for study for all the muscles of the paretic limb from distal to proximal.

**Understanding the role of the contralateral and ipsilateral projections to the paretic arm in the expression of abnormal coordination and determining whether a corticobulbospinal pathway is being employed will substantially enhance our understanding of mechanisms driving abnormal coordination following hemiparetic stroke and will provide new foundations for developing and investigating targeted interventions.**

## ***1.1 Specific Aims and Hypothesis***

The general aim of this thesis is to elucidate the roles of the ipsilateral and contralateral projections in the expression of abnormal synergies. Furthermore, the corticobulbospinal pathways were investigated as the possible substrate of the ipsilateral and contralateral projections by measuring the onset latency of the TMS responses and by investigating the effect of neck rotation on the magnitude of the responses.

The specific aims of the study are:

**1) To investigate the roles of the ipsilateral and contralateral descending motor projections to a paretic proximal arm muscle in recovery in mild to severe chronic hemiparetic stroke patients. Specifically we aimed to identify the relationship between the magnitude of the TMS muscle response and muscle strength, abnormal coordination and clinical motor scores.** Contralateral and ipsilateral responses in both the paretic and non-paretic pectoralis major muscles were recorded. Single pulse TMS was used with background adduction torque production. A laterality index was calculated using the peak-to-peak magnitude of the ipsilateral and contralateral responses. We tested the correlation between the laterality index and the Fugl-Meyer motor assessment score, the maximum adduction torque generated, and the magnitude of the elbow torque generated during maximum adduction torque. In addition, we calculated the onset latency as an indicator of the possible upregulation of corticobulbospinal pathways following stroke which would have longer latencies than the fast corticospinal tract. **We postulate that ipsilateral takeover will be correlated with abnormal coordination and**



**clinical score and that there will be a delay in onset supporting the usage of an oligosynaptic descending pathway.** This is the aim of Chapter 4 in this thesis.

**2) To identify an interstimulus interval (ISI) that is optimal for facilitating both distal and proximal muscles of the upper limb in both moderate to severely impaired chronic hemiparetic stroke subjects and healthy control subjects.** In an effort to enable future TMS research on a number of upper limb muscles simultaneously and to avoid biasing TMS results with voluntary background activation, we investigated the technique of paired pulse TMS for facilitation of both distal and proximal limb muscles in control subjects and in the paretic limb of stroke subjects. Proximal limb muscles as well as muscles in the paretic limb have high thresholds and are often very difficult to activate with TMS at rest, and, in some cases, also during background activation. As this phenomena strictly limits research of these muscles, we decided to investigate the effectiveness of the paired pulse technique to both increase the occurrence of the TMS evoked muscle response as well as the magnitude of the response. While studies have shown that the 10-30 ms ISIs facilitate the distal muscle response in control subjects, the proximal muscle and stroke muscle optimal ISIs are unknown. Eighteen ISIs were investigated for paired pulse TMS facilitation. We examined the peak-to-peak magnitude of the evoked responses in hand/wrist, elbow, shoulder and trunk muscles. **We postulate that a mid-range interpulse interval would be optimal for facilitating muscle responses in the paretic limb as well as in both the distal and proximal muscles of the control subjects.** This is the aim of Chapter 5 in this thesis.

**3) To quantify the relative contribution of the ipsilateral and contralateral cortical projections to flexor and extensor synergy muscles of the paretic upper extremity of moderate to severely impaired chronic hemiparetic stroke subjects.** Using the optimal ISI found in Aim 2, the contralateral and ipsilateral hemispheres to the paretic limb were stimulated using TMS. A hotspot on the scalp surface was found for each of eight arm muscles while at rest using a magnetic resonance imaging (MRI) generated subject-specific stimulation grid. A laterality index (LI) was calculated for each muscle and averaged across subjects. The degree of laterality was compared between muscles involved in the flexor synergy and those involved in the extensor synergy. The latency of the responses were measured and compared between muscle groups and projection type to investigate the descending pathway being used. **We postulate that the laterality index will shift to a dominant ipsilateral projection following stroke particularly in the muscles involved in the flexion synergy. Furthermore, we hypothesize that the onset will be delayed, providing evidence that a corticobulbospinal pathway is being used following stroke.** This is one of the aims of Chapter 6 in this thesis.

**4) To estimate the possible contribution of bulbospinal systems in the production of contralateral and ipsilateral MEPs in the paretic upper extremity using asymmetric tonic neck reflexes (ATNR) and TMS in moderate to severely impaired chronic hemiparetic stroke subjects.** In an effort to identify both the contralateral and ipsilateral pathways being employed following stroke, we tested the effects of ATNR on the muscle response to TMS of the

lesioned and non-lesioned hemispheres. Neck muscle afferents project to the reticular nuclei and can modulate the signals traveling in the cortico-reticulospinal tract. We applied TMS at the hotspots found in Aim 3 while the subject's chair was turned to the right or left 75 degrees such that the head remained stationary. We quantified the effect of head rotation on the magnitude of the TMS contralateral and ipsilateral motor evoked potential in eight muscles of the upper limb. **We postulate that the responses will be greater while the head is facing *towards* the paretic arm for muscles involved in the extensor synergy and responses will decrease in muscles involved in the flexor synergy, in accord with the expected effects of ATNR. Conversely, we believe the magnitude of the motor evoked potential in the extensor synergy muscles will decrease when the head is facing away from the paretic arm while the responses in the flexor synergy muscles will be facilitated. Conversely, we predict that no such effects will be observed in the non-paretic limb nor in control subjects.** This would provide evidence for an increased reliance on bulbospinal systems as a mechanism underlying the expression of both abnormal muscle synergies. We believe that both the contralateral and ipsilateral responses in the paretic limb may be modulated with neck rotation, as both may be a result of corticobulbospinal upregulation following corticospinal damage during stroke. The effects of ATNR may be less in the contralateral MEP depending on the degree of corticospinal damage and remaining descending corticospinal fibers. This is one of the aims of Chapter 6 in this thesis.

## 2

**BACKGROUND*****2.1 Motor Performance Following Stroke***

Hemiparetic stroke is accompanied by abnormalities of muscle tone (i.e. spasticity), muscle weakness, and disturbances of muscular coordination. Spasticity is defined as “a motor disorder characterized by a velocity-dependent increase in tonic stretch reflexes (muscle tone) with exaggerated tendon jerk, resulting from hyperexcitability of the stretch reflex, as one component of the upper motor neuron syndrome” (Lance, 1980). An increase in motoneuronal excitability and an increase in the amount of excitatory input elicited by muscle extension contribute to spasticity. **In the isometric experiments conducted for this thesis, the elicited muscle activation was small and did not evoke a stretch reflex.** A variety of factors may contribute to the paresis of individual muscles (see Bourbonnais and Vanden Noven, 1989 for a review). Motor unit recruitment and rate modulation have been shown to be impaired in hemiparetic patients. In general, only a fraction of a spastic muscle’s motor units can be recruited and firing rates of recruitable units may be inappropriately slow (e.g. Gemperline et al., 1995), resulting in a degradation of force generation. Changes in the properties of motor units may also be a factor. Specifically, studies have reported atrophy of putative fast-contracting fibers, an increase in the twitch contraction time in fast-contracting units, and the presence of slow-contracting, fatigable motor units (not present in normal muscle) in paretic muscles. Additionally, increased force production in the antagonist muscle (due to either co-contraction or a change in muscle

properties) may result in a functional weakness although the forces generated by agonist muscles may be fairly normal. **In chapter 4 of this thesis, the correlation between weakness and abnormal coordination, clinical recovery level, and expression of synergy was investigated. In the following chapters, it was considered in experimental planning and in the explanation of results.** Even when muscle tone and muscle weakness are treated effectively, abnormal muscle coactivation patterns are still present and are functionally disabling. Therefore the main thrust of this thesis focused on this aspect of motor disturbance following stroke. A detailed description of the abnormal movement patterns in the paretic limb, and the natural history of the evolution of the various components of these abnormal clinical signs was first provided by Twitchell in 1951, in which he delineated both the major features of the movement disturbance, and the time course of recovery from stroke in some detail. A prominent feature of the disturbed movement patterns was the emergence of “stereotypic” movements, in which there appeared to be relatively tight coupling of motion at adjacent joints in the upper and lower limbs. Brunnstrom (1970) subsequently classified these abnormal stereotypic movement patterns into so called “synergies” which were broadly of either flexor or extensor type (see table 2-1).

**Table 2-1** Flexor and Extensor Upper Limb Synergies (Based on Brunnstrom, 1970)

<b>Flexor Synergy</b>	<b>Extensor Synergy</b>
flexion of the elbow	extension of the elbow
supination of the forearm	pronation of the forearm
abduction of the shoulder	adduction of the arm in front of the body
external rotation of the shoulder	internal rotation of the shoulder
shoulder girdle retraction and/or elevation	shoulder girdle protraction

This classification of abnormal coordination patterns has recently been quantified with electromyographic recordings from a large number of upper extremity muscles and the simultaneous measurement of joint torques with a load cell during static, isometric muscle contractions (Dewald and Beer, 2001; Dewald et al., 1995). Electromyographic (EMG)/EMG scatterplots for different muscle pairs measured during these experimental conditions showed significant EMG-EMG correlations in the paretic arm, which were not evident in either the contralateral arm or in the arms of normal subjects. Abnormal muscle coactivation patterns were found especially between shoulder abductors and elbow flexors as well as between shoulder adductors and elbow extensors. The measurements of shoulder and elbow torques confirmed the earlier EMG results. A decrease was found in the number of coordination patterns involved between the paretic limb and the non-paretic limb or control subjects (Dewald et al., 2001). The flexion synergy is more prominent and can be observed in the resting state of the arm, with elbow, wrist and finger flexion. It is unknown if the wrist or finger extensors are included in the extension synergy. Voluntary finger extension is greatly impaired following stroke, with the deficits resulting not only from a decrease in voluntary excitability, but also a coactivation of finger flexors which often exceeds any extension generated (Kamper and Rymer, 2001). **The mechanisms involved in the expression of muscle synergies following stroke are unknown and the experiments in this thesis were aimed at elucidating the cortical connections to muscles in the upper extremity after stroke.**

## ***2.2 Motor System Anatomy***

In order to understand the changes that occur in the motor system after stroke, a brief review of the motor system anatomy is necessary.

### ***2.2.1 Primary Motor Cortex: Cortical Layers***

The cerebral cortex is divided into six layers based on cellular anatomy. The first layer has few neuronal bodies, it is mostly composed of glial cells and some horizontal interneurons. The second layer is dense with small pyramidal cells. The third lamina is composed of larger pyramidal cells and along with layer II, sends motor output to other cortical regions. The fourth layer receives afferent information primarily from the thalamus, however, it is virtually absent in primary motor cortex. Layer V contains large pyramidal cells, termed Betz cells, and gives rise to the descending pathways. Finally, layer VI contains neurons that project back to the thalamus. Horizontal fiber networks in layers IV and II provide short range connections while longer range connections are more superficial. These horizontal fiber systems tend to run perpendicular to the precentral gyrus (Meyer, 1987) and are preferentially activated by TMS (Mills et al., 1992).

### ***2.2.2 Major Motor Cortices***

There are three major regions in the cortex involved in motor control: the primary motor cortex (area 4 (Brodmann, 1909)) located anterior to the central sulcus in the frontal lobe, the premotor

cortex (Brodmann area 6) located anterior to the primary motor cortex on the lateral aspect of the brain hemisphere, and the supplementary motor cortex (Brodmann area 6) also located anterior to the primary motor cortex but on the medial and superior aspects of the hemisphere (see figure 2-1A). These regions are defined as areas that influence spinal motoneuron pools directly as determined with either electrical stimulation experiments (Penfield and Rasmussen, 1950) or neural tracing techniques (He et al., 1993; He et al., 1995). The primary motor cortex is primarily responsible for the voluntary execution of movement or muscle activation. The premotor cortex is involved in the preparation and sensory guidance of movement. The function of the supplementary motor cortex is not fully understood, but it has been implicated in the sequencing of complex movements and in bimanual movements. These three regions contribute the majority of corticospinal fibers (primary motor cortex: 50%; supplementary motor cortex: 10%; premotor cortex: 5%) (Mills, 1999). **The contributions of the secondary motor cortices to the corticospinal tract are considered possible substrates for recovery of motor function following stroke.**



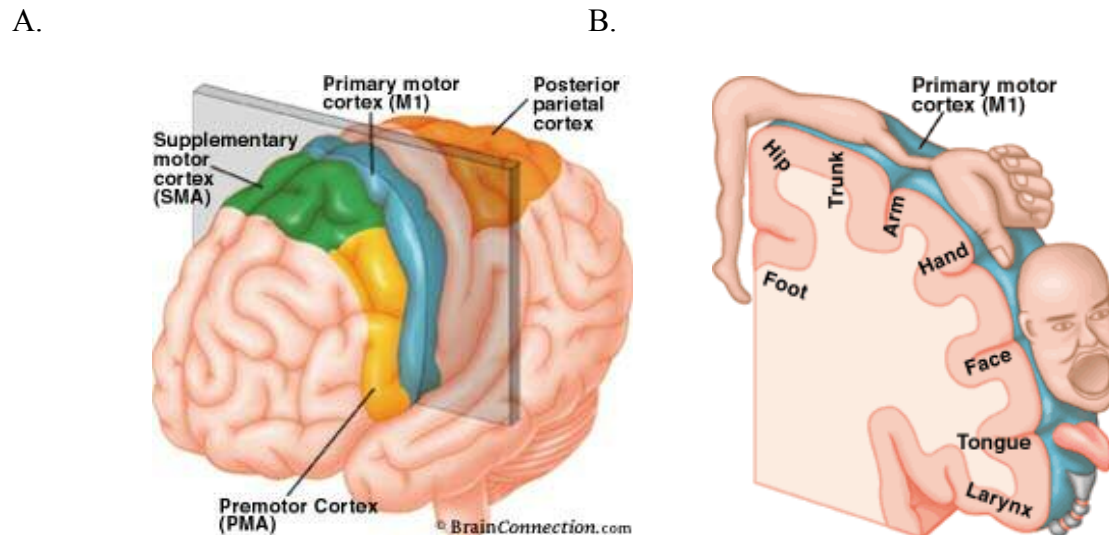


**Figure 2-1 Motor cortices and motor homunculus.** A. Major motor regions in the cortex. B. Motor Homunculus. Both figures are reproduced with permission from BrainConnection.com.

### 2.2.3 Gross Somatotopy

The organization of the primary motor cortex was first suggested to be somatotopic in early electrical stimulation experiments by Penfield and Rasmussen (1950). This study resulted in the classic homuncular representation of the M1 with the foot and leg lying medially, deep in the inter-hemispheric fissure and successive lateral representations of the trunk, arm, hand, and, most laterally along the precentral gyrus, the face and tongue. The homunculus is drawn to reflect the disproportionate amount of cortex devoted to the different body parts (e.g. the tongue has a large representation whereas the back has a small representation) (see figure 2-1B). Many studies since have supported the gross somatotopic organization of the primary motor cortex in man (TMS: Bondurant et al., 1997; PET: Grafton et al., 1991; fMRI: Rao et al., 1995; TMS: Wassermann et al., 1992). Recent studies have suggested at least a crude somatotopic arrangement in the premotor and supplementary motor cortices as well (Colebatch et al., 1991;

Fries et al., 1993; Grafton et al., 1993; Woolsey et al., 1952) with somatotopic cortico-cortical connections between the three motor regions (Stepniewska et al., 1993). **Similarities in gross somatotopy and inter-region connections support the possibility of secondary motor cortex takeover following stroke.**

#### *2.2.4 Fine Somatotopy in the Primary Motor Cortex*

Animal studies using intracortical electrical microstimulation demonstrate separate regions of activation for joints or arm segments as seen above. These regions are highly overlapping but maintain somatotopy (Kwan et al., 1978; Lemon, 1981; Murphy et al., 1978; Waters et al., 1990). However, within these regions there is no fine somatotopy, but rather a mosaic organization of muscles and movements. Individual muscles have also been found to have multiple representations spread widely throughout the primary motor cortex (Lemon et al., 1986). The overlap between regions, multiple representations and the mosaic nature within the regions may be a substrate for muscle/joint coordination. **Therefore, changes in the degree of overlap or other change in the location of muscle/joint representations within the primary motor cortex following stroke could reflect the constraint in coordination patterns observed during voluntary movement.**

## ***2.3 Descending Motor Tracts***

### ***2.3.1 Corticospinal Motor Pathway***

The corticospinal pathway is the only descending motor pathway that originates in the cerebral cortex and terminates directly onto spinal interneurons and motoneurons. The majority of corticospinal fibers originate from the primary motor cortex (50%), the supplementary motor cortex (10%), the premotor cortex (5%) and the somatosensory cortex (10%) (Mills, 1999). The fibers emanate from lamina V and course through the internal capsule (a common site of stroke), descend through the medullary pyramids, cross to the contralateral side and continue through the lateral portion of the spine to finally synapse onto spinal neurons in the ventral horn. A small percentage of the fibers (~ 10%) do not cross the midline and innervate ipsilateral spinal neurons. A single corticospinal axon may branch and terminate in several motoneuron pools, suggesting a possible role in muscle coactivation. Traditionally, it was believed that the corticospinal pathway affected primarily distal muscles, but recent studies in man show that it also has a significant effect on proximal limb muscles (Colebatch et al., 1990). The entire corticospinal pathway appears to be grossly topographically organized from the cortex to the spine. Within a spinal segment, the more proximal muscles are located more medially than the distal muscles. In addition, extensors are located in the gray matter along the border with the white matter and the flexors are located just medial to them. The corticospinal tract is the largest descending pathway with fibers of several diameters (90% of 1-4 $\mu$ m, 1.7% of 11-22 $\mu$ m) and fast conduction velocities (50-80 m/s). **The ipsilateral corticospinal projections are of particular interest as a substrate for recovery from hemiparetic stroke.**

### *2.3.2 Bulbospinal Motor Pathways*

The bulbospinal pathways are multi-synaptic and consist of small diameter fibers, both aspects contributing to slower conduction velocities than in the CS pathway. Bulbospinal axons are highly branching and innervate the more proximal and axial musculature. The bulbospinal pathways can be divided into the lateral and medial pathways based on their location in the spinal cord (Kuypers, 1964). The lateral pathways include rubrospinal tract and are traditionally thought to influence distal muscles whereas the medial pathways are composed of the vestibulospinal and reticulospinal tracts and are allegedly involved in axial and proximal muscle activation.

#### **2.3.2.1 Rubrospinal**

The rubrospinal tract is the other lateral pathway and originates from the red nucleus of the brainstem. It is primarily unilateral. Its function parallels that of the corticospinal tract offering a redundancy that can be called upon if the corticospinal tract is damaged. However, it does not have the capacity of the corticospinal tract for highly fractionated movements. Studies of this tract in man has shown that it is rudimentary and does not appear to extend caudal to the upper cervical segments (Nathan and Smith, 1982). In man, a lesion of the corticospinal tract causes considerable loss of function compared to the loss observed in lower primates where the rubrospinal tract is larger.

### **2.3.2.2 Vestibulospinal**

The vestibulospinal pathway originates in the vestibular nucleus. Cortical input to this system is limited (Wilson and Peterson, 1981).

**Medial.** The medial vestibulospinal tract projects mainly to midthoracic spinal levels and is bilateral. The medial vestibulospinal tract controls mostly neck and upper back musculature for postural adjustments during angular acceleration. It contains both slowly and rapidly conducting fibers. The medial vestibulospinal tract receives input from the semicircular canals and stretch receptors in the neck.

**Lateral.** The lateral vestibulospinal tract receives input from the labyrinth. There is no input from the cortex. The lateral vestibulospinal tract is concerned with the maintenance of posture. It descends primarily ipsilaterally and contains mostly fast conducting fibers (20-140 m/s). The lateral vestibulospinal tract extends the length of the cord. Branching is extensive in this tract; neurons which branch to the cervical enlargement may also project to the lumbrosacral cord (Abzug et al., 1974). This allows for coactivation of widely separated muscles. The lateral vestibulospinal tract has mono-synaptic excitatory inputs to extensor (antigravity) muscles and di-synaptic inhibitory inputs to flexor muscles.

The vestibulospinal system primarily depends on the input of the vestibular apparatus and is often concerned with excitatory fibers, some of which excite neck and hindlimb motoneurons monosynaptically. Despite the presence of monosynaptic connections on some motoneurons, actions of the lateral vestibulospinal tract, in particular, on limb extensors or flexors are mainly

achieved via interneurons. The branching of vestibulospinal fibers is extensive, allowing for coactivation of axial as well as proximal limb muscles.

### **2.3.2.3 Reticulospinal**

The reticulospinal pathway can be subdivided into its medial and lateral tracts. Reticulospinal neurons receive strong excitatory inputs from both the primary motor and premotor cortices.

**Medial.** The medial reticulospinal tract originates in the nucleus reticularis pontis oralis and nucleus reticularis pontis caudalis. It descends ipsilaterally in the ventromedial funiculus making synaptic connections with axial and limb flexor and extensor motoneurons, resulting in the facilitation of extensor (antigravity) muscles. It is a rapidly conducting tract of about 101 m/s (Nathan et al., 1996).

**Lateral.** The lateral reticulospinal tract originates in the nucleus reticularis gigantocellularis and nucleus reticularis ventralis. Lateral reticulospinal tract fibers descend mostly ipsilaterally although a small percentage of fibers also run contralaterally. The fibers terminate at all levels of the cord and within a segment the axonal branching can be so extensive it includes the entire ventral horn as well as the base of the dorsal horn (Nathan et al., 1996). The lateral reticulospinal tract innervates motoneurons of the neck and back and has a wide range of conduction velocities with an average of 69 m/s (Nathan et al., 1996). The lateral reticulospinal tract inhibits extensor (antigravity) muscles and facilitates flexor muscles.

*Recent animal studies of the reticulospinal tract.* Stimulation of the medial pontomedullary reticular formation in the primate most often resulted in facilitation of ipsilateral flexors in the arm and suppression of contralateral extensors with bilateral responses common (Davidson and Buford, 2004; Davidson and Buford, 2006). Recent work in the cat has shown that the reticular projections often cross the midline twice, once at the brainstem and once in the spine, thereby appearing to be an ipsilateral projection (Jankowska et al., 2003). These authors suggest this pathway as a replacement for damaged corticospinal projections from the pyramidal tract neurons (Jankowska et al., 2006).

**Both the reticulospinal and vestibulospinal tracts exhibit extensive branching and some bilateral connections. These aspects suggest their involvement in recovery from stroke based on the observations of muscle coactivation and bilateral brain activity after stroke. In addition, latency of muscle response may be prolonged after stroke which would correspond with the slower conducting velocities of the bulbospinal tracts as well as the increase in the number of synapses from the brain to the spinal cord.**

### *2.3.3 Propriospinal System*

Some corticospinal fibers terminate in the intermediate zone of the spinal grey. In the cat, they terminate on propriospinal interneurons. Propriospinal neurons also receive descending commands from the cortex, superior colliculus, red nucleus and reticular formation. The C<sub>3</sub>-C<sub>4</sub> propriospinal system has been extensively studied in the cat and has been shown to transmit corticospinal excitation to upper limb motoneurons (Alstermark and Lundberg, 1992). However,

data in the macaque monkey has shown that this transmission is uncommon, primarily because the direct cortico-motoneuronal pathway is more developed. As such, this pathway is thought to be suppressed in humans in whom strong cortico-motoneuronal connections exist. A recent study investigated whether the C<sub>3</sub>-C<sub>4</sub> propriospinal system in the macaque monkey has been overlooked because of the effects of anesthesia (Olivier et al., 2001). In awake or lightly sedated animals, they stimulated the medullary pyramidal tract and recorded single motor unit activity from either the adductor pollicis and abductor pollicis brevis, the extensor carpi radialis or the biceps. The poststimulus time histogram only consisted of one peak mediated by monosynaptic actions and did not have any later peaks which would have indicated non-monosynaptic activity. Thereby they confirmed that propriospinal activity in the monkey is weak or non-existent. Electrical stimulation of the motor cortex in man has shown a similar single peak result in the single motor unit (de Noordhout et al., 1999). The role of the propriospinal system in recovery from stroke was investigated in the extensor carpi radialis in humans (Mazevet et al., 2003). Stimulation of cutaneous afferents during on-going extensor carpi radialis activity caused asymmetrical suppression in stroke subjects, but not in healthy subjects. The authors suggest that this illustrates either an increased excitability of the propriospinal neurons, or an increase in the descending command projecting to these neurons, such as the reticulospinal tract.



## ***2.4 Possible Recovery Methods***

Several mechanisms could explain the recovery of movement after unilateral hemiparetic stroke. These mechanisms will be reviewed, along with their capacity to cause the abnormal coordination observed in stroke recovery.

### ***2.4.1 Reorganization Within the Motor Cortex***

**In the affected hemisphere, it is conceivable that the cortical innervation of a neighboring muscle could take over the function of a muscle whose cortical innervation has been damaged, resulting in obligatory coactivation between muscles.** Plasticity in the somatotopic representations of muscles, joints or body segments in the sensorimotor cortex have been shown in various studies. Amputation of the index finger resulted in the takeover of the somatosensory cortical region previously representing the index finger by the thumb and middle finger (Weiss et al., 1998). This effect has been observed in the motor cortex as well. In the motor cortex of Braille readers, the representation of the reading finger was enlarged and invaded the regions of the other fingers when compared with the contralateral hemisphere or controls (TMS: Pascual-Leone et al., 1993). Nudo and Milliken (1996) lesioned a portion of the cortical motor hand area in the monkey and observed that with training the spared hand region enlarged into the elbow region. Recovery from cortical stroke in humans results in peri-infarct activation as measured with fMRI (Cramer et al., 1997). Recovery from capsular stroke was associated with activation that appeared to have moved into the face region (Weiller et al., 1993). **Reorganization within the primary motor cortex would be indicated by a reduced number of stimulation induced**

**EMG and torque coordination patterns associated with a change in the somatotopic organization of the motor cortices in the affected hemisphere.**

#### *2.4.2 Non-Primary Motor Region Takeover*

**Another possible mechanism of cortical reorganization of motor function is for one of the non-primary motor regions to take over the lost function of the damaged primary motor area.** The primary motor cortex, premotor cortex and supplementary motor area occupy different regions of the internal capsule (primary motor cortex: posterior limb, premotor cortex: capsular genu, supplementary motor area: anterior limb), but a lesion in any of these areas results in a similar motor deficit indicating parallel function such that they may be able to substitute for each other at least partially (Fries et al., 1993). An increase in cortical activity in the premotor cortex and supplementary motor regions is often observed after stroke (Cramer et al., 1997; Weiller et al., 1993), however it is often accompanied by activity in the ipsilateral primary motor cortex which will be the next mechanism discussed. The somatosensory cortex is another region that could be involved in reorganization. A small percentage of corticospinal neurons originate in the somatosensory cortex (Fromm and Evarts, 1982). Evidence of somatosensory involvement has been found in spinal cord injury patients with EEG where activity related to movement was observed more posteriorly than in controls (Green et al., 1999). Moreover, a study of one stroke subject using fMRI, MEG and TMS showed, with all techniques, an enlargement of cortical activity and a posterior shift (Rossini et al., 1998). The role of the somatosensory cortex in stroke recovery cannot be ruled out. **Non-primary motor region**

**takeover would be indicated in the present study by a shift in the scalp sites where muscle and torque responses can be obtained with TMS as compared to the unaffected hemisphere. An anterior shift would implicate the increased involvement of the premotor cortex and/or supplementary motor regions and a posterior shift would implicate the somatosensory cortex.**

### *2.4.3 Descending Pathway Reorganization*

**The restricted patterns of muscle coactivation in hemiparetic stroke could be related to the loss of corticospinal pathways (see Kuypers, 1964).** A reduction of corticospinal input to the spinal cord, potentially results in an increased dependence on residual brainstem descending pathways (e.g. vestibulo- reticulo- spinal pathways; see Kuypers, 1964 and background section). These pathways project largely to motoneuron pools of axial and proximal limb muscles. They exhibit extensive branching, innervating neurons over many spinal segments. Takeover by brainstem descending pathways would lead to an obligatory coactivation of shoulder and elbow muscle groups and result in a reduced set of muscle coactivation patterns. Furthermore, a substitution of corticospinal fibers by corticobulbospinal connections would increase the latency between magnetic stimulation of the cortex and EMG responses in the paretic upper limb. Fries et al. (1991) electrically stimulated the lesioned hemisphere and observed a bilateral response, suggesting that recovery must rely on a descending pathway which is bilateral such as the corticoreticulospinal tract. Netz (1997) also suggests that the corticoreticulospinal tract is involved in recovery because of its small fiber diameter and multiple synapses which could

explain the long latency muscle activations observed after stroke. Several studies of stroke subjects have shown prolonged latencies (Benecke et al., 1991; Cicinelli et al., 1997; Traversa et al., 1997) **In the proposed study an increase in latency will indicate multi-synaptic brainstem descending pathway takeover.**

#### *2.4.4 Ipsilateral Motor Region Takeover*

**Ipsilateral M1 may take over lost motor function by using uncrossed corticospinal pathways.** Several imaging studies have recorded ipsilateral brain activity during contraction of the affected arm and hand muscles in stroke patients (PET: Chollet et al., 1991; fMRI: Cramer et al., 1997; EEG: Kopp et al., 1999; PET: Weiller et al., 1993). Initially, such activity was attributed to concurrent movement in the contralateral limb. However, both Kopp and Cramer made visual observations that there wasn't any movement of the non-responding hand and Kopp used sensitive force keys that did not record any finger movements from the non-responding hand. Cramer further argues that any non-visible muscle contractions of the non-responding hand could not create the strong intensity activation seen in the ipsilateral cortex. Along with ipsilateral primary motor cortex activity, activity was also observed in the ipsilateral supplementary motor cortex, primary motor cortex, insula and inferior parietal cortex. Bilateral activation was typically observed (Cao et al., 1998; Chollet et al., 1991; Cramer et al., 1997; Weiller et al., 1993), with pure ipsilateral activity seen rarely (Kopp et al., 1999).

Ipsilateral brain involvement has also been implied with brain stimulation studies. Fries et al.(1991) observed bilateral activation to stimulation of the unaffected hemisphere. Muscle activity elicited in the ipsilateral muscles following unaffected brain stimulation is of longer latency (6 ms, Netz et al., 1997) than would be expected from fast corticospinal paths. This suggests that other descending motor pathways may be involved with smaller fiber diameters and multiple synapses (see previous section). Corticobulbospinal pathways branch extensively and would be able to explain the abnormal coordination observed following stroke.

The benefit of ipsilateral takeover is questionable. Ipsilateral excitable activity is often seen with poor recovery from stroke, but not in patients with good recovery suggesting that this mechanism is not an effective recovery mechanism (Netz et al., 1997; Turton et al., 1996).

#### *2.4.5 Spinal Interneuron Excitability Alteration*

**An alternative possibility is that with the loss of descending input to the spinal cord after corticospinal pathway damage there is a change in the excitability of spinal interneurons.**

A potential increase in interneuron excitability would cause tonically active cutaneous afferents to have a continuous facilitatory effect on flexor motoneuron pools, which would be exaggerated in the lesioned nervous system. This could explain the predominance of flexor bias of the typical 'hemi-arm' (i.e., shoulder adduction, internal rotation, elbow flexion, forearm pronation and finger flexion). The fact that flexion reflex interneurons affect motoneuron pools located in several spinal segments would also potentially explain the abnormal muscle coactivation patterns

and resulting abnormal torque synergies which are the focus of this proposal. Work by Dewald and colleagues (1999) studying flexion withdrawal responses in the upper extremities of hemiparetic stroke subjects and controls suggest similar abnormal coactivational relations during electrically induced flexion withdrawal responses in the paretic upper limb as obtained during the voluntary isometric force exertions. In a comparison of torque profiles under voluntary conditions and flexion reflex conditions, it was found that no torque profiles matched in controls but that an average match of 2 of the 4 possible voluntary profiles to the flexion reflex profile occurred in stroke subjects. The flexion withdrawal responses were delayed in this study, suggesting that the transcortical long loop reflex may be involved. If the cortex has reorganized and is involved in the flexion withdrawal response, then it could explain the abnormal patterns seen with flexion withdrawal.

## ***2.5 Transcranial Magnetic Stimulation***

### ***2.5.1 Activation of the Motor Cortex by TMS***

Transcranial magnetic stimulation (TMS) is a noninvasive, nonpainful derivative of transcranial electrical stimulation. TMS acts by discharging a capacitor over a very short time period (100 ms risetime, 1 ms slow decay) and sending a current through a coil of tightly wound wires. This creates a magnetic field perpendicular to the coil which induces a horizontally oriented electric field in the brain (see figure 2.2). Excitation of neural structures occurs at axonal bends (Abdeen and Stuchly, 1994), where the threshold for excitation is lower the greater the degree of bending (Amassian et al., 1992; Maccabee et al., 1993) or at points where there is a change in diameter

such as at branch points or at the axon hillock (Durand et al., 1992). TMS activates pyramidal neurons in the cortex transynaptically (Day et al., 1989; Hess et al., 1987) via horizontally oriented interneurons such as stellate or cortico-cortical fibers (Rothwell, 1997). At least the onset of EMG activity can be attributed to activation of monosynaptic fast corticospinal axons (Hess et al., 1987). The depth of stimulation is dependent on stimulation intensity. A study in monkeys did not find any activation of corticospinal fibers below the grey matter (Edgley et al., 1990). This is attributed to the higher impedance of white matter than grey matter and to the fact that the magnetic field is cut in half 4-5 cm from the coil surface which is about equal to the distance from the surface of the skull to the depth of the central sulcus (Rothwell, 1997). Rothwell has suggested that at higher intensities pyramidal neurons that lie deep in the anterior bank of the central sulcus and are horizontally oriented may be activated or that at high intensities corticospinal fibers may be stimulated as they bend toward the internal capsule.

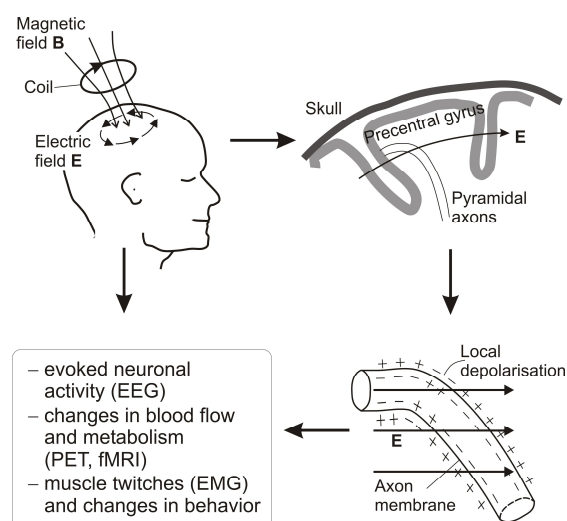


**Figure 2-2 Mechanism of TMS neural excitation.** Illustration of the magnetic and electric fields generated by TMS (note a circular coil is used and we used a figure-of-eight coil) and a mechanism by which it activates axons. Used with permission of the author (Ruohonen and Ilmoniemi, 1999).

### *2.5.2 TMS in Studying Motor Recovery Following Stroke*

TMS has been widely used to study the changes that occur in the motor system after stroke (See Talelli et al., 2006 for review). Only a few studies have investigated muscles of the paretic proximal upper limb after stroke; biceps brachii (Alagona et al., 2001; Eyre et al., 2001; Heald et al., 1993; Turton and Lemon, 1999; Turton et al., 1996), triceps (Heald et al., 1993), deltoid (Turton and Lemon, 1999; Turton et al., 1996), pectoralis major (Eyre et al., 2001; Heald et al., 1993) with more thorough investigation hampered by the heightened motor threshold post-stroke (Cicinelli et al., 2003; Cicinelli et al., 1997; Traversa et al., 1997; Turton et al., 1996). Even with background contraction, some proximal muscles are unavailable for study with single pulse TMS in moderate to severely impaired stroke subjects. These patients, in whom study is arguably needed the most, are often unable to provide background contraction. In addition, more recent studies have focused on the role of the ipsilateral descending motor pathways in recovery, which also have high thresholds (Netz et al., 1997; Turton et al., 1996). Using two pulses of the same intensity has been shown to intensify subliminal or nonexistent responses to single pulse TMS through temporal and spatial summation at the spinal as well as facilitation at the cortical levels (Nakamura et al., 1995). These studies have shown that an ISI of 10-50 ms with pulses of high stimulation intensity produce facilitatory effects in healthy controls in both hand (Abbruzzese et al., 1999; Chen et al., 1998; Claus et al., 1992; Kujirai et al., 1993; Valls-Sole et al., 1992) and biceps brachii (Abbruzzese et al., 1999; Chen et al., 1998). The majority of studies investigating the activation of distal arm muscles have found the presence of ipsilateral activity to be associated with poor motor recovery (Ward et al., 2003; Werhahn et al., 2003). In contrast,



studies of axial muscle activity have found a positive correlation between ipsilateral activity and recovery level (Fujiwara et al., 2001; Hamdy and Rothwell, 1998; Muellbacher et al., 1999). Several longitudinal studies have shown that early in recovery the ipsilateral (non-lesioned) sensorimotor cortex is hyperactive compared to controls and as recovery progresses activity shifts back to the contralateral (lesioned) hemisphere as determined with transcranial magnetic stimulation (TMS) (Turton et al., 1996) and other brain imaging techniques (transcranial doppler ultrasonography: Cuadrado et al., 1999; functional magnetic resonance imaging (fMRI): Marshall et al., 2000; fMRI: Tombari et al., 2004). However, in cases of poor recovery, the ipsilateral cortex retains control of the paretic arm (electroencephalography: Serrien et al., 2004; TMS: Turton et al., 1996; fMRI: Ward et al., 2003). The role of the ipsilateral projection, as well as the identification of the ipsilateral projection has not yet been determined.

### 3

## **SIGNIFICANCE**

### *Scientific implications*

This is the first time that TMS has been used to investigate abnormal coordination following stroke. By determining the best interstimulus interval for paired pulse TMS, and investigating the best ISI across distal and proximal muscles, we are enabling the study of proximal muscles in control subjects as well as enabling the study of the paretic arm following stroke using TMS, without biasing the results by using background muscle contractions, or disallowing subject participation because of their inability to provide background contraction. The results of the laterality study and effects of neck rotation as well as latency results will provide evidence to determine whether there has been a modification in the use of the descending motor pathways following stroke which could be responsible for constraining movement into the synergistic behaviors. In conclusion, the results of this study will substantially enhance our understanding of neural mechanisms driving abnormal coordination following stroke-induced brain-injury.

### *Clinical implications*

Abnormal coordination in moderate to severely impaired stroke patients has been shown to severely limit reaching workspace and overall usage of the impaired limb. The underlying mechanisms of abnormal coordination in these patients are unknown. This study has provided evidence that the ipsilateral projection is upregulated in these patients and may underlie the expression of the synergistic movements. We have also provided evidence of a delayed onset

and similarity between the muscles with preferential ipsilateral input to muscles that are facilitated by stimulation of the reticular formation in the monkey, and suggest that the upregulated pathway may be the corticoreticulospinal tract. The identification of the descending motor pathway involved in the expression of abnormal coordination is extremely important for developing rehabilitation strategies. Therapeutic drugs based on altering the effects of neurotransmitters used in that pathway could be tested. In addition, knowledge of the pathway's connections would be a starting point for studies attempting to adjust the synaptic gain for some muscles and not others and could possibly result in an increase in arm function. Furthermore, the use of asymmetric tonic neck reflexes, to train movements outside of the abnormal synergies, would permit rehabilitation clinicians to regain lost workspace in the paretic upper limb. In conclusion, this study has provided information regarding the mechanisms underlying abnormal coordination which could form the basis for designing novel therapeutic approaches following stroke-induced brain injury.

## 4

# **IPSI- VERSUS CONTRA-LATERAL CORTICAL MOTOR PROJECTIONS TO A SHOULDER ADDUCTOR IN CHRONIC HEMIPARETIC STROKE: IMPLICATIONS FOR THE EXPRESSION OF ARM SYNERGIES**

## *4.1 Introduction*

After a stroke which has damaged the corticospinal tract, ipsilateral projections from the intact hemisphere are more active as measured with functional magnetic resonance imaging (fMRI) (Cao et al., 1998; Carey et al., 2002; Cramer et al., 1997; Feydy et al., 2002; Marshall et al., 2000; Ward et al., 2003), positron emission tomography (PET) (Chollet et al., 1991; Honda et al., 1997; Weiller et al., 1993), electroencephalography (EEG) (Green et al., 1999; Kopp et al., 1999; Serrien et al., 2004; Verleger et al., 2003) and transcranial magnetic stimulation (TMS) (Alagona et al., 2001; Chen et al., 2003; Fujiwara et al., 2001; Strens et al., 2003; Ward et al., 2003). The majority of studies investigating the activation of distal arm muscles have found the presence of ipsilateral activity to be associated with poor motor recovery (Ward et al., 2003; Werhahn et al., 2003). In contrast, studies of axial muscle activity have found a positive correlation between ipsilateral activity and recovery level (Fujiwara et al., 2001; Hamdy and Rothwell, 1998; Muellbacher et al., 1999).

The disparity between the muscle groups may be explained by the fact that axial muscles receive extensive bilateral input (Ferber et al., 1992; Hamdy and Rothwell, 1998) whereas distal muscles are primarily innervated by contralateral projections (Palmer and Ashby, 1992). Therefore, even when contralateral projections are damaged, the axial muscles may be able to depend on a strong ipsilateral projection for some function.

The role of ipsilateral projections in the recovery of the proximal upper limb muscle function is still unknown. After a hemiparetic stroke, the proximal limb is less affected than the distal limb (Colebatch and Gandevia, 1989), however, the normal function of the upper arm is severely disrupted as evidenced by weakness (Adams et al., 1990; Bohannon and Smith, 1987; Colebatch and Gandevia, 1989; Lum et al., 2003; Mercier and Bourbonnais, 2004) and abnormal coordination between elbow and shoulder muscles expressed as flexor and extensor synergies (Beer et al., 1999b; Brunnstrom, 1970; Dewald and Beer, 2001; Dewald et al., 1995; Twitchell, 1951). These impairments significantly affect reaching abilities in patients with poor recovery (Beer et al., 2004).

In healthy subjects, ipsilateral projections to the proximal limb are more common than in the distal limb. Using TMS, ipsilateral motor evoked potentials (iMEPs) in the pectoralis major and the trapezius muscles were most easily evoked during tonic contraction, whereas iMEPs in the deltoids and biceps occurred only with biphasic contractions (Bawa et al., 2004) and iMEPs in distal muscles were rare. However, iMEPs have been recorded in some distal muscles using

high stimulation intensities and background contraction (Ziemann et al., 1999). A study in rhesus monkeys showed that the ipsilateral corticospinal tracts primarily innervate proximal and axial muscles (Brinkman and Kuypers, 1973). Furthermore, cortico-bulbospinal pathways descend bilaterally and innervated mainly axial and proximal limb muscles (Kuypers, 1964). This anatomical arrangement may facilitate recovery of the proximal limb following stroke. However, it could be that the loss of direct contralateral corticospinal input to the proximal limb results in the loss of independent joint control observed as abnormal coordination in the proximal limb after stroke. Moderate to severely affected stroke patients exhibit an obligatory coactivation between shoulder adductors and elbow extensors (extensor synergy) as well as between shoulder abductors and elbow flexors (flexor synergy) (Brunnstrom, 1970; Dewald and Beer, 2001; Dewald et al., 1995).

The purpose of this study was to determine if the relative presence and magnitude of the ipsilateral and contralateral projections to the proximal muscle PMJ were correlated with muscle strength, abnormal coordination, and/or Fugl-Meyer score in mild to severely impaired stroke subjects.

## ***4.2 Materials and Methods***

### ***4.2.1 Subject Selection***

Ten male subjects with left hemiparesis volunteered to participate in the study. All subjects were recruited from the stroke database at the Sensory Motor Performance Program within the Rehabilitation Institute of Chicago. The experiments were performed with informed consent and

approval of the local ethics committee. Subjects were evaluated with the upper extremity motor portion of the Fugl-Meyer Motor Assessment (FMA) (Fugl-Meyer et al., 1975) and the Chedoke-McMaster Stroke Assessment (CMSA) (Gowland et al., 1993) prior to the experiment (see table 4-1). Lesion location was identified by a neuroradiologist from an anatomical MRI if it was available.

**Table 4-1** Clinical data for hemiparetic stroke participants

Participant	Age	Lesion Location	FMA <sup>a</sup>	CMSA <sup>b</sup>	Recovery Group
<b>S1</b>	51	N/A	14	2	MS
<b>S2</b>	58	N/A	22	2	MS
<b>S3</b>	56	N/A	23	3	MS
<b>S4</b>	57	thalamus, posterior putamen, posterior limb of internal capsule	24	3	MS
<b>S5</b>	48	insula, thalamus, basal ganglia, internal capsule	26	3	MS
<b>S6</b>	57	lateral/posterior frontal lobe, caudate, basal ganglia, internal capsule	43	6	MM
<b>S7</b>	66	occipital lobe, thalamus, basal ganglia	49	5	MM
<b>S8</b>	38	temporal lobe, internal capsule	50	7	MM
<b>S9</b>	69	frontal-parietal cortex and coronal radiata, internal capsule	51	3	MM
<b>S10</b>	65	N/A	58	7	MM

<sup>a</sup>Based on Fugl-Meyer scale (maximum score = 66)

<sup>b</sup>Based on the Chedoke-McMaster scale (maximum score = 7)

#### 4.2.2 Experimental Set-Up

Subjects were secured in a Biodex experimental chair (Biodex Medical systems, Shirley, NY) using waist and shoulder belts to restrict trunk movement. Both the paretic and non-paretic arms were held in the following arm configuration: 90° elbow angle, 55° shoulder abduction angle, and 20° shoulder flexion angle. A fiberglass cast was put on the hand, wrist and forearm of the paretic arm which was fixed at the wrist to a six degrees of freedom load cell (Model 45E15A; JR3, Inc., Woodland, CA). The non-paretic arm was strapped to a single degree of freedom load

cell (Model FT04433; ATI Industrial Automation, Garner, NC) under the elbow center of rotation. Forces and moments measured by the six degrees of freedom load cell were converted on-line to torques at the elbow and shoulder of the paretic limb (Beer RF, 1999). Maximum voluntary shoulder adduction and elbow flexion/extension torques were measured for the paretic arm. Only maximal shoulder adduction was measured in the non-paretic arm. Real-time visual feedback of the downward force produced by each elbow during shoulder adduction was provided to the subject on a computer monitor. During the experiment, the subject was asked to simultaneously adduct both arms to a level of 5-10% of the voluntary max of the non-paretic limb. Surface electromyographic (EMG) signals were recorded from the right and left pectoralis major vertical fibers (PMJ). Active electrodes (Delsys, Boston, MA), with a 1 cm inter-electrode distance were placed over the muscle belly. The EMG signals were sampled at 2500 Hz, amplified 1000 times and band-pass filtered at 6-450 Hz.

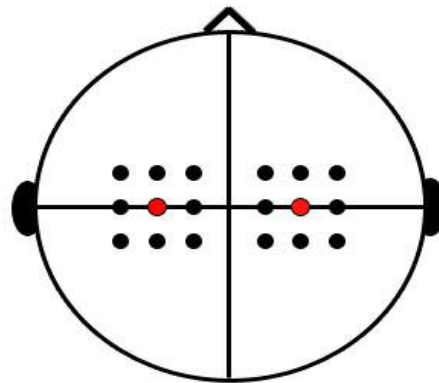


**Figure 4-1 Stimulation grid.** Red circle indicates the point 4 cm lateral from the vertex. Points are spaced 2 cm apart.

### **4.2.3 Transcranial Magnetic Stimulation**

Single pulse transcranial magnetic stimulation (TMS) of 90% maximal stimulator intensity was applied over an eighteen site stimulation grid on the scalp surface (nine sites on each hemisphere, see figure 4.1) with a 70 mm figure-of-eight coil (Magstim Co., UK). The 2 cm spaced grid was



centered on a site located 4 cm lateral to the vertex of the head, which has previously been found to be the optimal site for activation of PMJ in healthy subjects (MacKinnon et al., 2004). A grid was investigated to account for any shift that may have occurred in the lesioned hemisphere with cortical reorganization after the stroke. In addition, the investigation of a grid would be able to detect if the ipsilateral hotspot is in a position distinct from the contralateral hotspot as has been previously reported (Chen et al., 2003; Nirkko et al., 2001; Wassermann et al., 1994; Ziemann, 1999). The coil was held with the handle straight backward and was oriented to produce currents in a posterior-to-anterior direction. During the experiment, the subject was asked to maintain the target level of adduction force in both arms for thirty seconds while five TMS stimuli were applied. The experimenter verified that both arms were adducting within the target range before stimulating the subject. Two trials of five stimuli were recorded for each stimulation site for a total of ten stimuli per site.

### ***4.3 Analysis***

Data were analyzed off-line using custom software developed in Matlab (Mathworks, Inc., Natick, MA). For each stimulation site, the ten trials of unrectified EMG were ensemble averaged. The size of the motor evoked potential (MEP) was calculated by measuring the peak-to-peak magnitude of the ensemble averaged signal. The presence of an MEP was determined by evaluating the ensemble averaged signal as well as an overlay of all ten trials. At least five of the ten trials needed to deviate in the same direction from baseline at a similar time-point for the determination that an MEP occurred. The site with the largest peak-to-peak response was

defined as the hotspot. Four hotspots were found; the contralateral and ipsilateral hotspots for the non-paretic arm and the contralateral and ipsilateral hotspots for the paretic arm. The signals elicited from these four sites were further analyzed and compared across subjects. The statistical analysis was performed using Data Desk (version 6.1, Data Description, Inc., Ithaca, NY) or STATPAC for Windows. A significance level of .05 was used for all the statistical tests.

#### *4.3.1 MEP prevalence*

The prevalence of iMEPs and cMEPs were compared between the paretic and non-paretic limbs using the Fisher's Exact test which is suited for small sample sizes.

#### *4.3.2 Relative Size of Responses in Paretic Limb*

The MEPs were normalized to the maximum voluntary contraction. The peak-to-peak magnitude of the cMEPs and iMEPs in the paretic limb were compared with the non-paretic limb responses using paired t-tests.

#### *4.3.3 Hemispheric Laterality*

The laterality index (LI) was calculated for both the paretic and non-paretic PMJ for each subject to determine the relative magnitude of the contralateral and ipsilateral projections as follows:

$$LI = (cMEP - iMEP) / (cMEP + iMEP)$$

where an LI = 1 signifies that only a cMEP was recorded in the muscle and an LI of -1 indicates that only an iMEP was elicited. The correlation between the laterality index and the Fugl-Meyer score was tested using the non-parametric Spearman's correlation coefficient.

#### *4.3.4 Strength*

The maximum voluntary shoulder adduction torque was recorded in the paretic limb and normalized to the non-paretic limb maximum torque as an indicator of the level of recovery of strength. The correlation between strength and laterality index was tested using the parametric Pearson's correlation coefficient.

#### *4.3.5 Secondary Elbow Torque*

In abnormal coordination after stroke, shoulder adduction is abnormally combined with elbow extension. In this experiment, the secondary torque at the elbow was measured while subjects performed maximal voluntary shoulder adduction. The laterality index was tested for correlation with the amount of elbow extension across subjects using Pearson's correlation coefficient. The correlation between the degree of elbow coactivation and the Fugl-Meyer score was tested using the non-parametric Spearman's correlation coefficient.

#### *4.3.6 Spatial Analysis*

The location of the ipsilateral hotspot in each hemisphere was compared to the contralateral hotspot in the medial-lateral and anterior-posterior directions. The amount of relative shift was described in terms of the grid sites, such that if the ipsilateral hotspot was one grid site anterior (2 cm) to the contralateral grid site, the shift was positive 1 in the anterior-posterior direction. A one sample sign test of the direction of the shift was used to test for a significant change in the hotspot location across subjects. A sign test was used simply to determine if a consistent shift occurred across subjects in a particular direction. If a shift was evident across subjects, it was quantified in terms of the average number of grid sites.

#### **4.3.7 Latency Analysis**

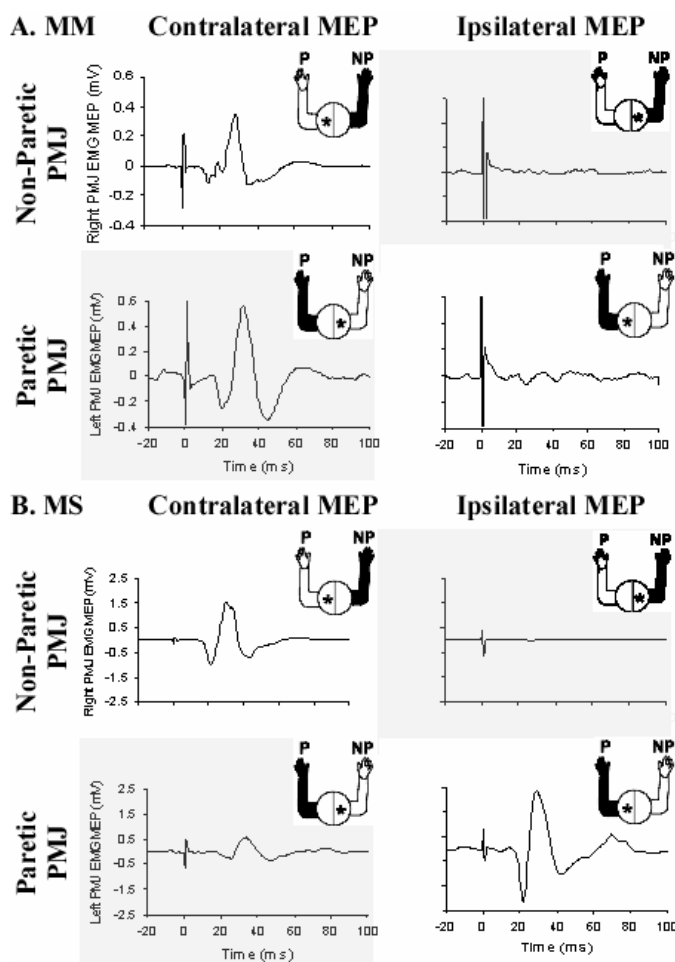
The onset of the MEP was identified as the time-point where at least 5/10 trials deviated from baseline in the same direction. An ANOVA was used to test for the effect of arm (paretic vs. non-paretic) and projection type (contralateral vs. ipsilateral). Scheffe posthoc tests were used to determine significant differences between groups in terms of the onset latency.

### **4.4 Results**

#### **4.4.1 Raw Data**

An example of MEPs evoked in the non-paretic and paretic PMJ from either the contralateral or ipsilateral hemispheres is shown in figure 2 for two subjects (one with mild to moderate impairment and one with moderate to severe impairment). Both subjects had some ipsilateral response in the paretic limb, however, the response was much larger in the moderate to severe subject. The ipsilateral response in this subject was even larger than the contralateral response in the paretic limb. We observed ipsilateral responses much more often in our more severely affected subjects (see table 2) and therefore for some analysis we divided the subjects into the mild to moderate (MM) impairment group (five subjects) with Fugl-Meyer scores in the 1-33 range and Chedoke-McMaster scores of 2 or 3 or into the moderate to severe (MS) impairment group (five subjects) with Fugl-Meyer scores of 31-66. Only one subject in the MM group had a Chedoke-McMaster score of less than 5. (see tables 1 & 2).

**Figure 4-2 Raw data.** Motor evoked potentials (MEPs) elicited in the non-paretic and paretic pectoralis major muscle by transcranial magnetic stimulation (TMS) of the contra-lateral and ipsilateral hotspots in two subjects. A. mild to moderate subject. B. moderate to severe subject. Plots show the average MEP waveform from ten trials. The figure in the upper right shows which arm is being recorded from and which hemisphere is being stimulated. The shaded plots are MEPs recorded when stimulating the lesioned hemisphere.

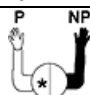
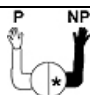
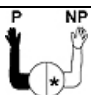
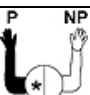


#### 4.4.2 Prevalence of cMEPs and iMEPs

Contralateral MEPs (cMEPs) were evoked in the non-paretic PMJ in all ten subjects (see table 2). In the paretic arm, cMEPs occurred almost as frequently as in the non-paretic PMJ (7/10 versus 10/10 respectively;  $p = .2105$ ; two-tailed Fisher's Exact Test, FET). Ipsilateral MEPs in the paretic arm occurred with a similar frequency as in the non-paretic PMJ (7/10 versus 5/10 respectively;  $p = .6499$ ; two-tailed FET). By recovery group, the subjects in the MS group were more likely to exhibit iMEPs in the paretic limb than the MM group (5/5 versus 2/5 respectively;  $p = .0833$ ; one-tailed FET) and were overall significantly more likely to have iMEPs in either

limb (9/10 versus 3/10 respectively;  $p = .0099$ ; two-tailed FET). The prevalence of cMEPs was similar between the MS and MM groups for both the paretic and non-paretic limbs. In only four subjects could all four types of responses be evoked, with three of the four being in the MS group and the fourth having the lowest FM score of the MM group.

**Table 4-2** Summary of results

Subject <sup>a</sup>	Group	Non-Paretic cMEP	Non-Paretic iMEP	Paretic cMEP	Paretic iMEP	Strength <sup>c</sup> (%)	Secondary Torque <sup>d</sup> (%)	Paretic LI	Non-Paretic LI
									
S1	MS	√ <sup>b</sup>	√	√	√	33.18	-67.78	-0.66	0.94
S2	MS	√	√		√	5.63	-81.20	-1.00	0.88
S3	MS	√	√	√	√	57.48	-74.57	-0.35	0.92
S4	MS	√	√	√	√	56.13	31.92	0.19	0.75
S5	MS	√			√	57.19	-162.79	-1.00	1.00
S6	MM	√	√	√	√	53.04	-28.82	-0.02	0.44
S7	MM	√				59.03	N/A	N/A	1.00
S8	MM	√		√	√	90.06	18.41	-0.11	1.00
S9	MM	√		√		55.93	-42.38	1.00	1.00
S10	MM	√		√		57.80	1.30	1.00	1.00

<sup>a</sup>subjects are listed in order of impairment level; from most impaired at the top to least impaired at the bottom

<sup>b</sup>√ indicates the presence of an MEP

<sup>c</sup>maximal adduction of the paretic arm normalized to the non-paretic arm

<sup>d</sup>elbow torque that was generated during maximal adduction

#### 4.4.3 Relative Size of MEPs in the Paretic Limb

Across all subjects, the normalized cMEPs in the paretic limb were significantly smaller than in the non-paretic limb ( $p = .0425$ ). In the MS group alone, the paretic limb cMEPs were smaller than the non-paretic limb ( $p = .0162$ ), but there was no difference in size in the MM group ( $p = .4539$ ). The normalized iMEPs in the paretic limb were not significantly different from those in the non-paretic limb across all subjects ( $p = .1524$ ). A comparison of iMEPs within the MM

group was not possible because the majority of subjects did not have ipsilateral responses in either arm. In the MS group, there was no significant difference between arms for iMEP magnitude ( $p = .3418$ ). While the non-paretic cMEP was, with one exception, larger than the paretic iMEP, the magnitude of the two responses were not significantly different across subjects ( $p = .2793$ ).

#### 4.4.4 Laterality

Comparison of the laterality index between the stroke MM and MS groups in the paretic and non-paretic arms was completed using a two-factor (group and arm) mixed design analysis of variance (ANOVA) with repeated measures on the last factor (arm). Results (see figure 4.2)

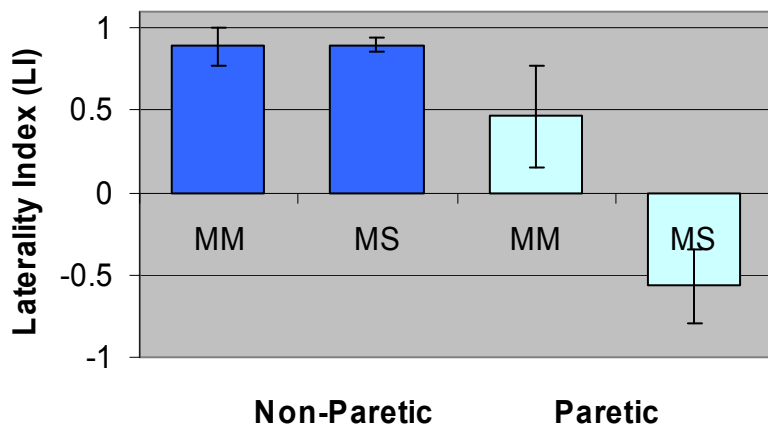


**Figure 4-3 Laterality index.** LI in the non-paretic muscle (dark blue) and paretic muscle (light blue). The LI in the paretic arm of the moderate-severe group (MS) is negative and significantly different from both the LI of the MS non-paretic arm and the MM non-paretic arm.

show an effect of group, arm and interaction between arm and group ( $F = 7.9211$ ,  $P < .0131$ ). A  $t$ -test with Bonferroni correction was used for post hoc comparisons between

different factors and their interactions. Results show significant difference

between group ( $F = 7.58$ ,  $P < .0148$ ), arm ( $F = 25.876$ ,  $P < .001$ ), and the following pairs: MS,

paretic and MM, non-paretic ( $P < .000246$ ); MS, paretic and MM, paretic ( $P < .0099$ ); and MS, paretic and MS, non-paretic ( $P < .000226$ ). There was no significant difference between the other pairs. In one subject (S7) the laterality index could not be determined because no cMEP or iMEP was recorded in the paretic limb.

#### 4.4.5 Correlation of Laterality Index with Impairment

The laterality index in the paretic arm is correlated with impairment level as measured by the Fugl-Meyer score (Spearman's correlation coefficient,  $R^2_s = .6108$ ,  $p < .05$ , see figure 4.3).

There is no correlation found between LI and strength (Pearson's correlation coefficient,  $R^2_p = .1806$ ,  $p = .2543$ ). Finally, LI is correlated with the amount of elbow flexion/extension torque generated during maximal shoulder adduction ( $R^2_p = .4247$ ,  $p = .0232$ ).

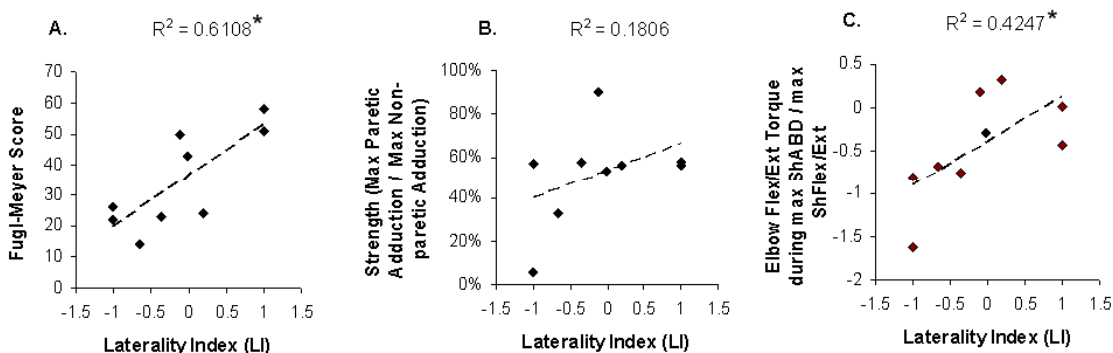


**Figure 4-4 Correlation results.** Correlation between the laterality index and: A. Fugl-Meyer score B. strength and C. secondary elbow torque. \* Indicates the correlation is significant at the  $p < .05$  level.



#### **4.4.6** *Correlation of Paretic cMEP and iMEP Magnitude with Clinical Score*

In order to determine whether it was the loss of contralateral projections or the increased usage of ipsilateral projections that caused the change in the laterality index, we normalized the paretic cMEP and iMEP to the non-paretic cMEP. The correlation between the respective normalized cMEP and iMEP and the Fugl-Meyer score was tested. There is a trend in the cMEPs such that more impaired subjects (lower Fugl-Meyer score) have smaller cMEPs (Spearman correlation coefficient  $R^2 = .2803$ ,  $p < .10$ ). In addition, most subjects either had an iMEP around 17% of the non-paretic cMEP (13%, 13%, 16%, 22%, 22%) or no iMEP at all (3 subjects) with 2 subjects having very large iMEPs (86%, 174%), therefore no significant correlation was obtained (Spearman correlation coefficient  $R^2 = .2278$ ,  $p < .50$ ).

#### **4.4.7** *Relative Spatial Location of Optimal cMEPs and iMEPs*

In the non-lesioned hemisphere, a one sample sign test failed to show a significant shift in either the medial-lateral direction ( $p = .250$ ) or the anterior-posterior direction ( $p = .375$ ) between the contralateral and ipsilateral hotspots. For the lesioned hemisphere, only four subjects had both an ipsilateral and a contralateral hotspot, with two subjects having no difference in location at all.

#### **4.4.8** *Onset Latency*

A significant interaction was found between the arm involved (non-paretic versus paretic) and the type of projection (contralateral versus ipsilateral) ( $p = .0265$ ), but no effect of group type (moderate to severe versus mild to moderate) ( $p = .3930$ ). A Scheffe post-hoc analysis showed a significant delay in onset for the non-paretic iMEPs (23.92 +/- 7.46 ms) compared to the non-paretic cMEPs (14.22 +/- 5.13 ms) ( $p = .0332$ ). The paretic arm iMEP onset latency (16.41 +/-

2.59 ms) was not significantly different from the paretic arm cMEP (19.59 +/- 2.27 ms) or either projection in the non-paretic arm.

## ***4.5 Discussion***

The results of this study indicate that an increase in the presence of the ipsilateral MEP which causes a shift in the laterality index towards the ipsilateral hemisphere may contribute to the expression of the extensor synergy in patients with poor motor recovery from stroke. Furthermore, there is a trend to a reduction in cMEP amplitude as stroke subjects become more impaired as determined with the Fugl-Meyer motor assessment scores.

### ***4.5.1 Ipsilateral MEP Prevalence***

Ipsilateral MEPs can be elicited in healthy adults with high stimulation intensity and background activation of the muscle (Carr et al., 1994; Colebatch et al., 1990; Ziemann et al., 1999). The iMEPs are more easily elicited in proximal than distal muscles, however, even when present, the contralateral projections are much stronger (Bawa et al., 2004). iMEPs are elicited more frequently in stroke subjects than in healthy subjects. In this study, iMEPs were evoked as often in the non-paretic and paretic limbs, but significantly more often in the moderate to severe group than in the mild to moderate group. In healthy subjects, iMEPs in the PMJ muscles were only about 20% of the cMEP amplitude in healthy subjects (MacKinnon et al., 2004). The results from this study in stroke subjects has similar results in that the majority of iMEPs in the paretic

limb are about 17% of the “normal” cMEP elicited in the non-paretic limb, suggesting that the ipsilateral pathways evoked by TMS in healthy and stroke subjects is the same.

#### *4.5.2 Evidence for an Increased Reliance on Indirect Descending Motor Pathways Following Stroke*

After stroke, a reduction of the crossed corticospinal input to the muscle could result in an increased dependence on residual brainstem descending pathways (e.g. vestibulo-, reticulo- and tecto-spinal pathways) (Kuypers, 1964). These pathways project bilaterally to motoneuron pools of axial and proximal limb muscles. They exhibit extensive branching, innervating neurons over many spinal segments thus providing the infrastructure for obligatory coactivation of muscles acting at different joints. In fact, recent work in felines has shown a connectivity between pyramidal tract neurons and ipsilateral motoneurons which involves pathways that cross the midline twice-once at the level of the brainstem and once at the spinal level (Jankowska et al., 2003). Latency studies on ipsilateral MEPs suggest that they are mediated by a cortico-bulbospinal pathway (MacKinnon et al., 2004; Ziemann, 1999). While we did not observe significant differences between the latencies of the cMEPs and iMEPs in the paretic limb in this study, their onsets were all delayed compared to the latencies reported for cMEPs in the PMJ in healthy subjects (mean onset = 9.9 ms) (MacKinnon et al., 2004). The initial portion of an MEP has been contributed to the fast corticospinal projection, but the medium latency component (occurring about 6 ms after the initial portion) has been proposed to originate from cortico-brainstem pathways (MacKinnon et al., 2004). The delayed onsets observed here in the paretic limb cMEP could indicate that only the medium latency component (Colebatch et al., 1990) of

the MEP is present, with a loss of the short latency corticospinal projection which would be plausible after stroke. A recent study showed the modulation of a wrist extensor iMEP with neck rotation in accord with the asymmetric tonic neck reflex (Ziemann et al., 1999). The authors suggest that the ipsilateral pathways are routed through the reticular formation which receives input from neck receptors. Stimulation of the reticular formation in monkeys has shown a pattern of muscle suppression/facilitation which would result in the flexion of the ipsilateral arm indicating a possible role in the flexor synergy (Davidson and Buford, 2004). Asymmetric tonic neck reflex is present in infants and young children, but disappears with development (Marinelli, 1983; Parmenter, 1975; van Kranen-Mastenbroek et al., 1997; Vles et al., 1988; Zemke, 1985), which could reflect an inhibition of these primitive reflex pathways. In addition, ipsilateral MEPs can be evoked in children up to 10 years, strengthening the possible connection between ATNR effects and ipsilateral projections (Muller et al., 1997). Following a stroke, these pathways could be unmasked and produce the flexor and extensor synergies.

#### **4.5.3** *Clinical Correlates*

In this study the recovery level, as measured by the Fugl-Meyer index, was correlated with the laterality index such that more severely affected stroke patients had greater ipsilateral than contralateral projections to the PMJ. In addition, the laterality index was correlated with the secondary elbow torque during shoulder adduction, reflecting a greater expression of the extensor synergy in subjects with a lower Fugl-Meyer score. This is in agreement with previous studies of distal arm muscles that have shown that the presence of iMEPs is correlated with poor

recovery (Ward et al., 2003; Werhahn et al., 2003). The loss of independent joint control, demonstrated in this study by the extensor synergy, may be either a result of the loss of contralateral projections, or the upregulation of the ipsilateral projection-as both can contribute to the shift of the laterality index in the MS group. This work only looked at MEPs in a single adductor muscle (PMJ) and other muscles in the paretic upper limb need to be studied to further establish the exact link between ipsilateral projections and the expression of abnormal muscle synergies in the paretic arm following stroke induced brain injury.

#### ***4.6 Conclusion***

While some studies have shown a correlation between the use of ipsilateral pathways after stroke and poor recovery, we propose that the usage of these pathways actually may be a form of recovery where otherwise all function might be lost. This form of recovery may however be at the expense of independent joint control which limits the functional usage of the paretic upper extremity. In an effort to test this possibility we investigated the PMJ muscle because iMEPs in this muscle have been previously recorded in healthy subjects therefore increasing the likelihood of eliciting iMEPs in stroke. However, PMJ is involved in the extensor synergy which is less strongly expressed following stroke than the flexor synergy, therefore the results presented here may be stronger if applied to the study of muscles/joints involved in the flexor synergy. Nonetheless, this study is the first to demonstrate preliminary evidence of the connection between ipsilateral projections and the expression of abnormal coordination patterns following stroke. Further research investigating the loss of corticospinal contralateral projections and the

employment of oligosynaptic ipsilateral projections in relation to abnormal coordination following stroke needs to be done.

## 5

# **FACILITATION OF CONTRA- AND IPSI-LATERAL MEPS IN UPPER EXTREMITY MUSCLES IN CHRONIC HEMIPARETIC STROKE USING PAIRED PULSE TMS**

### ***5.1 Introduction***

Transcranial magnetic stimulation (TMS) has been widely used to study the changes that occur in the motor system after stroke (See Talelli et al., 2006 for review). TMS studies have provided valuable information such as shifts in the cortical topography of arm and hand muscle motor representations (Byrnes et al., 1999; Cicinelli et al., 1997; Delvaux et al., 2003; Rossini et al., 1998; Thickbroom et al., 2004), increased latency of muscle activation which provides clues to changes in the descending motor pathways (Cicinelli et al., 1997; Rossini et al., 1998; Traversa et al., 1997; Turton et al., 1996), and changes in intracortical excitability (Byrnes et al., 2001; Cicinelli et al., 2003; Liepert et al., 2000; Manganotti et al., 2002; Traversa et al., 2000) after stroke.

The majority of TMS studies in the paretic upper limb have focused on the more distal muscles, presumably because of the severe effect of a stroke on hand function as well as the fact that distal muscles are more accessible to TMS. However, the paretic proximal limb also suffers from debilitating attributes such as weakness (Adams et al., 1990; Bohannon and Smith, 1987;

Colebatch and Gandevia, 1989; Lum et al., 2003; Mercier and Bourbonnais, 2004), spasticity (Benecke et al., 1983; Delisa et al., 1982) and abnormal coordination in the form of the flexor and extensor synergies (Beer et al., 1999a; Beer et al., 2000; Beer et al., 1999b; Brunnstrom, 1970; Dewald and Beer, 2001; Dewald et al., 1995; Landau and Sahrman, 2002; Levin, 1996; Lum et al., 2003; Twitchell, 1951). Abnormal coordination can severely interfere with reaching and therefore, studying the changes that occur in the descending cortical projections to these arm muscles could be very important for understanding the underlying mechanisms of movement disorder in the arm following stroke.

Only a few studies have investigated muscles of the paretic proximal upper limb after stroke; biceps brachii (Alagona et al., 2001; Eyre et al., 2001; Heald et al., 1993; Turton and Lemon, 1999; Turton et al., 1996), triceps (Heald et al., 1993), deltoid (Turton and Lemon, 1999; Turton et al., 1996), pectoralis major (Eyre et al., 2001; Heald et al., 1993) (also see our study in chapter 4) with more thorough investigation hampered by the heightened motor threshold post-stroke (Cicinelli et al., 2003; Cicinelli et al., 1997; Traversa et al., 1997; Turton et al., 1996). Even with background contraction, some proximal muscles are unavailable for study with single pulse TMS in moderate to severely impaired stroke subjects. These patients, in whom study is arguably needed the most, are often unable to provide background contraction. In addition, more recent studies have focused on the role of the ipsilateral descending motor pathways in recovery, which also have high thresholds (Netz et al., 1997; Turton et al., 1996). To overcome these high thresholds for single pulse motor activation and to enable the study of paretic muscles at rest as



well as the study of multiple muscles at once, this study is aimed at investigating the technique of paired pulse TMS in the stroke population. Using two pulses of the same intensity has been shown to intensify subliminal or nonexistent responses to single pulse TMS through temporal and spatial summation at the spinal as well as facilitation at the cortical levels (Nakamura et al., 1995). These studies have shown that an ISI of 10-50 ms with pulses of high stimulation intensity produce facilitatory effects in healthy controls in both hand (Abbruzzese et al., 1999; Chen et al., 1998; Claus et al., 1992; Kujirai et al., 1993; Valls-Sole et al., 1992) and biceps brachii (Abbruzzese et al., 1999; Chen et al., 1998). To date, this technique has not been investigated for its effectiveness in shoulder muscles of healthy subjects or in any muscles in the stroke population. Anatomical studies have shown that the proximal limb receives less corticospinal projections and may receive greater brainstem input than distal muscles (Kuypers, 1964) which could affect the mechanism involved in paired pulse TMS facilitation. Furthermore, facilitation may not occur after stroke because damage may have occurred in the pathways involved in paired pulse TMS facilitation. In this study, we investigated the optimal interstimulus interval (ISI) for facilitation of thirteen upper limb muscles in stroke and healthy subjects using high intensity paired pulses aiming at determining a single ISI that could be used to study both healthy and stroke subjects in comparative studies. Differences between facilitation of distal and proximal muscles were also investigated. Finally, the onset latency of the TMS response at the optimal ISI was calculated as a means to identify the descending pathway employed in paired pulse TMS. Parts of this work have appeared in abstract form (Schwerin and Dewald, 2003).

## 5.2 Materials and Methods

### 5.2.1 Subject Selection

Eight stroke patients (age:  $60.75 \pm 12.76$  years, 6 male) with unilateral hemiparesis (see table 1) and six controls in the same age range (age:  $57.50 \pm 9.85$  years, 5 male, 4 right hand dominant) were tested. Stroke patients were more than one year post-stroke ( $7.88 \pm 6.90$  years) and were moderately to severely impaired as determined by the Fugl-Meyer upper limb assessment (Fugl-Meyer et al., 1975). A neuroradiologist identified the lesion locations from anatomical MRIs acquired specifically for this study. All subjects were recruited from the stroke database at the Sensory Motor Performance Program within the Rehabilitation Institute of Chicago. Written informed consent was obtained from all subjects. The Institutional Review Board at Northwestern University approved the experimental protocol.

**Table 5-1** Clinical data for hemiparetic stroke participants

Participant	Gender	Age (years)	Years Since Onset	FMA <sup>a</sup>	Original Handedness	Lesion Location (hemisphere: structures)
S1	M	46	3	11	R	L: motor cortex, corona radiata, insula, basal ganglia, internal capsule
S2	M	61	23	13	R	R: thalamus, PLIC <sup>b</sup>
S3	M	58	5	24	R	R: thalamus, posterior putamen, PLIC <sup>b</sup>
S4	M	49	10	26	R	R: temporal cortex, insula, thalamus, basal ganglia, genu of the internal capsule
S5	M	75	10	30	R	L: thalamus, PLIC <sup>b</sup>
S6	M	62	1	34	L	R: thalamus, PLIC <sup>b</sup>
S7	F	83	4	35	R	L: thalamus
S8	F	52	7	35	R	L: premotor cortex, caudate, basal ganglia, ALIC <sup>c</sup>

<sup>a</sup>Based on Fugl-Meyer Assessment (FMA) scale (maximum score = 66)

<sup>b</sup>PLIC = posterior limb of the internal capsule

<sup>c</sup>ALIC = anterior limb of the internal capsule

### *5.2.2 Experimental Set-Up*

The subject was supine in a Biodex experimental chair (Biodex Medical systems, Shirley, NY) with the chair back tilted up 25° from horizontal. The torso was secured using restraining straps over the shoulders and another across the waist. The target arm was held in the following configuration: 90° elbow angle, 75° shoulder abduction angle, and 0° shoulder flexion angle. A fiberglass cast was put over the target hand, wrist and forearm and was fixed at the wrist to a stationary base to maintain arm position.

### *5.2.3 Electromyography*

Surface electromyographic (EMG) signals were recorded with active differential electrodes (Delsys, Boston, MA) with a 1 cm inter-electrode distance placed over the muscle belly. The EMG signals were pre-amplified with a gain of 1000 and high pass filtered at 20 Hz. In a second stage, the signals were low pass filtered at 500 Hz (8-pole Butterworth, Frequency Devices Model 9016, Havelhill, MA) and amplified depending on the strength of the signal during maximum muscle contraction to optimize for the range of the amplifier. The amplified EMG signals were then sampled at 1000 Hz and stored on a computer for subsequent analysis. EMG electrodes were placed on thirteen arm muscles including: first dorsal interosseus (FDI), extensor carpi radialis (ECR), wrist flexors in the region of the flexor carpi radialis (WF), biceps brachii (BIC), brachioradialis (BRD), triceps brachii long head and lateral head (TRILO and TRILA), anterior (ADL), intermediate (IDL), and posterior (PDL) deltoids, pectoralis major vertical fibers (PMJ), latissimus dorsi (LAT), and superior trapezius (TPS). Correct electrode placement was

verified by examination of EMG activity using methods described by Kendall et al. (1983). After EMG electrode placement, maximum voluntary contraction of each arm muscle was collected for normalization purposes. During TMS application, the muscles were at rest and were monitored for activity prior to data collection. In order to analyze the effect of muscle group (i.e., proximal vs. distal) on the optimal ISI, muscles were divided into four groups: hand/wrist (FDI, WF, ECR), elbow (BRD, BIC, TRILO, TRILA), shoulder (ADL, IDL, PDL) and trunk (PMJ, TPS, LAT).

#### *5.2.4 Transcranial Magnetic Stimulation*

TMS was performed with a thinly coated 70 mm diameter figure-of-eight coil connected to a magnetic stimulator (Magstim 250, Magstim, U.K.) with a maximal field strength of 1.97 Tesla. A 1 cm grid on the scalp surface was examined for the optimal ipsilateral and contralateral site using a 25 ms interstimulus interval (ISI) and 100% stimulator intensity while the subject was at rest. The center of the coil (3 cm posterior to the anterior bifurcation of the external coating) was positioned tangential to the head at each site with the handle at 30° from the parasagittal plane. In an effort to keep the subject awake and alert, a movie was shown during TMS stimulation.

#### *5.2.5 Optimal Stimulation Site Exploration*

TMS was performed at a single site to minimize experimental time and to enable us to gather data for this large number of upper limb muscles. Instead of stimulating at each muscle's hotspot, we found an optimal stimulation site where all the muscles being investigated could be

activated to at least 1% of maximum voluntary contraction. If any muscles could not be activated from any point on the scalp, an optimal site was found for the subset of muscles that could be activated. Since the proximal muscles have higher thresholds, the optimal site was closer to their true hotspot than it was to the distal muscles. However, by using 100% stimulation intensity we maximized our chances of activating all of the target muscles at a single site by taking advantage of current spread (Thickbroom et al., 1998). In further support, TMS maps of muscles in the upper limb are largely overlapping (Devanne et al., 2006). Since this study is looking at a relative change in the magnitude of the response due to different ISIs and not the actual magnitude, this method was deemed acceptable. If multiple sites could elicit responses in all the target muscles, then we lowered the stimulation intensity until only one site met our criteria and employed that site for the experiment. Two or more locations where different groups of muscles could be activated was not encountered in this study.

#### *5.2.6 ISI Investigation*

The stimulating coil was held in place at the optimal site with a multi-jointed arm attached to the Biodex Chair. Single pulse and paired pulse at ISI = 1, 3, 5, 8, 10, 12, 15, 20, 25, 30, 40, 50, 60, 70, 80, 99.9 ms were applied randomly with six sequential trials recorded for each ISI. The intensity of each of the paired pulses was 100% of the stimulator output.

#### *5.2.7 Experimental Sessions*

In stroke subjects, the contralateral projections from the lesioned hemisphere and non-lesioned hemisphere as well as the ipsilateral projections from the non-lesioned hemisphere were studied

on three separate occasions. In controls, the contralateral projections from the left and right hemispheres were studied on two separate days, with a search for ipsilateral activity from each respective hemisphere at the end of each day. If ipsilateral activity was found for any of the muscles, it was investigated in detail on a third occasion. For analysis, there were six subject/projection types: control right hemisphere stimulation (Right), control left hemisphere stimulation (Left), control ipsilateral stimulation (Ipsilateral), stroke non-lesioned hemisphere stimulation (Non-Lesioned), stroke lesioned hemisphere stimulation (Lesioned) and stroke ipsilateral stimulation (Ipsilateral).

### **5.3 Analysis**

Compared to the response obtained with single pulse TMS, the optimal ISI must 1) lead to a higher occurrence of motor evoked potential, 2) result in a larger magnitude response and 3) be consistent across different muscle/subject groups. The MEP analysis for each criteria is described below. For criteria 1 & 2 we selected a range of best ISIs in order to facilitate getting a single (or small range) optimal ISI after applying criteria 3.

#### **5.3.1 Motor Evoked Potential Occurrence**

Data were analyzed off-line using custom software developed in Matlab (Mathworks, Inc., Natick, MA). For a single trial, the occurrence of a motor evoked potential (MEP) was determined by visually inspecting the single trial in comparison to an overlay of all six trials. Specifically, we investigated two indices: optimal ISI range for MEP occurrence and the gain in

MEP occurrence. We defined an optimal ISI range for MEP occurrence across subjects and muscles as the range of ISIs in which the MEP occurrence is no less than 25% of the occurrence rate of the highest resulting occurrence across ISIs. The gain in MEP occurrence ( $\text{gain}^0$ ) attributed to the paired pulse technique was defined as the occurrence rate for a particular ISI divided by the occurrence rate with single pulse stimulation:

$$\text{gain}^0 = \text{Occurrence}_{\text{ISI}} / \text{Occurrence}_{\text{SINGLE}}$$

### 5.3.2 *MEP Magnitude*

The six unrectified trials for an individual subject/muscle were ensemble averaged and the peak-to-peak magnitude of the MEP was calculated. If one MEP was observed, the peak-to-peak of that response was calculated. If two distinguishable MEPs occurred, the peak-to-peak was calculated for the second response. If two indistinguishable responses occurred, the peak-to-peak of the fused response was measured. Since each subject and muscle combination has a different motor threshold and therefore may respond more or less than another muscle or person at any specific ISI simply because of the relationship between its threshold and the stimulation intensity, we normalized each muscle's response within subject to its respective highest magnitude response across all ISIs, such that the best ISI has a magnitude of 1. The normalized responses were averaged across subjects/projection types. We then defined the range of optimal ISIs for achieving the highest magnitude responses within each subject/projection type as the range in which the ISI produced responses that were significantly greater than the single pulse response but were not significantly different from the greatest magnitude response across ISIs. A t-test with the .05 level was used to test for significance. We quantified the gain in magnitude

( $\text{gain}^M$ ) by dividing the largest magnitude response across ISIs ( $\text{Magnitude}_{\text{MAX}}$ ) by the magnitude of the response with single pulse stimulation:

$$\text{gain}^M = \text{Magnitude}_{\text{MAX}} / \text{Magnitude}_{\text{SINGLE}}$$

### **5.3.3 Muscle Groups**

The magnitude of response within muscle groups was analyzed to investigate differences in the distal/proximal nature of the results. The nonparametric Kolmogorov-Smirnov goodness of fit test was used to determine if the ISI response curve distributions for each muscle group were significantly different from one another and to determine if there were differences for a muscle group between subject group/projection type.

### **5.3.4 MEP Latency**

The latency was determined for the single pulse response and the optimal ISI response. If a single response was observed, the latency to that response was used. If two responses were observed, the latency to the second response was used. If two responses were observed, but they were not clearly distinguishable, the latency to the initial response was employed for subsequent analysis.

## **5.4 Results**

### **5.4.1 Optimal Stimulation Site**

The optimal stimulation site was always in either the primary motor cortex or premotor cortex for all subject group/projection types (see figure 5.1). There was not a consistent shift across



subjects in the location of the ipsilateral projection site in the non-lesioned hemisphere compared to the contralateral projection site.

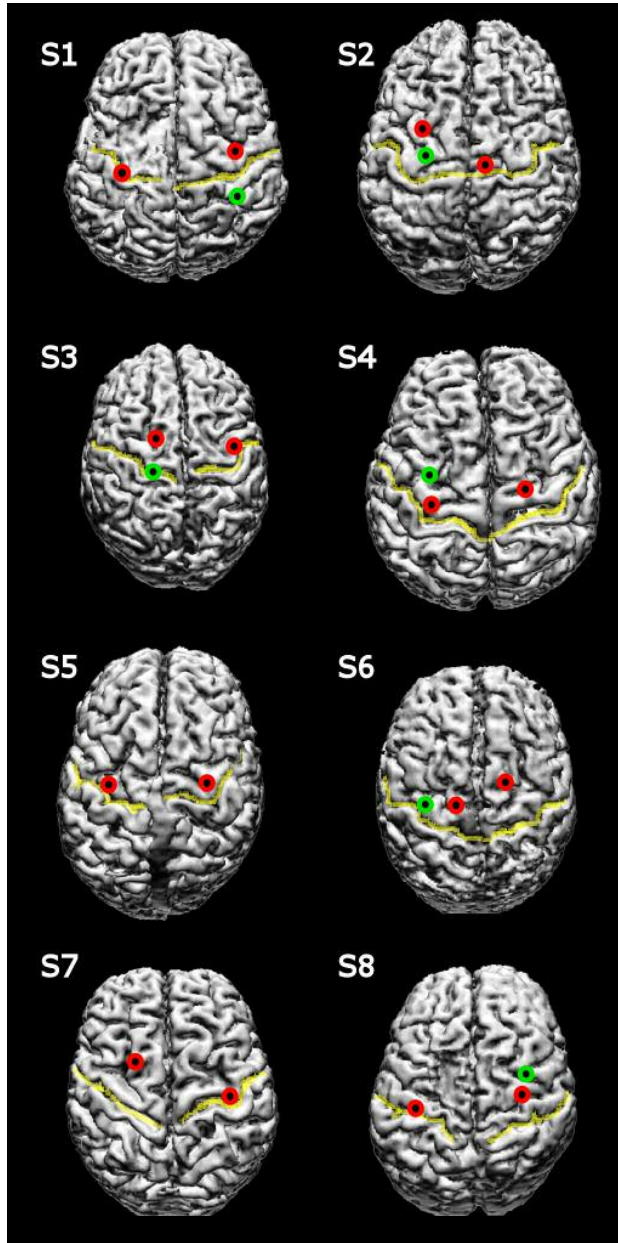


**Figure 5-1 Stimulation sites.** The optimal stimulation site in stroke subjects. The central sulcus is highlighted in yellow. The contralateral optimal site is shown in red for both hemispheres. In subjects where responses to stimulation of the ipsilateral hemisphere to the paretic arm were recorded, the optimal ipsilateral site is shown with a green circle.

### 5.4.2 Raw Data

Figure 5.2 shows examples of MEPs elicited in both control and stroke subjects using either single or paired pulse TMS in the anterior deltoid muscle. In the more distal muscles, 2 responses (one to the first stimulus and one to the second stimulus) were more often recorded in the control subjects as well as in the non-lesioned hemisphere. Two responses were rare when stimulating the ipsilateral cortex regardless of muscle.

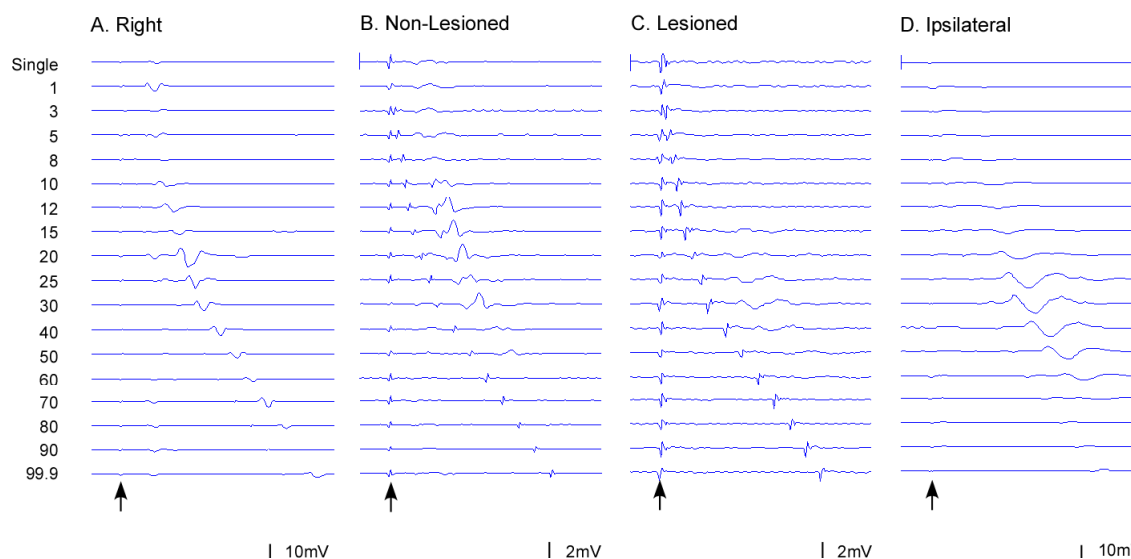


**Figure 5-2 Raw data.** Effect of TMS dual pulse stimulation compared to single pulse stimulation exemplified in the anterior deltoid muscle following stimulation of the control right hemisphere (A), the stroke non-lesioned hemisphere (B), the stroke lesioned hemisphere (C) and the stroke ipsilateral hemisphere to the paretic arm. The arrows indicate the time-point of the first stimulus. Note the different mV scales for each graph. In the right and non-lesioned hemisphere paired pulse promotes facilitation at shorter ISIs than in the lesioned and ipsilateral hemispheres. Also, the magnitude of the response in the non-lesioned and lesioned hemispheres is much smaller than for the right or ipsilateral hemispheres.

### 5.4.3 Occurrence

In the control group, a wide range of ISIs consistently evoked contralateral MEPs (cMEPs) across all muscles (see figure 5.3A and B). With stimulation of the right hemisphere, ISIs of 8-40 ms almost doubled ( $\text{gain}^0 = 2.36$ ) the occurrence of cMEPs compared to the single pulse stimulation and were within 25% of the best ISI (20 ms). In the left hemisphere, ISIs of 3-50 ms were within 25% of the best ISI (20 ms) with a  $\text{gain}^0$  of 1.70. Occurrence levels were high at the best ISI for the control contralateral hemisphere stimulation (Right hemisphere = 95% at 20 ms ISI, Left hemisphere = 94% at 20 ms ISI). Ipsilateral MEPs (iMEPs) were rare in the control group muscles with any ISI. As such, the control ipsilateral results were excluded from further analysis. In the stroke group, the cMEP occurrence resulting from stimulation of the non-lesioned hemisphere was similar to the control group results (see figure 5.3D), with a range of 8-50 ms and the best ISI of 25 ms (occurrence = 95%) and a  $\text{gain}^0$  of 2.23. However, for the lesioned hemisphere (see figure 5.3E), the likelihood of evoking a response decreased drastically (best ISI occurrence = 46.20%), while the range of optimal ISIs was similar (12-50 ms). The best ISI was 30 ms with a  $\text{gain}^0$  of 2.22. The ipsilateral response in the paretic arm was rare with single pulse stimulation (3.77%), but reached a greater occurrence level (56.58%) than even the paretic cMEPs at the 30 ms ISI, with a  $\text{gain}^0$  of 15.01 over the single pulse occurrence (see figure 5.3F). Unlike the contralateral responses in both the control and stroke, the ipsilateral response prevalence across ISIs in the paretic arm was narrow (25-40 ms) and peaked at 30 ms.

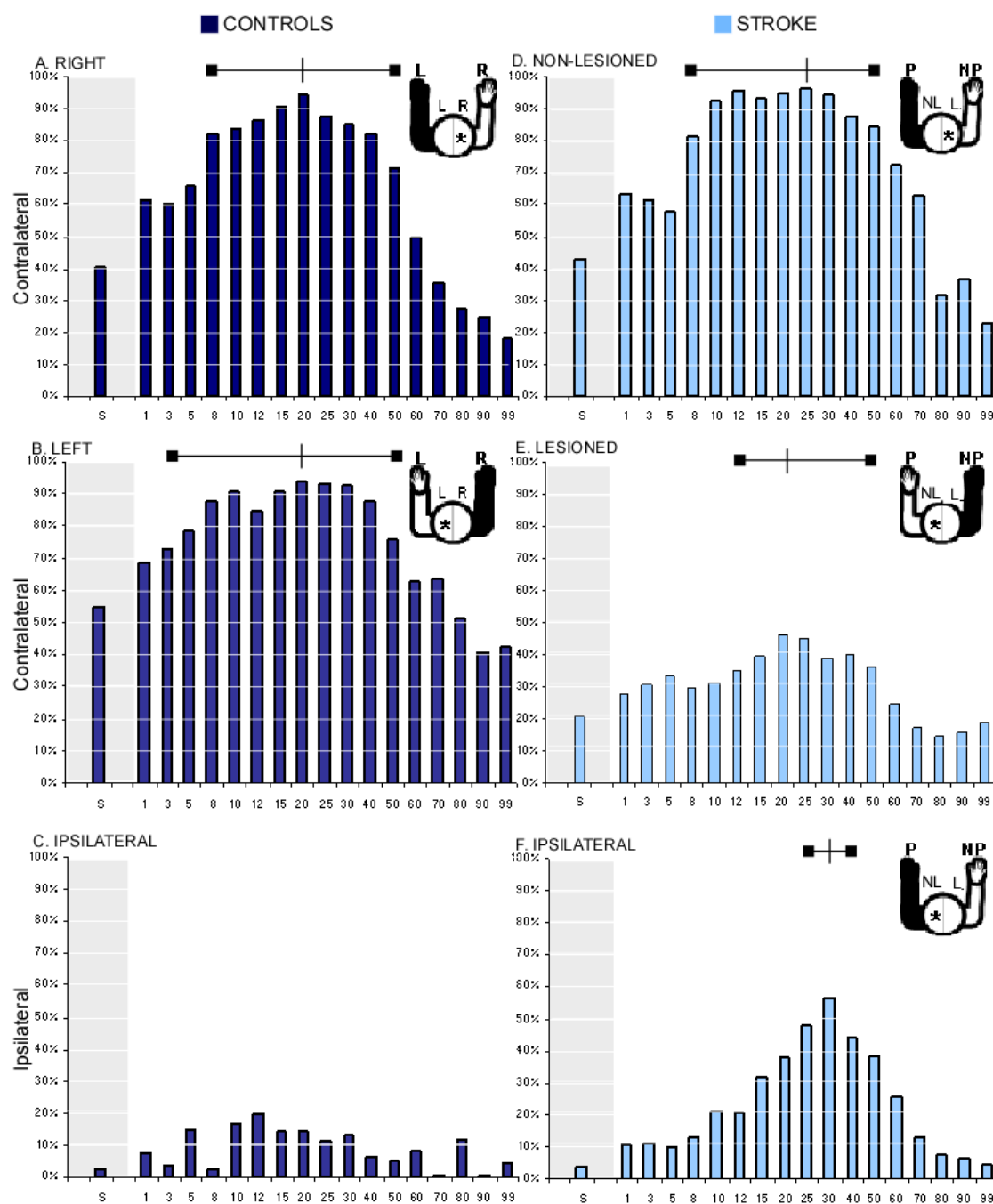


**Figure 5-3 Occurrence.** Percentage of trials where an MEP was evoked for both single and paired pulse stimulation in both control (A-C) and stroke (D-F) groups. The figure in the upper right shows which arm is being recorded from and which hemisphere is being stimulated. Paired pulse using any ISI increased the occurrence rate compared to single pulse. Very few responses were observed in the control ipsilateral stimulation and is excluded from further analysis. The range of ISIs with occurrence rates within 25% of the max occurrence rate are shown by the bar at the top of each graph. Ipsilateral responses in the paretic arm had the highest rate of occurrence around 30ms with a very narrow range.

#### **5.4.4 Magnitude**

Similar to the occurrence results, the ipsilateral MEP magnitudes in the paretic arm were greatest in a range of ISIs centered at 30 ms. (see figure 5.4F). The ISIs of 15-50 ms all produced responses significantly larger than with the single pulse and not significantly different from the response at 30 ms. This range is shifted slightly to the right compared to the range observed in the control right (8-40 ms) and control left (10-30 ms) and stroke non-paretic (8-25 ms) but was similar to the stroke paretic range (20-40 ms). The gain in magnitude at the best ISI over single pulse for ipsilateral stimulation in stroke was quite large (68%) compared to the control results (right = 6%, left = 5%) and the contralateral responses in stroke with stimulation of the non-lesioned hemisphere (4%) or the lesioned hemisphere (3%).

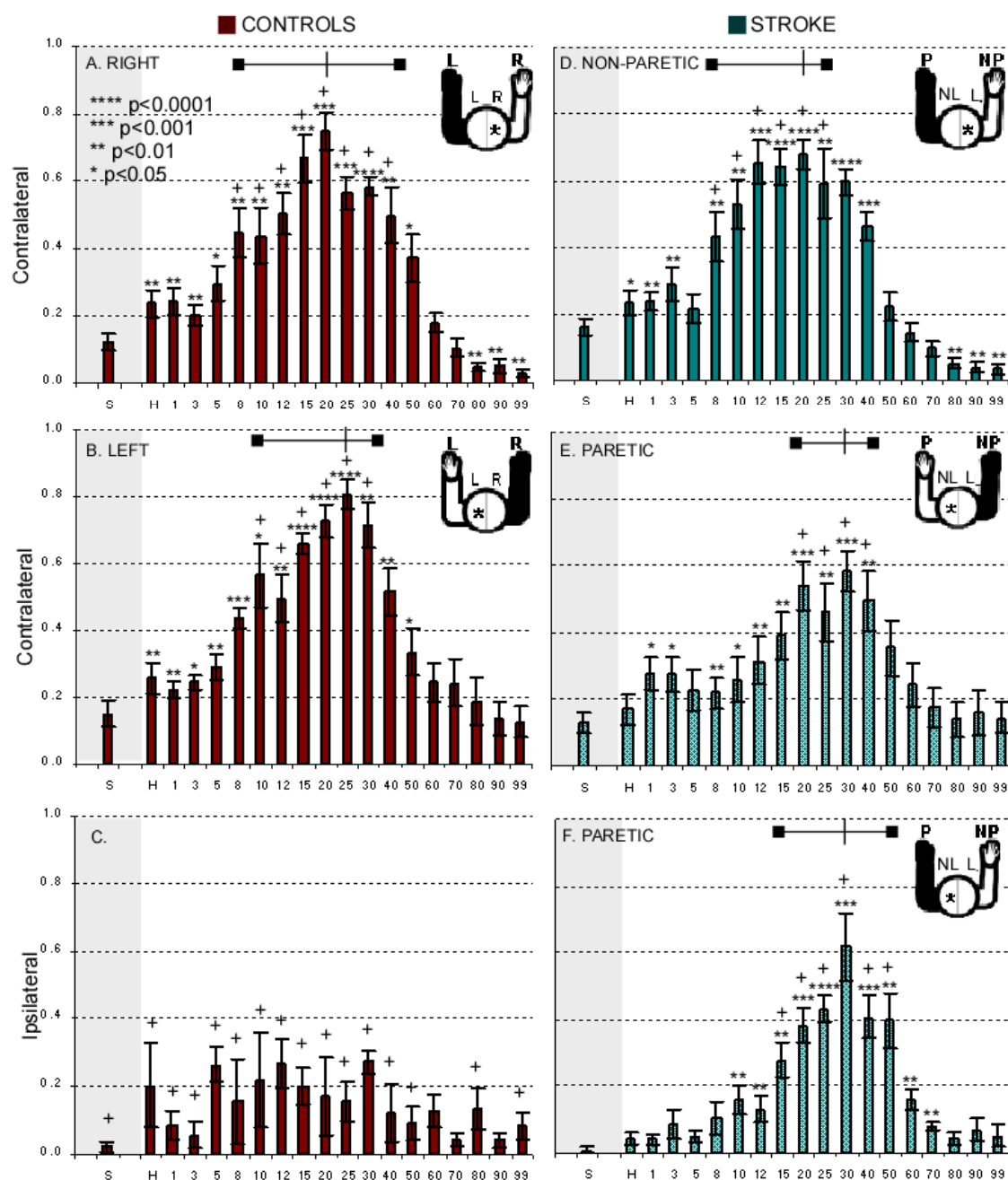


**Figure 5-4 Magnitude.** Normalized magnitude of MEPs across control (A-C) and stroke (D-F) groups. Asterisks denote responses that were significantly different in magnitude from the single pulse stimulation responses. Plus signs denote the responses that were not significantly different from the maximal response for that subject group/projection ( $p < .05$ ). The range of ISIs that produced responses that were significantly greater than the single pulse response but were not significantly different from the greatest magnitude response across ISIs are shown by the bar at the top of each graph. The figure in the upper right shows which arm is being recorded from and which hemisphere is being stimulated.

#### 5.4.5 *Muscle Groups*

The Kolmogorov-Smirnov test did not show a significant difference in the ISI response curve distributions between muscle groups within each subject/projection type (see figure 5.5). At the .05 level of significance there was a significant difference in the hand/wrist muscles between the stroke ipsilateral projection response curve and each of the other subject/projection types (left:  $p < .0001$ ; right;  $p = .004$ ; non-lesioned:  $p = .0001$ ; lesioned:  $p < .0001$ ) and between control left and stroke lesioned curves ( $p = .039$ ). In the elbow muscle group there was a significant difference between control left and stroke ipsilateral curves ( $p = .039$ ) and stroke lesioned and stroke ipsilateral curves ( $p = .014$ ). In the shoulder muscle group there was a significant difference between the stroke ipsilateral and the control left curves ( $p = .039$ ). There was no statistical significant difference between subject/projection type ISI response curves for the trunk muscle group.

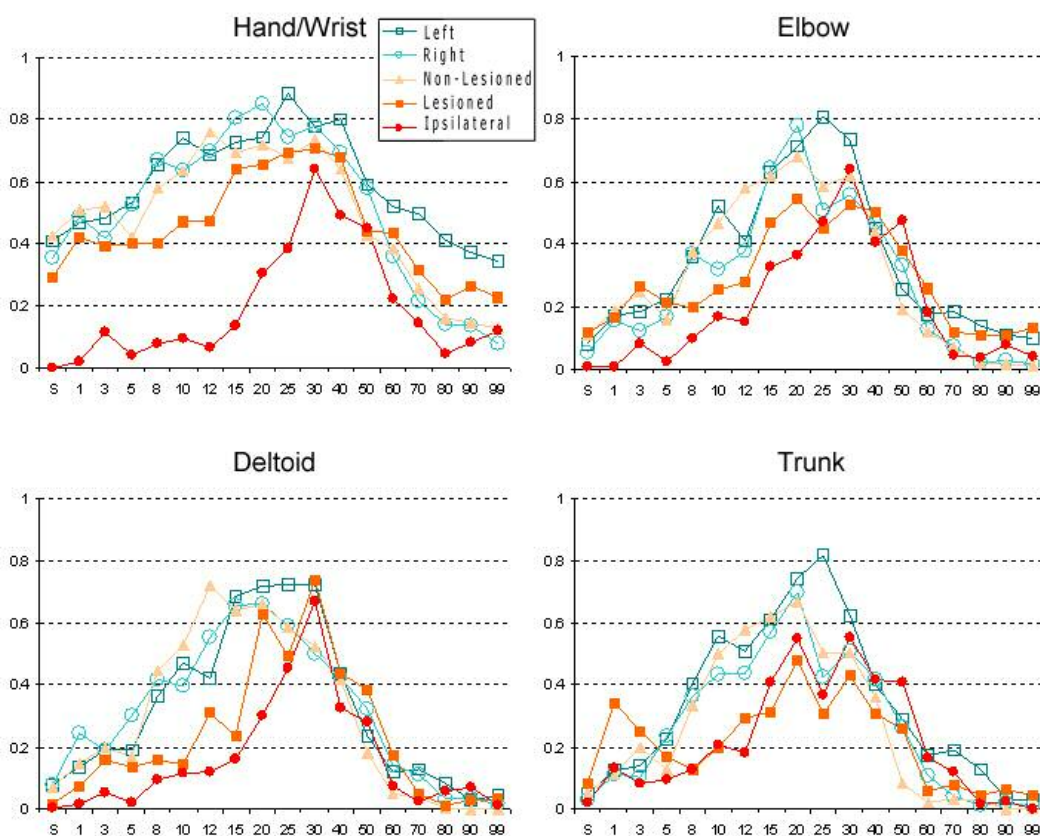


**Figure 5-5 Muscle groups.** ISI response curves plotted for muscle groups. The normalized magnitude of the response at each ISI was averaged across the muscles in each group. Note how the curves are more narrow in the more proximal muscles and also for the stroke ipsilateral projection.

#### 5.4.6 Onset Latency

Within each muscle group there was no significant difference in the onset latencies between the left and right hemispheres of control subjects. The non-lesioned hemisphere responses were not significantly different in onset from the control responses. The lesioned hemisphere responses in the hand/wrist muscles were significantly delayed compared to the non-lesioned hand/wrist responses (5.08 ms  $\pm$  1.49 ms). The ipsilateral responses in the hand/wrist, elbow and trunk muscle groups (but not shoulder) were all significantly delayed (hand/wrist: 22.35 ms  $\pm$  7.13



ms; elbow: 15.80 ms +/- 0.95 ms; trunk: 8.16 ms +/- 3.27 ms) compared to the non-lesioned hemisphere responses, but not to the lesioned hemisphere responses.

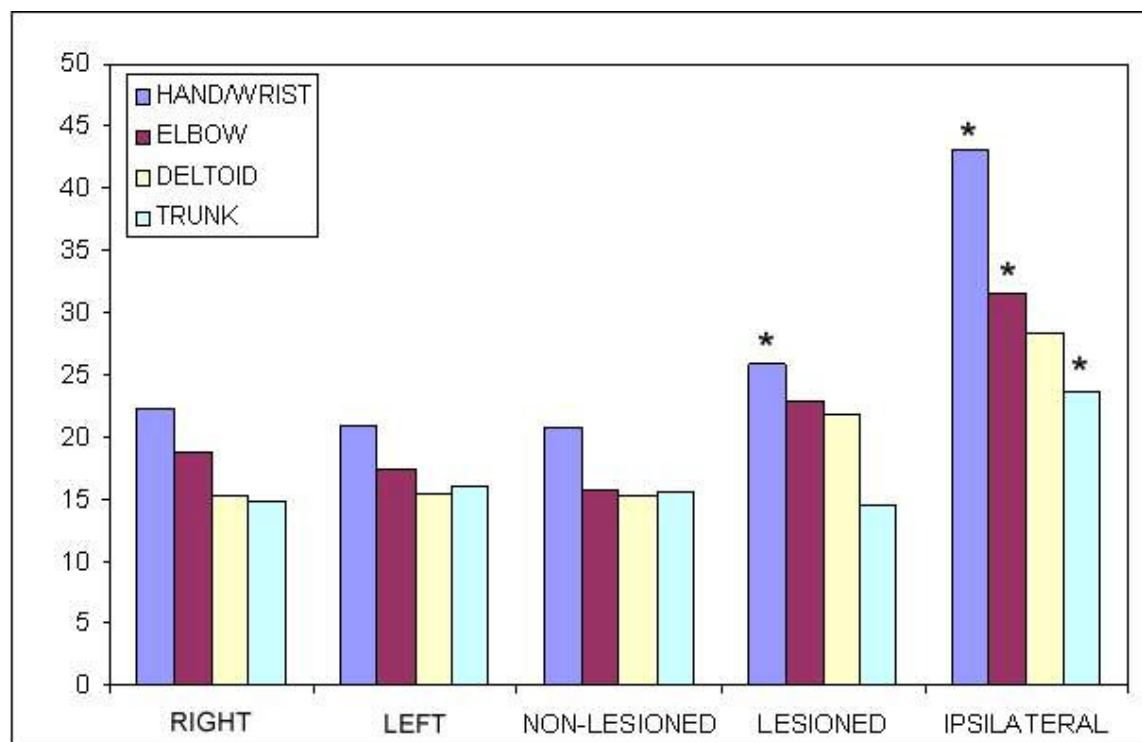


**Figure 5-6 Latency.** The contralateral responses elicited from the lesioned hemisphere showed a trend towards a delay in onset compared to the non-lesioned hemisphere cMEPS while the ipsilateral MEPs in the paretic arm were significantly delayed in the hand/wrist, elbow, trunk but not shoulder muscle groups. There was no significant difference in onset latencies between the control RIGHT and LEFT responses, the control and stroke non-lesioned responses, or the between the lesioned and ipsilateral responses.

## 5.5 Discussion

The use of high intensity paired pulses drastically increased the occurrence of cMEPs and iMEPs in the paretic limb as well as caused the greatest facilitation in all muscle groups. The iMEPs had the most narrow range of optimal ISIs. The greatest facilitation of the magnitude of ipsilateral MEPs occurred at 15-50 ms and the best range for optimal occurrence was 25-40 ms. Therefore the optimal ISI range, taking into account both the occurrence and magnitude ranges,

for the *ipsilateral* projections is 25-40 ms. The optimal range for occurrence with stimulation of the lesioned hemisphere was 20-40 ms and the optimal range for facilitation was 12-50 ms, resulting in an optimal ISI range for the *contralateral* projections of 20-40 ms. Therefore the optimal range for studying the paretic limb across projection type was 25-40 ms. The contralateral MEPs in the non-paretic limb and in the control subjects all had optimal ranges that included the narrower range observed in the paretic limb. Therefore, the best ISI for studies of multiple muscles, or between ipsilateral and contralateral projections to the paretic limb, or between stroke and control groups would be 25-40 ms. This study has provided evidence of the efficacy of paired pulse TMS in eliciting responses in distal and proximal muscles and enables the study of these muscles following stroke whereby previously it was not possible.

### ***5.5.1 Possible Mechanisms of Facilitation at Medium Interval ISIs***

The exact mechanism causing the facilitation at the 25-40 ms ISIs is unknown. At medium latency ISIs of 10-50 ms, facilitation has been observed to occur in healthy subjects with a subthreshold first (conditioning) stimulus paired with a suprathreshold second (test) stimulus, or with both stimuli at threshold or with both stimuli suprathreshold (Abbruzzese et al., 1999; Claus et al., 1992; Nakamura et al., 1997; Valls-Sole et al., 1992). Cervical epidural recordings from the spine show that the volley of descending excitatory potentials (I-waves) produced by two stimuli 25 ms apart is augmented, demonstrating that MEP facilitation with this protocol (with a suprathreshold conditioning stimulus) is at least partly cortical in origin (Nakamura et al., 1997). The increased size and number of I waves in the descending volley most likely results in

temporal and spatial facilitation at the spinal level as well. The excitatory post-synaptic potential in the spinal motoneuron can be prolonged for up to 30 ms by multiple descending volleys (Kernell and Chien-Ping, 1967). In addition to corticospinal volleys, TMS may activate oligosynaptic corticofugal pathways such as corticobulbospinal or corticopropriospinal projections (MacKinnon et al., 2004; Ziemann et al., 1999) which could also contribute to the descending volleys or synapse onto spinal interneurons and result in facilitation. In the MacKinnon et al., study, the medium latency portion of the MEP, occurring 6 ms later than the short latency portion, was attributed to oligosynaptic connections which reach the muscle later than the fast corticospinal projections. Olivier stimulated the medullary pyramid in the macaque monkey and did not record any later peaks in the post stimulus time histogram which would have indicated propriospinal activity, even when using paired pulse TMS (Olivier et al., 2001).

### *5.5.2 Muscle Group ISI Curves*

The magnitude ISI response curve was very similar between the control group and the non-lesioned hemisphere of the stroke group for each of the 4 muscle groups studied. The major difference in the curves was seen in the ipsilateral responses in the paretic limb. In all muscle groups, the responses at the short interval ISIs (1, 3 and 5 ms) as well as for slightly longer ISIs (8, 10, 12, 15 ms) were all suppressed compared to the response at the medium interval ISIs (25, 30, 40 ms). This seems to suggest 1) that both distal and proximal muscles use a similar descending ipsilateral pathway 2) either the mechanism causing facilitation at the short interval

ISIs is disrupted following stroke, or the mechanism does not exist in the ipsilateral descending pathway, or 3) the mechanism causing facilitation at the medium interval ISIs is upregulated following stroke to an extent that the normally sized responses at the short ISIs now appear smaller when normalized to the maximal response across all ISIs. Intracortical facilitation using excitatory cortical circuitry is the mechanism causing the facilitation at the shorter ISIs. Studies have shown that intracortical facilitation in the lesioned hemisphere is not significantly different from the intracortical facilitation observed from the non-lesioned hemisphere (Liepert, 2006). However, a decrease in intracortical facilitation was observed in patients with a lesion in the region of the superior cerebellar artery and therefore may depend on the lesion location (Liepert et al., 2004). Studies of intracortical facilitation of the ipsilateral projection are lacking. However, a decrease in intracortical facilitation in the unaffected hemisphere could be the cause of the relative decrease in magnitude in the ipsilateral projection at the short ISIs. If this were the case, one would expect a concomitant decrease in the magnitude of response at the short ISIs in the contralateral MEPs elicited from the unaffected hemisphere and that is not observed. Therefore, we believe that mechanism involved in facilitation at medium interval ISIs is upregulated after stroke. This would make sense if these responses are the result of activation of an oligosynaptic pathway which is typically suppressed for the most part, but is unmasked or upregulated following stroke. This data supports the theory that ipsilateral responses result from oligosynaptic activation in that the medium latency ISI responses are preserved or upregulated after stroke.

### *5.5.3 Possible Mechanisms for Delayed Onsets of iMEPs Following Stroke*

In general, the ipsilateral responses in the paretic limb were all significantly delayed compared to the contralateral responses in the control group. This agrees with several studies of ipsilateral responses in stroke subjects (Ziemann et al., 1999) and supports the hypothesis that the ipsilateral projections are not uncrossed corticospinal projections or even the result of branching of corticomotoneurons, but oligosynaptic corticofugal projections. Ziemann showed that the ipsilateral MEP in a distal muscle is modulated with neck turn, according to the asymmetric tonic neck reflex which could imply that the reticulospinal tract (which is innervated by neck afferents) is being utilized (Ziemann et al., 1999). Furthermore they ruled out the possibility that the ipsilateral projection runs through the corpus callosum by observing an increase magnitude ipsilateral MEP in a patient with complete callosal agenesis.

It is interesting that the response in the hand/wrist muscle group were also delayed, demonstrating that the ipsilateral pathway involves a common neural mechanism between distal and proximal muscle groups. The ipsilateral projection to the deltoid muscle group was not delayed in this study and could be a result of the small subject size or might represent a different descending pathway. The delay in onset that we report here for the ipsilateral projection suggests that we are activating an oligosynaptic pathway.

## ***5.6 Scientific Implications***

This paired pulse TMS technique allows us to study muscles not accessible with single pulse TMS at rest, and muscles where voluntary activation is difficult as is the case in some stroke subjects. In addition, studying the arm at rest allows for the study of multiple muscles at a time thereby limiting experiment lengths and avoiding fatigue. Also, by applying TMS with all the muscles at rest, there is no question about biasing the results towards the muscles that are abnormally coactivated in hemiparetic stroke subjects when generating volitional forces/torques (Dewald and Beer, 2001; Dewald et al., 1995). The results of this study provide the methodological platform for studying proximal muscles in general and muscles in the paretic limb following brain injury using TMS. This method represents an invaluable tool for studying the changes that occur in the motor system after stroke.

## 6

# **IPSILATERAL AND CONTRALATERAL CORTICOBULBOSPINAL PROJECTIONS INVOLVED IN THE EXPRESSION OF ABNORMAL COORDINATION PATTERNS IN MODERATE TO SEVERE HEMIPARETIC STROKE SUBJECTS**

## ***6.1 Introduction***

Recently, activity in the ipsilateral hemisphere following hemiparetic stroke has been investigated for its role in motor recovery. Several longitudinal studies have shown that early in recovery the ipsilateral (non-lesioned) sensorimotor cortex is hyperactive compared to controls and as recovery progresses activity shifts back to the contralateral (lesioned) hemisphere as determined with transcranial magnetic stimulation (TMS) (Turton et al., 1996) and other brain imaging techniques (transcranial doppler ultrasonography: Cuadrado et al., 1999; functional magnetic resonance imaging (fMRI): Marshall et al., 2000; fMRI: Tombari et al., 2004). However, in cases of poor recovery, the ipsilateral cortex retains control of the paretic arm (electroencephalography: Serrien et al., 2004; TMS: Turton et al., 1996; fMRI: Ward et al., 2003). This has left most investigators wondering: what is the function of the ipsilateral hemisphere in poorly recovered stroke patients? And how does the balance between the contralateral and ipsilateral projections affect movement?

At the same time, moderate to severely impaired stroke subjects exhibit stereotypical problems in voluntary movement coordination (Brunnstrom, 1970; Dewald and Beer, 2001; Dewald et al., 1995). The abnormal coordination is exhibited as either the stronger flexion synergy (shoulder abduction combined with shoulder extension and elbow flexion) or the extension synergy (shoulder adduction combined with shoulder flexion and elbow extension). The mechanisms underlying the constraint in movement are not well understood. Clearly, with the loss of fibers in the fast corticospinal tract occurring with stroke, substitution by remaining neural substrates may be a form of neural plasticity that results and explains the expression of constraining abnormal coordination patterns. For instance, an increased reliance on pre-existing *ipsilateral* fiber projections (i.e., uncrossed corticospinal pathway or a corticobulbospinal pathway, such as the corticoreticulospinal pathway or an increased reliance on corticobulbar *contralateral* pathways) that have been unmasked or upregulated is a clear possibility. The extensive branching of brainstem pathways could be responsible for the obligatory coactivation of muscles thus explaining the synergistic behaviors. TMS studies have shown that the ipsilateral projections have a much longer onset latency supporting the hypothesis that of an increased dependence on oligosynaptic pathways rather than the uncrossed corticospinal pathway. Another question is whether the ipsilateral takeover (in terms of the balance between the strength of the ipsilateral and contralateral projections) is equal between muscles involved in the flexion or extension synergies. Clinical and scientific observations (Ellis et al., 2006) show a stronger expression of the flexion synergy. If this is indeed the case one would postulate that the muscles involved in the flexion synergy will have stronger ipsilateral takeover than other muscles, as well



as a greater increase in onset latency following transcranial magnetic stimulation (TMS). The neurophysiological correlates for such a hypothesis are supported by a recent study stimulating the reticular nucleus of the monkey. This study has shown the facilitation of ipsilateral elbow and shoulder flexors and a suppression of ipsilateral extensors (Davidson and Buford, 2004), similar to the abnormal coordination observed following stroke. In an effort to investigate this possibility in human subjects, we investigated whether asymmetric tonic neck reflexes (ATNR) activated during neck rotation can alter muscle activity during TMS. Afferent activity resulting from neck rotation is expected to affect brain stem nuclei such as reticular nuclei. If TMS evoked muscle responses in response to the ATNR are more significant following stroke then the hypothesis of an increased reliance on cortico-bulbospinal reliance can be supported. Parts of this work have appeared in abstract form (Schwerin and Dewald, 2004; Schwerin and Dewald, 2005).

## ***6.2 Materials and Methods***

### ***6.2.1 Subject Selection***

Eight hemiparetic stroke subjects (age: 58.13 +/- 9.2 years, seven male) participated in the experiments. All subjects experienced a unilateral brain lesion not involving the brainstem at least one year prior to the study (onset: 8.0 +/- 6.82 years ago - (see table 1). All subjects were recruited from the stroke database at the Sensory Motor Performance Program within the Rehabilitation Institute of Chicago. Subjects were selected on the basis of their responsiveness to paired pulse TMS while at rest. We required a palpable TMS evoked response in either the

anterior, intermediate or posterior heads of the deltoid muscle using a 30 ms interpulse interval and up to 100% stimulus intensity. Subjects were moderately to severely impaired as measured by the Fugl-Meyer upper limb assessment score (FM: 24.88 +/- 8.85, range 11-35; maximal score=66) (Fugl-Meyer et al., 1975). The lesion locations varied (six left hemisphere lesions) and were identified by a neuroradiologist using an anatomical MRI acquired specifically for this study. Five healthy control subjects, in a similar age range (age: 53.2 +/- 4.5 years, range: 47-59; three male), also participated and were selected with the same TMS response criteria. Written informed consent was obtained from all subjects. The Institutional Review Board of Northwestern University approved the experimental protocol.

**Table 6-1** Clinical data for hemiparetic stroke participants

Participant	FM <sup>a</sup>	Lesion Location (hemisphere: structure)	Gender	Age (years)	Years Since Onset	Original Handedness
S1	11	L: motor cortex, corona radiata, insula, basal ganglia, internal capsule	M	46	3	R
S2	13	R: thalamus, PLIC <sup>b</sup>	M	61	23	R
S3	24	R: thalamus, posterior putamen, PLIC <sup>b</sup>	M	58	5	R
S4	26	R: temporal cortex, insula, thalamus, basal ganglia, genu of internal capsule	M	49	10	R
S5	26	R: PLIC <sup>b</sup>	M	62	5	R
S6	30	L: thalamus, PLIC <sup>b</sup>	M	75	10	R
S7	34	R: thalamus, PLIC <sup>b</sup>	M	62	1	L
S8	35	L: premotor cortex, caudate, basal ganglia, ALIC <sup>c</sup>	F	52	7	R

<sup>a</sup>Based on Fugl-Meyer scale (maximum score = 66)

<sup>b</sup>PLIC = posterior limb of the internal capsule, <sup>c</sup>PLIC = anterior limb of the internal capsule

### 6.2.2 Experimental Set-Up

The subject was seated in a Biodex experimental chair (Biodex Medical systems, Shirley, NY) and at rest during the experiment. The torso was secured using restraining straps over the shoulders and another across the waist. The target arm was held in the position of 65° shoulder

abduction, 10° shoulder flexion and 90° elbow flexion using a plastic hand/forearm mold attached to a support (see figure 6.1).

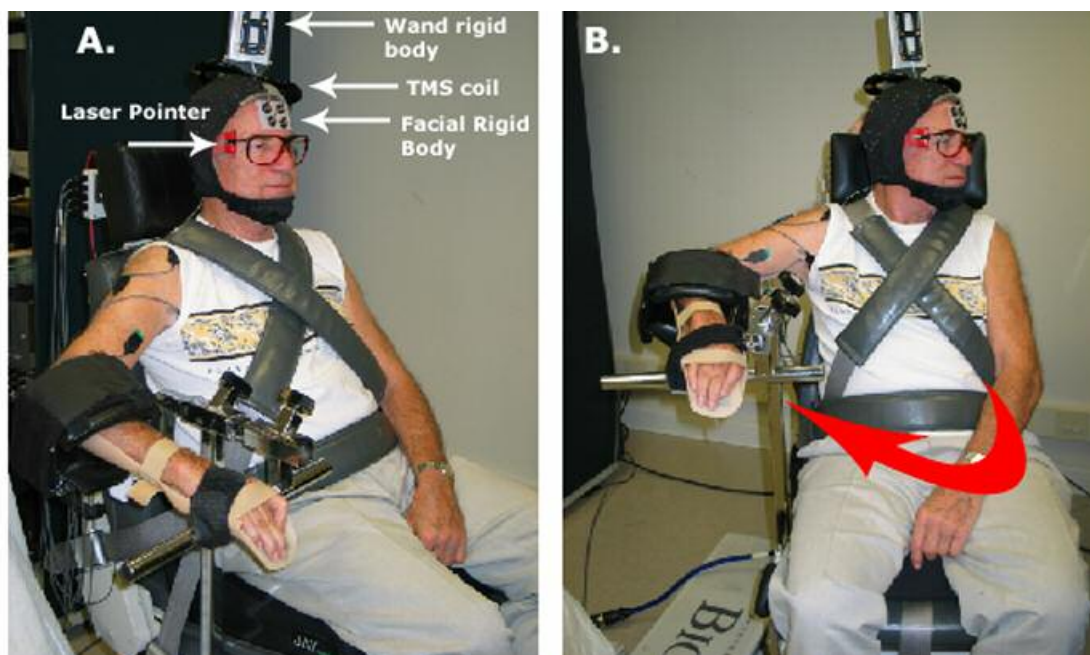


**Figure 6-1 Experimental setup.** A. Laterality was investigated in the chair facing forward position. B. ATNR was tested with the chair turned 75° to the right or left while the head remain stationary. Head position was maintained by the subject by preserving the location of a laser light point on a computer screen in front of the subject. The laser light is attached to the eyeglasses frame. Notice the infrared markers on the facial rigid body and on the TMS stimulating coil.

### 6.2.3 Electromyography

Surface electromyographic (EMG) signals were recorded with active differential electrodes (Delsys, Boston, MA) with a 1 cm inter-electrode distance placed over the muscle belly. The EMG signals were pre-amplified with a gain of 1000 and high pass filtered at 20 Hz. In a second stage, the signals were low pass filtered at 500 Hz (8-pole Butterworth, Frequency Devices Model 9016, Havelhill, MA) and amplified depending on the strength of the signal during maximum muscle contraction to optimize for the range of the amplifier. The amplified EMG

signals were then sampled at 1000 Hz and stored on a computer for subsequent analysis. Eight muscles were examined in each arm. These included the flexor muscles of the hand and wrist at the skin surface location of the flexor carpi radialis (DF-distal flexors) and extensor muscles of the hand and wrist at the skin surface location of the extensor carpi radialis (DE-distal extensors), biceps brachii (BIC), and triceps lateral head (TRI) at the elbow, anterior (ADL), intermediate (IDL), and posterior heads of deltoid (PDL), and pectoralis major vertical fibers (PMJ) at the shoulder. Correct electrode placement was verified by examination of EMG activity on an oscilloscope program while performing muscle testing procedures as described by Kendall and Kendall (1983). After EMG electrode placement, maximum voluntary contraction of each arm muscle was collected for normalization purposes. During TMS application, subjects were asked to maintain their muscles at rest and their activity was monitored immediately prior to data collection. Muscles were divided into the flexion synergy muscles (DF, BIC, IDL, PDL) and the extension synergy muscles (DE, TRI, ADL, PMJ) based on previously reported results for the flexion synergy (where BIC, IDL, PDL were reported in: Dewald et al., 1995), and DF) and the extension synergy (where ADL is assumed because shoulder flexion was reported in combination with shoulder adduction and elbow extension in: Dewald and Beer, 2001; where TRI, PMJ were reported in: Dewald et al., 1995) and DE). For comparison, joint flexor muscles (DF, BIC, ADL) were compared with joint extensor muscles (DE, TRI, PDL) and distal muscles (DF, DE) were compared with the more proximal elbow (BIC, TRI), shoulder (ADL, IDL, PDL) and trunk (PMJ) muscles.

#### **6.2.4** *Transcranial Magnetic Stimulation*

Transcranial magnetic stimulation (TMS) was performed with a 70 mm figure-of-eight shaped coil connected to a MagStim Model 250 stimulator (MagStim 250, MagStim Inc). The coil was held at a 30 degree angle with reference to the interhemispheric fissure and was oriented to produce currents in a posterior-to-anterior direction. A point (TMS coil stimulation point) on the bottom of the coil that was 3 cm posterior to the anterior divergence of the two loops of the coil was used to line up the coil with the stimulation sites. Paired pulse transcranial magnetic stimulation with a 30 ms inter-stimulus interval and 100% stimulator intensity was applied at each stimulation site. In a previous study, we found the 30 ms ISI to be optimal for eliciting MEPs using paired pulse TMS in both distal and proximal muscles from both control, stroke contralateral and stroke ipsilateral hemispheres (see chapter 5). Six stimuli were applied consecutively at each site. In an effort to keep the subject awake and alert, a movie was shown during TMS stimulation.

#### **6.2.5** *TMS Stimulation Grid Generation and MRI Co-Registration*

Laterality and the effects of ATNR were tested in this study by applying TMS at each muscle's specific hotspot on both the contralateral and ipsilateral hemisphere to the paretic arm (left arm in control subjects). The hotspot was defined as the stimulation site resulting in the largest ensemble averaged peak-to-peak motor evoked potential in the target muscle. A 1 cm spaced grid on the scalp surface was investigated to locate each hotspot. The subject specific grid was generated using the subject's anatomical MRI. MR imaging was performed on a 1.5 T

superconducting magnet. A T1-weighted, 3D standard gradient echo sequence with a sagittal slice orientation was used. The field of view was 256 mm, yielding a slice thickness of 1.0 mm.

Curry neuroimaging software (CURRY neuroimaging software package Philips Research, Hamburg, Germany) was used to process the MRI and create a surface mesh of the head surface. Orthogonal axial, coronal and sagittal planes were generated using the surface landmarks (nasion, inion, left and right pre-auricular points): the sagittal plane was defined by the nasion and inion and the longitudinal fissure, the coronal plane by the pre-auricular points, and the axial plane was the plane perpendicular to the other two, positioned superior to the ears. The Cz was defined as the skin surface location of the intersection of the sagittal and coronal planes. The grid points were defined as the skin surface locations of the intersection of 1 cm spaced planes parallel to the coronal and sagittal planes. The grid continued along the skin surface down to the axial plane. Grid points lying above the primary motor cortex, somatosensory cortex, and premotor cortex were chosen as stimulation sites for the experiment. From the Cz, this generally corresponded to a lateral skin surface distance of 6 cm, an anterior distance of 3 cm and a posterior distance of 3 cm for a total of 30-60 stimulation sites for each hemisphere.

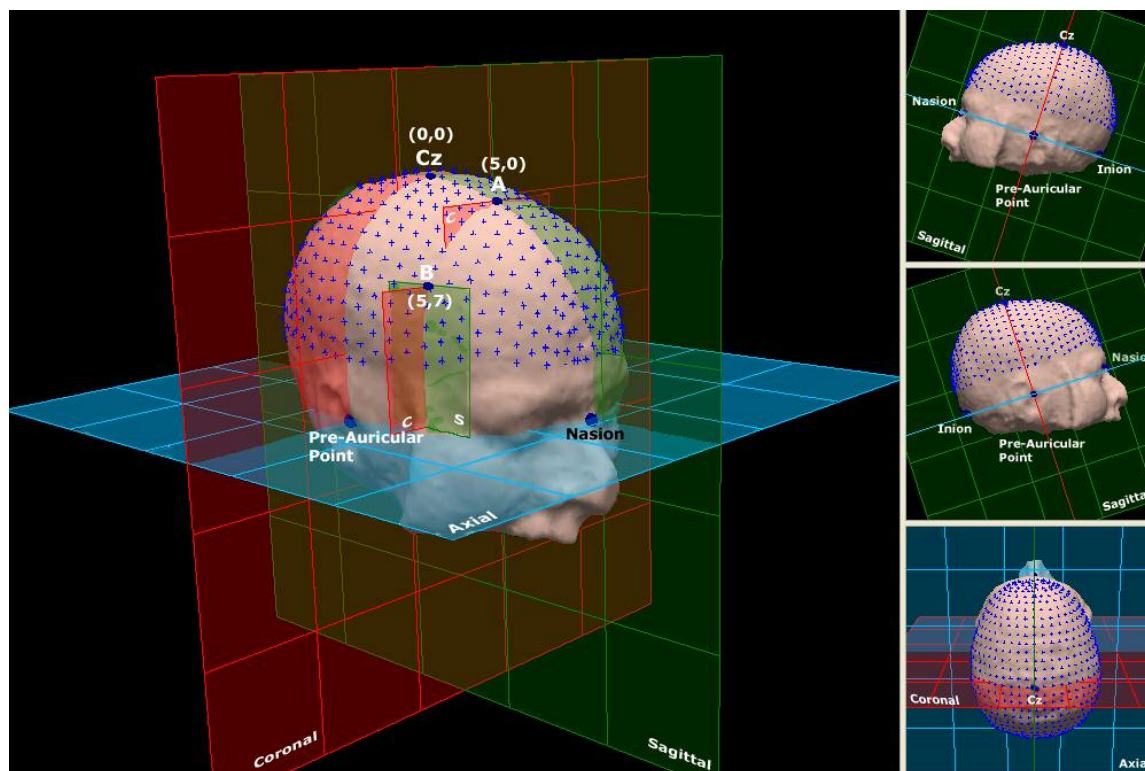


**Figure 6-2 Planes used to generate stimulation grid.** The Cz is the intersection point on the scalp of the coronal and sagittal planes. Successive 1 cm gridpoints were determined by the scalp location where planes parallel to the coronal and sagittal planes intersected. Point A is the intersection of the sagittal plane and a plane parallel to the coronal plane and 5 cm anterior it. Point B is the intersection of that same parallel coronal plane and a plane that is parallel to the sagittal plane but 7 cm lateral to it.

On the day of the experiment, each subject's head was coregistered with the MRI using the surface landmarks. A best least-squares fit method was used to create a transformation matrix between the subject's head and MRI coordinate systems.

During the experiment, the spatial location and orientation of the stimulating wand was tracked using a motion analysis system (OptoTrak 2010, Northern Digital, Inc., City State) to allow specification of the exact coordinates of each stimulation site. The 3D coordinates of infrared light emitting diodes (IREDS), placed on the stimulating wand and on the head of each subject

were recorded and transformed online using custom software to generate the 3D coordinates of the TMS coil stimulation point in each subject's coordinate system as defined by the anatomical landmarks (see above). The custom software also used the transformation matrix generated above to guide the localization of the wand to the individual points on the stimulating grid and oriented tangential to the head surface and at a 30 degree angle with reference to the interhemisphere fissure. The location of the stimulating wand in reference to the head and each angle was recorded during each stimulus for offline analysis. This allowed for interpretation of TMS results from each stimulation site based on the subject's specific brain anatomy (for a full description regarding the grid generation using the MRI, coregistration of the subject's head with the MRI and the program developed to guide the stimulating wand to a gridpoint and save the location, and the coregistration of the stimulation points back onto the MRI, please see the Appendix).

#### **6.2.6** *Grid Testing*

On Day One, first the grid over the contralateral and then the ipsilateral hemisphere was randomly stimulated, with six stimuli applied consecutively at each site. The grid was analyzed after the experiment was completed. The hotspot was defined as the grid site resulting in the ensemble averaged largest peak-to-peak motor evoked potential in the target muscle.

#### **6.2.7** *Laterality and ATNR Testing*

On Day Two, laterality and the effects of ATNR were tested. Because reliability of the optimal site, or hotspot, has not been shown conclusively across days (Wolf et al., 2004), on the second



day the sites immediately surrounding the hotspot, as well as the hotspot were stimulated 3 times each and the site with the largest average response was used. The strength of the ipsilateral and contralateral projections to each muscle was investigated by stimulating the specified hotspots six times with the subject looking straight forward (ST). The effects of the asymmetric tonic neck reflex (ATNR) on MEPs evoked by either contralateral or ipsilateral TMS were studied by rotating the Biodex chair 75° to the left or to the right while subjects maintained the straight forward head position. Subjects preserved head position during the 75° trunk rotation by aiming a laser light attached to eyeglasses onto a computer screen directly in front of them. The conditions were labeled either toward (TO) or away (AW) depending on the position of the head looking toward the target arm or away from it. The six stimuli were applied consecutively at each site with 30 ms between each stimulus. For each muscle, the contralateral and ipsilateral sites were stimulated first in the ST position, then in the TO position, and then in the AW position.

## **6.3 Analysis**

### **6.3.1 Laterality**

The peak-to-peak of each trial was calculated within a 100 ms window following the second pulse and then averaged. The strength of the contralateral (C) and ipsilateral (I) projections, as indicated by the magnitude of the peak-to-peak measurement, to each of the target muscles in the paretic limb (left limb in controls) were compared by calculating a laterality index (LI):

$$LI = (C - I) / (C + I)$$

If each of the projections resulted in EMG responses with a peak-to-peak of equal sizes, then LI = 0. If there was only a measurable contralateral response the LI = 1 and LI = -1 if there was only an ipsilateral response. For each muscle the LI was averaged across subjects and comparisons were made between stroke and control subjects using a paired t-test.

### **6.3.2** *Correlation with Recovery Level in Stroke Subjects*

The correlation between the laterality index and the Fugl-Meyer score was tested using the non-parametric Spearman's correlation coefficient.

### **6.3.3** *MEP Onset Latency and Duration*

The latency and duration were calculated for each trial with the head and chair facing forward. If a single response was observed, the latency and duration of that response was used. If two responses were observed, the latency and duration of the second response was used. If two responses were observed, but they were not clearly distinguishable, the latency of the initial response was used and the duration of the entire response was measured for subsequent analysis.

### **6.3.4** *Asymmetric Tonic Neck Reflex*

The effects of lateral head rotation were determined by calculating the difference in the peak-to-peak amplitude of the MEP in either the toward or away condition and the straight forward position and then normalizing by the straight forward position:

$$\Delta\text{MEP}_{\text{condition}} = (\text{MEP}_{\text{condition}} - \text{MEP}_{\text{straight}}) / \text{MEP}_{\text{straight}}$$

The effects of head rotation (away or toward the target muscle) on MEP size across subjects were tested using a paired t-test.

## 6.4 Results

### 6.4.1 Raw Data

Stroke subjects varied considerably with which muscles we were able to get responses from when stimulating either the contralateral or ipsilateral

hemisphere. Responses were less consistent in shape and size and onset than in the

controls. In the control subjects, the distal muscles typically had 2 responses (one for the first and one for the second stimulus). This was rarely observed in the stroke subject where typically just a single response was observed (see figure 6.3).

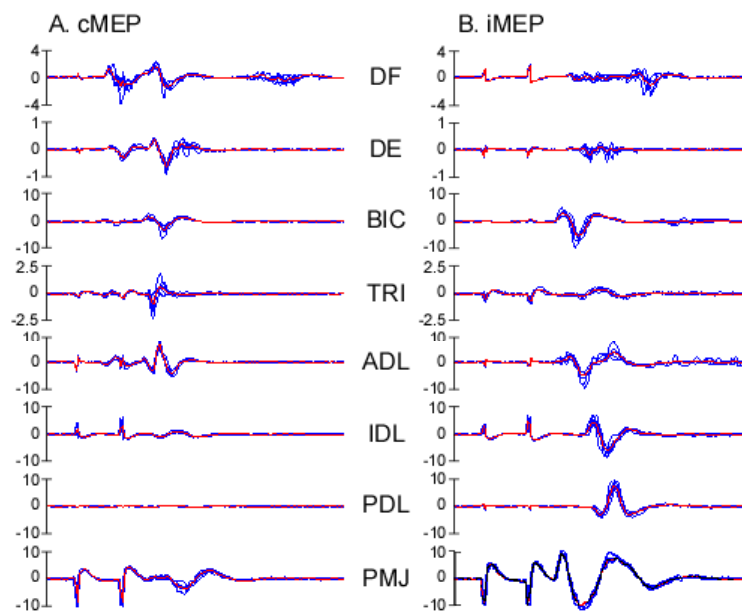


**Figure 6-3 Raw data.** Contralateral (A) and ipsilateral (B) motor evoked responses in eight muscles of the paretic upper limb for one stroke subject. Six trials are shown with the mean trial in red. Note the different y-axis scales.

### 6.4.2 *Laterality*

The laterality results are shown in figure 2. Note that the control subjects all have primarily contralateral (LI = +1) responses with little to no ipsilateral responses in the limb. The stroke subjects however, have the majority of muscles (BIC, TRI, ADL, IDL, PDL, PMJ) whose dominant input is now from the ipsilateral hemisphere resulting in a significantly different LI than the control subjects. The distal extensors, which are difficult to activate voluntarily after stroke, have the least amount of ipsilateral takeover. The laterality of the stroke paretic muscles had statistically different laterality indexes than the control muscles ( $p < .01$ ). Within the paretic limb, the muscles involved in the flexion synergy (DF, BIC, IDL, PDL) had significantly more ipsilateral LIs than the muscles involved in the extension synergy (DE, TRI, ADL, PMJ) ( $p = .05994$ ). The flexor muscles (DF, BIC, ADL) were not significantly different from the extensor muscles (DE, TRI, PDL) within the paretic limb ( $p = .5420$ ). A repeated measures ANOVA testing the wrist, elbow, shoulder and trunk muscle groups did show an effect of muscle group ( $p = .0133$ ). The wrist muscles were significantly different (less ipsilateral) than the elbow ( $p = .0288$ ), shoulder ( $p = .0022$ ), and trunk muscles ( $p = .0185$ ). There was no significant difference between the more proximal muscle groups.

### 6.4.3 Correlation with Recovery Level in Stroke Subjects

Only the LIs for the DF ( $R^2 = .3866$ ,  $p = .1$ ), BIC ( $R^2 = .379$ ,  $p = .05$ ) and TRI ( $R^2 = .2397$ ,  $p = .1$ ) were significantly correlated with the Fugl-Meyer score (see figure 6.4). For these three muscles, the more impaired the subject, the more ipsilateral the LI.

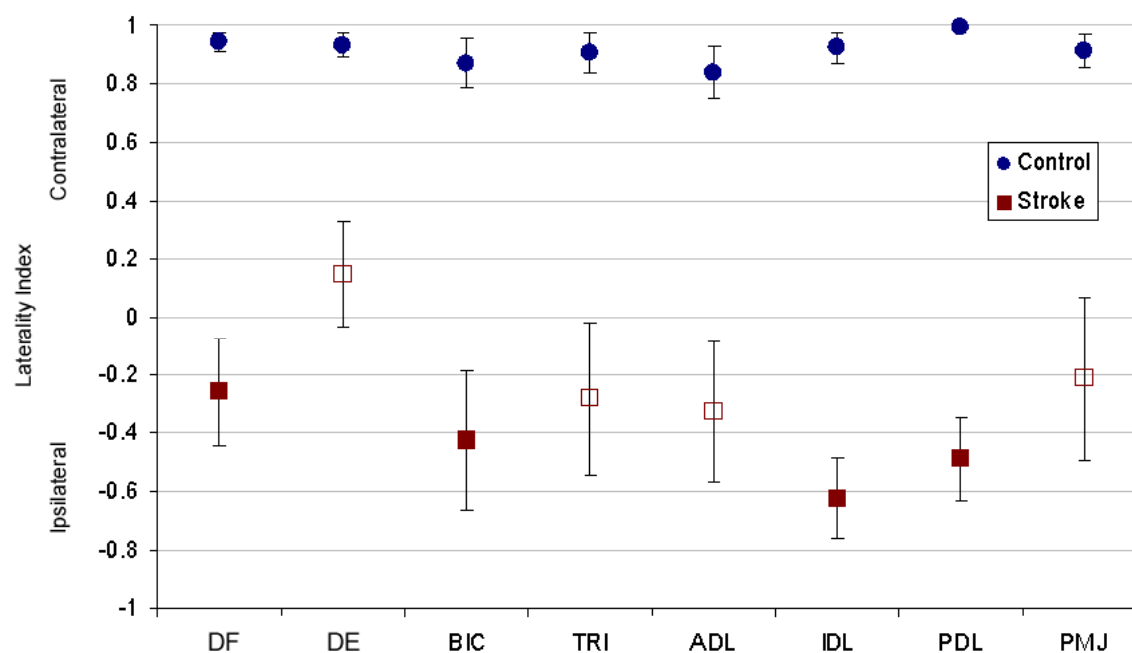


**Figure 6-4 Lateral index.** Plotted with standard error. The zero indicates an equal size MEP elicited from both the ipsilateral and contralateral cortices. Within the stroke data, the closed squares are those muscles involved in the flexion synergy, the open squares are the muscles involved in the extension synergy.

### 6.4.4 Latency

Stroke iMEPs (mean across muscles: 31.99 +/- 9.40 ms) are significantly delayed compared to the control cMEP (mean across muscles: 15.99 +/- 2.17 ms) ( $p < .0001$ ), the control iMEP (mean across muscles: 21.48 +/- 3.85 ms) ( $p = .01253$ ) and the stroke cMEP (mean across muscles:

21.60 +/- 3.85 ms) ( $p = .01381$ ) (see figure 6.5). There was no significant difference between control cMEP, control iMEP and the stroke cMEP. Within the stroke ipsilateral muscles, the extensor synergy muscles had significantly different onsets (24.65 +/- 2.72 ms) than the flexor synergy muscles (39.34 +/- 7.42 ms) (paired t-test,  $p = .0183$ )

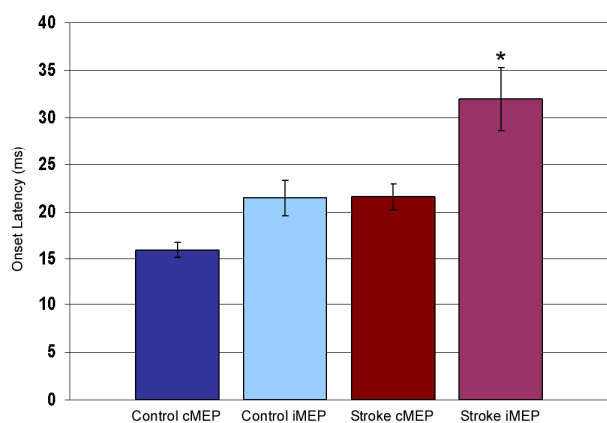


**Figure 6-5 Onset latency.** Only the stroke iMEP was significantly different from each of the other subject group/projection types. Shown standard error bars. \* indicates significance at the  $p = .05$  level.

#### 6.4.5 Duration

There was no significant difference in the duration of the MEP in each muscle between the control cMEPs (average across all muscles = 41.08 +/- 8.86 ms), the stroke cMEPs (average across all muscles = 37.96 +/- 6.29 ms) or the stroke iMEPs (average across all muscles = 43.08 +/- 8.02 ms).

#### 6.4.6 Spatial Location

All hotspots were on the sensorimotor cortices in both control and stroke subjects (see figure 6.6). There was no consistent shift in the ipsilateral or contralateral hotspots in stroke subjects. In addition, somatotopy was not consistently observed, except for PMJ in the control subjects which was always more medial than the remaining muscles.

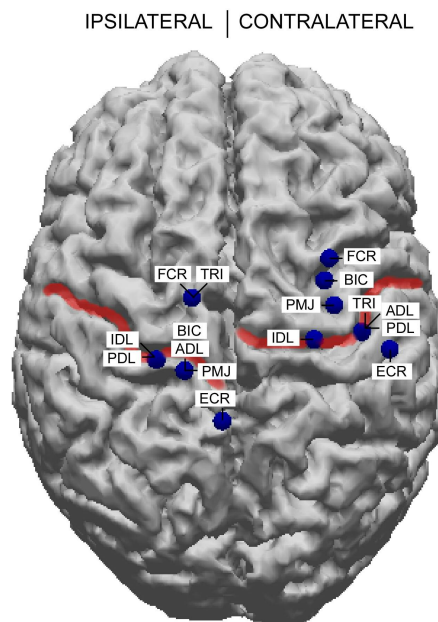


**Figure 6-6 Hotspot location.** Hotspots for each muscle for the ipsilateral and contralateral projections in one example stroke subject. The red highlighting indicates the central sulcus. Note that a single hotspot was frequently the optimal stimulation location for multiple muscles, which could span from distal to proximal muscles.

#### 6.4.7 ATNR

An example of the effects of neck rotation are shown in figure 6.7. In the control subjects there was a significant facilitation of the contralateral MEPs by head rotation toward the BIC compared with the condition when the head was turned away from the muscle ( $p = .0511$ ) (see figure 6.8). There was no significant change in Tricep response

by head rotation away from the muscle compared with toward ( $p = .6262$ ). Contrastingly, in the stroke subjects, both the ipsilateral and contralateral projections to the TRI showed an increase in MEP size with head rotation toward the muscle compared with away, with only the ipsilateral projection reaching significance ( $p = .0708$ , contralateral:  $p = .1358$ ). For the BIC, only the contralateral projection with head rotation away from the muscle had a significant facilitation ( $p$

= .0302) compared with away whereas the ipsilateral MEP did show a trend towards facilitation ( $p = .1567$ ). The only other muscle that exhibited a significant modulation with ATNR was PDL of the control subject group which was significantly facilitated with the head turned away compared with toward ( $p = .0943$ ). When the muscles were grouped into flexor synergy and extensor synergy groups, there was no significant difference between the iMEPs in the toward and away conditions for either the flexor synergy group ( $p = .523$ ) or the extensor synergy group ( $p = .2066$ ), however there was a significant difference in the cMEPs in the flexor synergy group ( $p = .0003$ ) and a trend in the extensor synergy group ( $p = .1142$ ) such that the flexors were facilitated in the TO condition and the extensors were facilitated in the AW condition. When the muscles were divided into the joint flexors and joint extensors no significant differences in the conditions was found.



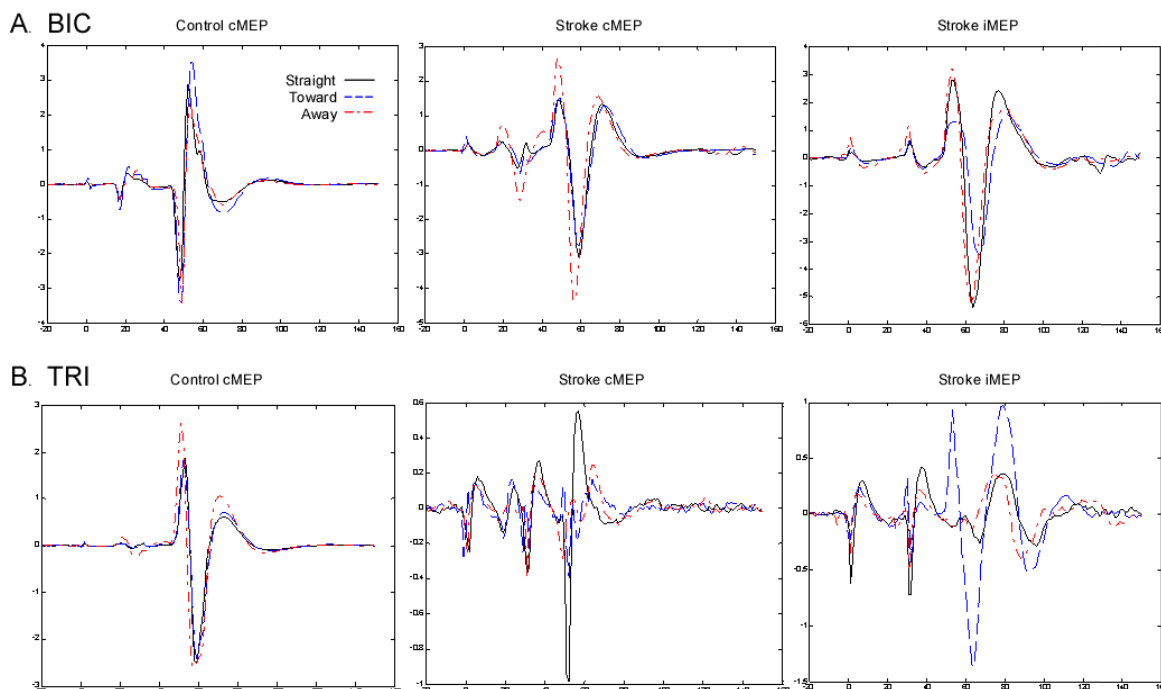


**Figure 6-7 ATNR raw data results.** Row A–biceps muscle in control cMEP, and in Stroke cMEP and iMEP. Row B –triceps muscle in control cMEP, and in Stroke cMEP and iMEP. The y-axis of each graph is optimized for the display of the data and is different between graphs. TMS evoked MEP in the head position: straight forward in solid black, facing toward the target arm in dashed blue, and facing away from the target arm in dash-dot red.

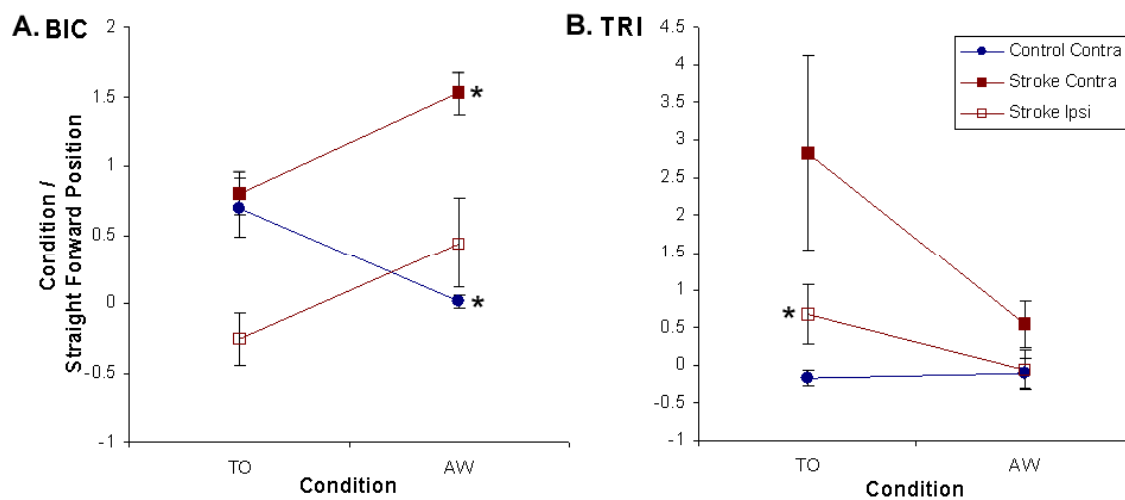


**Figure 6-8 ATNR results.** The biceps and triceps muscles were the only muscles that seemed to be modulated with neck rotation for several subject/projection types. Data are shown for the MEPs elicited when the chair was rotated such that the stationary head faced to or away from the target arm. Standard error bars are shown. \* indicate significance at the  $p = .1$  level.

## **6.5 Discussion**

Our findings suggest that the ipsilateral projection is an oligosynaptic pathway which is more prevalent in muscles involved in the pathological flexor synergy. ATNR only modulated the responses in the muscles of the elbow. However, if the muscles involved in the pathological flexor and extensor synergies were grouped and the effects of ATNR were compared, there was a significant modulation within each group, within the contralateral projection only.

### **6.5.1 Bias Towards Pathological Flexor Synergy Muscles in Ipsilateral Takeover**

The laterality index showed that across the paretic limb a shift towards dominance of the ipsilateral projection was occurring in moderate to severe stroke subjects. This is consistent with many studies that have reported an increased likelihood of ipsilateral activity in poorly recovered patients (Ward et al., 2003; Werhahn et al., 2003); (Serrien et al., 2004; Turton et al., 1996; Ward et al., 2003). Few studies have investigated the relative strength of the ipsilateral and contralateral projections. Kimberley et al. used fMRI to look at the activity that occurred in the cortex while imagining moving the paretic wrist and recorded greater ipsilateral than contralateral activity in the primary motor cortex and supplementary motor cortex (2006). In a previous study, we found that the laterality index for the proximal pectoralis major muscle was correlated with recovery (see chapter 4). The current study may be the first to investigate the relative strength of the projections for such a large number of upper limb muscles. The ipsilateral shift was weakest for the distal muscles. This result is in accordance with the

hypothesis that the ipsilateral projection observed after stroke results from the unmasking or upregulation of an existing oligosynaptic pathway in that anatomical evidence has shown a predominant mono-synaptic corticospinal input to the distal muscles (Kuypers, 1960). The observation that wrist extensors exhibit very poor recovery (Kamper and Rymer, 2001) may be related to the fact that these muscles exhibit the least amount of ipsilateral takeover.

The shift toward ipsilateral dominance was strongest for those muscles involved in the pathological flexor synergy, but not across the pure joint flexor muscles. The difference in hemispheric laterality between the extensor and flexor synergy muscles may be a result of preferential connections of contralateral and ipsilateral bulbospinal tracts to different muscle subsets. Stimulation of the medial pontomedullary reticular formation in the primate most often resulted in facilitation of ipsilateral flexors in the arm and suppression of contralateral extensors with bilateral responses common (Davidson and Buford, 2004; Davidson and Buford, 2006). However, in this study, we included in the pathological flexor synergy muscles that are not all pure joint flexors - such as the posterior deltoid. In Davidson and Buford (2006), the PDL is included and responds similarly to the other joint extensors, contrary to our results. Similarly, we put the anterior deltoid with the pathological extensor synergy muscles, but in the Davidson and Buford paper, ADL responded similarly to other joint flexors. While the behavioral evidence in stroke patients would point towards an anatomical grouping between the pathological flexor and extensor synergy muscles (Dewald et al., 1995), this needs to be investigated further.

### ***6.5.2 Delayed Onset Latency in Flexor Synergy Muscles of the Ipsilateral Projection***

The onset latency for ipsilateral MEPs was delayed compared to control MEPs and also compared to the contralateral MEP in the paretic limb. Furthermore, the flexor synergy muscles were significantly delayed compared to the extensor synergy muscles. This shows that the ipsilateral projection has multiple synapses and could be a trans-brainstem pathway. The delay in onset in the ipsilateral MEP has been widely reported (Netz et al., 1997; Turton et al., 1996). We propose that this pathway involves the reticulospinal tract because of the preferential input to the flexors that we have observed in this study.

### ***6.5.3 Effects of Head Rotation***

The observed facilitation of the stroke ipsilateral MEP in the triceps with the head turned towards the muscle, and in the biceps with the head turned away from the muscle are in accordance with the asymmetrical tonic neck reflex and indicate a privileged input of tonic neck afferents to the pathways for the ipsilateral MEP. In contrast, the opposite modulation of the control contralateral triceps and biceps MEPs is inconsistent with the tonic neck reflex and suggests that the modulation observed may be explained by changes in motoneurone excitability. Similar results were obtained in the wrist extensors of healthy subjects during background contraction, where ipsilateral MEPs were modulated according to the tonic neck reflex and contralateral MEPs reflected opposite effects (Ziemann, 1999). In the current study, the impaired triceps MEP in stroke subjects resulting from contralateral stimulation was also

modulated according to ATNR, suggesting that both the ipsilateral and contralateral projections to the impaired arm pass through the brainstem which receives input from the neck receptors. In addition, when the muscles were grouped according to abnormal coordination synergy (flexor or extensor) they were significantly modulated by head rotation during contralateral TMS, but not ipsilateral TMS. As the effects of ATNR could be small, a study with more subjects could provide some interesting results. That we were able to record significant modulation in the elbow could simply be because the elbow does not receive predominant input from either the corticospinal tract or the bulbospinal tracts but a combination of both. These stimulated results are similar to other results in this laboratory in stroke patients where the effects of head rotation were studied during maximum voluntary activation of the paretic arm (unpublished results). This study too only saw modulation of the elbow muscles with neck rotation. The elbow may therefore have the most to gain from a modulation of the corticobulbospinal tracts.

#### *6.5.4 Cortical Origin of Ipsilateral Responses*

Previous studies have shown a shift between the contralateral projection and the ipsilateral projection to the paretic limb, however, we did not see a similar shift. In addition, we did not observe somatotopy among the optimal stimulation sites for each muscle. This may be a result of the resolution of the stimulation grid. We used a 2 cm resolution grid which is based on the width of the stimulation coil at the intersection of the windings. The anterior-posterior resolution of the stimulation coil has also been questioned as the coil intersection is about 3 cm long. This could be the reason why we observed multiple muscles across joints with the same hotspot, and

why we did not observe somatotopy within the arm region. A recent TMS study on FDI, ECR and ADL in healthy subjects with a 1cm grid also failed to show significant differences in either the medial-lateral or anterior-posterior direction for all cases except in the medial-lateral direction between the optimal sites for FDI and ADL with a separation of just over 1 cm (Devanne et al., 2006). These authors also saw considerable overlap in the area where responses could be elicited in each muscle. Overlapping representations have also been reported in microstimulation experiments in animals but maintain somatotopy (Kwan et al., 1978; Lemon, 1981; Murphy et al., 1978; Waters et al., 1990). However, within these regions there is no fine somatotopy, but rather a mosaic organization of muscles and movements. Individual muscles have also been found to have multiple representations spread widely throughout the primary motor cortex (Lemon et al., 1986).

## ***6.6 Clinical Implications***

This study suggests that in moderate to severe stroke patients, an upregulation of ipsilateral oligosynaptic pathways (such as the corticoreticulospinal pathway), may explain the flexion bias observed in the paretic limb. The moment a stroke subject lifts their arm against the force of gravity their movements are constrained to the flexion synergy. This results in a significant reduction in reaching workspace (Beer et al., 2004). Using ATNR following stroke can reduce the overwhelming effects of the flexion synergy. An identification of the descending pathway involved in the constraint in movement will provide new foundations for developing and investigating targeted interventions.

## 7

**SUMMARY**

This dissertation examined the role of the ipsilateral and contralateral corticobulbospinal projections in the expression of abnormal muscle coordination patterns using transcranial magnetic stimulation. The effectiveness of paired pulse TMS was investigated and used to study the paretic distal and proximal upper limb. During single pulse TMS with background activation, as well as during paired pulse TMS we found evidence of corticobulbospinal pathways contributing to synergistic muscle activations in subjects with hemiparetic stroke.

In the first study (chapter 4), we investigated a single proximal muscle using single pulse TMS and background activation. We were able to correlate the relative magnitude of the ipsilateral response in that muscle with the Fugl-Meyer score as well as with the degree of abnormal coordination observed. Previous studies have shown that ipsilateral responses are correlated with poor recovery, however this is the first study to implicate the ipsilateral responses in the behaviors exhibited by subjects with poor recovery namely the expression of abnormal limb synergies resulting in abnormal coordination following stroke.

In an effort to avoid biasing the TMS results with volitional background contractions, which would result in abnormal muscle coactivation patterns and TMS activation of the associated

muscles, we investigated paired pulse TMS at rest (chapter 5). Previous studies have shown the optimal range of interpulse interval facilitation in distal muscles and some elbow muscles to be in the same range that we discovered, however, this had not been studied systematically in the proximal muscles prior to the current study, nor had it been investigated in the stroke population. The observation that this mechanism of facilitation is present across distal and proximal muscles, and preserved following stroke is an interesting finding in itself. Paired pulse TMS with interpulse intervals of 25-40 ms is able to increase the occurrence of ipsilateral MEPs in the paretic arm by 15% and is able to increase the magnitude of the response by 68% over the responses observed across subjects with the traditional single pulse TMS. The reason why the ipsilateral MEPs may be more responsive to paired pulse facilitation may be because the ipsilateral projections primarily consist of oligosynaptic connections. The results of this study determined the optimum interpulse interval for TMS of upper extremity muscles in stroke patients while at rest.

Using the optimal paired pulse TMS ISI of 30 ms, we investigated the relative strength of the ipsilateral and contralateral projections to the paretic arm in moderate-to-severely impaired patients (chapter 6). We found that every muscle had greater ipsilateral input than in the control subjects, and that muscles involved in the pathological flexor synergy had significantly greater ipsilateral dependence than the muscles in the pathological extensor synergy. This finding, along with a delay in onset compared to the pathological extensor muscles, and recently published literature regarding stimulation of the reticular formation in monkeys resulting in a similar



finding, prompted us to study the effects of head rotation on the TMS responses. Neck receptors have preferential input to the reticular formation and can thereby modify signals traveling through the reticular formation. In the monkey, stimulation of the medial pontomedullary nucleus of the reticular formation results in the facilitation of ipsilateral joint flexor muscles and the suppression of contralateral joint extension muscles. Interestingly, we only observed modulation of the ipsilateral and contralateral biceps and triceps. This is similar to other results in this laboratory in stroke patients where the effects of head rotation were studied during maximum voluntary activation of the paretic arm (unpublished results). This study too only saw modulation of the elbow muscles with neck rotation. This could be because the elbow does not receive predominant input from either the corticospinal tract or the bulbospinal tracts but a combination of both. The elbow has therefore the most to gain from an upregulation of the corticobulbospinal tracts.

The results presented in this dissertation demonstrate the preferential input of the ipsilateral projections to the pathological flexor synergy muscles of the upper limb of stroke subjects. The paired pulse technique is providing a new way to investigate motor system reorganization following stroke.

## 8

### **FUTURE WORK**

The experimental approach developed in this thesis will provide the platform for not only studying paretic limb muscles with TMS while at rest, but will also allow for the study of proximal limb muscles in the healthy subjects at rest. One of the major benefits of TMS is the ability to activate the underlying nervous system, and to compare it with the pathways that the body activates under voluntary conditions. It is with this comparison that new rehabilitative strategies could be discovered.

This study is the first to look at the relative contribution of the ipsilateral and contralateral hemispheres to the muscles of the paretic limb in light of the abnormal coordination that these patients exhibit during voluntary force/torque exertions in the paretic upper limb. Abnormal coordination is a function of the entire arm and traditional TMS studies of a single muscle would not be as informative as investigating the connectivity of sets of muscles that are involved in this dysfunction.

The results presented here suggest that the ipsilateral hemisphere may have a role in the expression of the pathological flexor synergy. However, the ATNR results did not provide evidence of a purely reticulospinal origin for the coactivation of these muscles. Therefore, further research needs to be done to determine which ipsilateral pathway is being upregulated

following stroke. In the background section a number of possible pathways were reviewed, and, as is typically the case in science, the answer probably lies in some combination of them. A study that tries to elucidate the roles of monoaminergic bulbospinal pathway in abnormal movement coordination following stroke is currently under way.

## 9

**REFERENCES**

- Abbruzzese G, Assini A, Buccolieri A, Schieppati M, Trompetto C. Comparison of intracortical inhibition and facilitation in distal and proximal arm muscles in humans. *J Physiol* 1999; 514 ( Pt 3): 895-903.
- Abdeen MA, Stuchly MA. Modeling of magnetic field stimulation of bent neurons. *IEEE Trans Biomed Eng* 1994; 41: 1092-5.
- Adams RW, Gandevia SC, Skuse NF. The distribution of muscle weakness in upper motoneuron lesions affecting the lower limb. *Brain* 1990; 113 ( Pt 5): 1459-76.
- Alagona G, Delvaux V, Gerard P, De Pasqua V, Pennisi G, Delwaide PJ, et al. Ipsilateral motor responses to focal transcranial magnetic stimulation in healthy subjects and acute-stroke patients. *Stroke* 2001; 32: 1304-9.
- Alstermark B, Lundberg A. The C3-C4 propriospinal system: target reach and food-taking. In: Jami L, Pierrot-Deseilligny E and Zytnicki D, editors. *Muscle Afferents and Spinal Control of Movement*. London: Pergamon, 1992: 327-354.
- Amassian VE, Eberle L, Maccabee PJ, Cracco RQ. Modelling magnetic coil excitation of human cerebral cortex with a peripheral nerve immersed in a brain-shaped volume conductor: the significance of fiber bending in excitation. *Electroencephalogr Clin Neurophysiol* 1992; 85: 291-301.
- Bawa P, Hamm JD, Dhillon P, Gross PA. Bilateral responses of upper limb muscles to transcranial magnetic stimulation in human subjects. *Exp Brain Res* 2004; 158: 385-90.
- Beer RF DJ. The relationship between abnormal static torque synergies and disturbances of planar arm movements in hemiparetic subjects: Preliminary results. *Soc. of Neurosci. Abstr* 1999; 25.

- Beer R, Dewald J, Rymer Z. Disturbances of voluntary movement coordination in stroke: problems of planning or execution? *Prog Brain Res* 1999a; 123: 455-60.
- Beer RF, Dewald JP, Dawson ML, Rymer WZ. Target-dependent differences between free and constrained arm movements in chronic hemiparesis. *Exp Brain Res* 2004; 156: 458-70.
- Beer RF, Dewald JP, Rymer WZ. Deficits in the coordination of multijoint arm movements in patients with hemiparesis: evidence for disturbed control of limb dynamics. *Exp Brain Res* 2000; 131: 305-19.
- Beer RF, Given JD, Dewald JP. Task-dependent weakness at the elbow in patients with hemiparesis. *Arch Phys Med Rehabil* 1999b; 80: 766-72.
- Benecke R, Conrad B, Meinck HM, Hohne J. Electromyographic analysis of bicycling on an ergometer for evaluation of spasticity of lower limbs in man. *Adv Neurol* 1983; 39: 1035-46.
- Benecke R, Meyer BU, Freund HJ. Reorganisation of descending motor pathways in patients after hemispherectomy and severe hemispheric lesions demonstrated by magnetic brain stimulation. *Exp Brain Res* 1991; 83: 419-26.
- Bohannon RW, Smith MB. Assessment of strength deficits in eight paretic upper extremity muscle groups of stroke patients with hemiplegia. *Phys Ther* 1987; 67: 522-5.
- Bondurant CP, Haghighi SS, Oro JJ. Experience with transcranial magnetic stimulation in cortical mapping. *Neurol Res* 1997; 19: 435-40.
- Bourbonnais D, Vanden Noven S. Weakness in patients with hemiparesis. *Am J Occup Ther* 1989; 43: 313-9.
- Brinkman J, Kuypers HG. Cerebral control of contralateral and ipsilateral arm, hand and finger movements in the split-brain rhesus monkey. *Brain* 1973; 96: 653-74.
- Brodmann K. Vergleichende Lokalisationslehre der Grosshirnrinde in ihren Prinzipien dargestellt auf Grund des Zellenbaues. Bath, England: Leipzig, 1909.
- Brunnstrom S. Movement therapy in hemiplegia : a neurophysiological approach. New York: Medical Dept. Harper & Row, 1970.
- Byrnes ML, Thickbroom GW, Phillips BA, Mastaglia FL. Long-term changes in motor cortical organisation after recovery from subcortical stroke. *Brain Res* 2001; 889: 278-87.

- Byrnes ML, Thickbroom GW, Phillips BA, Wilson SA, Mastaglia FL. Physiological studies of the corticomotor projection to the hand after subcortical stroke. *Clin Neurophysiol* 1999; 110: 487-98.
- Cao Y, D'Olhaberriague L, Vikingstad EM, Levine SR, Welch KM. Pilot study of functional MRI to assess cerebral activation of motor function after poststroke hemiparesis. *Stroke* 1998; 29: 112-22.
- Carey JR, Kimberley TJ, Lewis SM, Auerbach EJ, Dorsey L, Rundquist P, et al. Analysis of fMRI and finger tracking training in subjects with chronic stroke. *Brain* 2002; 125: 773-88.
- Carr LJ, Harrison LM, Stephens JA. Evidence for bilateral innervation of certain homologous motoneurone pools in man. *J Physiol* 1994; 475: 217-27.
- Chen R, Tam A, Butefisch C, Corwell B, Ziemann U, Rothwell JC, et al. Intracortical inhibition and facilitation in different representations of the human motor cortex. *J Neurophysiol* 1998; 80: 2870-81.
- Chen R, Yung D, Li JY. Organization of ipsilateral excitatory and inhibitory pathways in the human motor cortex. *J Neurophysiol* 2003; 89: 1256-64.
- Chollet F, DiPiero V, Wise RJ, Brooks DJ, Dolan RJ, Frackowiak RS. The functional anatomy of motor recovery after stroke in humans: a study with positron emission tomography. *Ann Neurol* 1991; 29: 63-71.
- Cicinelli P, Pasqualetti P, Zaccagnini M, Traversa R, Oliveri M, Rossini PM. Interhemispheric asymmetries of motor cortex excitability in the postacute stroke stage: a paired-pulse transcranial magnetic stimulation study. *Stroke* 2003; 34: 2653-8.
- Cicinelli P, Traversa R, Rossini PM. Post-stroke reorganization of brain motor output to the hand: a 2-4 month follow-up with focal magnetic transcranial stimulation. *Electroencephalogr Clin Neurophysiol* 1997; 105: 438-50.
- Claus D, Weis M, Jahnke U, Plewe A, Brunholzl C. Corticospinal conduction studied with magnetic double stimulation in the intact human. *J Neurol Sci* 1992; 111: 180-8.
- Colebatch JG, Deiber MP, Passingham RE, Friston KJ, Frackowiak RS. Regional cerebral blood flow during voluntary arm and hand movements in human subjects. *J Neurophysiol* 1991; 65: 1392-401.

- Colebatch JG, Gandevia SC. The distribution of muscular weakness in upper motor neuron lesions affecting the arm. *Brain* 1989; 112 ( Pt 3): 749-63.
- Colebatch JG, Rothwell JC, Day BL, Thompson PD, Marsden CD. Cortical outflow to proximal arm muscles in man. *Brain* 1990; 113 ( Pt 6): 1843-56.
- Cramer SC, Nelles G, Benson RR, Kaplan JD, Parker RA, Kwong KK, et al. A functional MRI study of subjects recovered from hemiparetic stroke. *Stroke* 1997; 28: 2518-27.
- Cuadrado ML, Egido JA, Gonzalez-Gutierrez JL, Varela-De-Seijas E. Bihemispheric contribution to motor recovery after stroke: A longitudinal study with transcranial doppler ultrasonography. *Cerebrovasc Dis* 1999; 9: 337-44.
- Darian-Smith I, Brookhart JM, Mountcastle VB, Geiger SR, American Physiological Society (1887- ). *The Nervous system. Vol. 3, part 1, Sensory processes.* Bethesda, Maryland: American Physiological Society, 1984.
- Davidson AG, Buford JA. Motor outputs from the primate reticular formation to shoulder muscles as revealed by stimulus-triggered averaging. *J Neurophysiol* 2004; 92: 83-95.
- Davidson AG, Buford JA. Bilateral actions of the reticulospinal tract on arm and shoulder muscles in the monkey: stimulus triggered averaging. *Exp Brain Res* 2006; 173: 25-39.
- Day BL, Dressler D, Maertens de Noordhout A, Marsden CD, Nakashima K, Rothwell JC, et al. Electric and magnetic stimulation of human motor cortex: surface EMG and single motor unit responses. *J Physiol* 1989; 412: 449-73.
- de Noordhout AM, Rapisarda G, Bogacz D, Gerard P, De Pasqua V, Pennisi G, et al. Corticomotoneuronal synaptic connections in normal man: an electrophysiological study. *Brain* 1999; 122 ( Pt 7): 1327-40.
- Delisa JA, Mikulic MA, Melnick RR, Miller RM. Stroke rehabilitation: Part II. Recovery and complications. *Am Fam Physician* 1982; 26: 143-51.
- Delvaux V, Alagona G, Gerard P, De Pasqua V, Pennisi G, de Noordhout AM. Post-stroke reorganization of hand motor area: a 1-year prospective follow-up with focal transcranial magnetic stimulation. *Clin Neurophysiol* 2003; 114: 1217-25.
- Devanne H, Cassim F, Ethier C, Brizzi L, Thevenon A, Capaday C. The comparable size and overlapping nature of upper limb distal and proximal muscle representations in the human motor cortex. *Eur J Neurosci* 2006; 23: 2467-76.

- Dewald JP, Beer RF. Abnormal joint torque patterns in the paretic upper limb of subjects with hemiparesis. *Muscle Nerve* 2001; 24: 273-83.
- Dewald JP, Beer RF, Given JD, McGuire JR, Rymer WZ. Reorganization of flexion reflexes in the upper extremity of hemiparetic subjects. *Muscle Nerve* 1999; 22: 1209-21.
- Dewald JP, Pope PS, Given JD, Buchanan TS, Rymer WZ. Abnormal muscle coactivation patterns during isometric torque generation at the elbow and shoulder in hemiparetic subjects. *Brain* 1995; 118 (Pt 2): 495-510.
- Dewald JP, Sheshadri V, Dawson ML, Beer RF. Upper-limb discoordination in hemiparetic stroke: implications for neurorehabilitation. *Top Stroke Rehabil* 2001; 8: 1-12.
- Durand D, Ferguson AS, Dalbasti T. Effect of surface boundary on neuronal magnetic stimulation. *IEEE Trans Biomed Eng* 1992; 39: 58-64.
- Edgley SA, Eyre JA, Lemon RN, Miller S. Excitation of the corticospinal tract by electromagnetic and electrical stimulation of the scalp in the macaque monkey. *J Physiol* 1990; 425: 301-20.
- Ellis MD, Acosta AM, Yao J, Dewald JP. Position-dependent torque coupling and associated muscle activation in the hemiparetic upper extremity. *Exp Brain Res* 2006.
- Eyre JA, Taylor JP, Villagra F, Smith M, Miller S. Evidence of activity-dependent withdrawal of corticospinal projections during human development. *Neurology* 2001; 57: 1543-54.
- Ferbert A, Caramia D, Priori A, Bertolasi L, Rothwell JC. Cortical projection to erector spinae muscles in man as assessed by focal transcranial magnetic stimulation. *Electroencephalogr Clin Neurophysiol* 1992; 85: 382-7.
- Feydy A, Carlier R, Roby-Brami A, Bussel B, Cazalis F, Pierot L, et al. Longitudinal study of motor recovery after stroke: recruitment and focusing of brain activation. *Stroke* 2002; 33: 1610-7.
- Fries W, Danek A, Scheidtmann K, Hamburger C. Motor recovery following capsular stroke. Role of descending pathways from multiple motor areas. *Brain* 1993; 116 ( Pt 2): 369-82.
- Fries W, Danek A, Witt TN. Motor responses after transcranial electrical stimulation of cerebral hemispheres with a degenerated pyramidal tract. *Ann Neurol* 1991; 29: 646-50.
- Fromm C, Evarts EV. Pyramidal tract neurons in somatosensory cortex: central and peripheral inputs during voluntary movement. *Brain Res* 1982; 238: 186-91.



- Fugl-Meyer AR, Jaasko L, Leyman I, Olsson S, Steglind S. The post-stroke hemiplegic patient. 1. a method for evaluation of physical performance. *Scand J Rehabil Med* 1975; 7: 13-31.
- Fujiwara T, Sonoda S, Okajima Y, Chino N. The relationships between trunk function and the findings of transcranial magnetic stimulation among patients with stroke. *J Rehabil Med* 2001; 33: 249-55.
- Gemperline JJ, Allen S, Walk D, Rymer WZ. Characteristics of motor unit discharge in subjects with hemiparesis. *Muscle Nerve* 1995; 18: 1101-14.
- Gowland C, Stratford P, Ward M, Moreland J, Torresin W, Van Hullenaar S, et al. Measuring physical impairment and disability with the Chedoke-McMaster Stroke Assessment. *Stroke* 1993; 24: 58-63.
- Grafton ST, Woods RP, Mazziotta JC. Within-arm somatotopy in human motor areas determined by positron emission tomography imaging of cerebral blood flow. *Exp Brain Res* 1993; 95: 172-6.
- Grafton ST, Woods RP, Mazziotta JC, Phelps ME. Somatotopic mapping of the primary motor cortex in humans: activation studies with cerebral blood flow and positron emission tomography. *J Neurophysiol* 1991; 66: 735-43.
- Green JB, Bialy Y, Sora E, Ricamoto A. High-resolution EEG in poststroke hemiparesis can identify ipsilateral generators during motor tasks. *Stroke* 1999; 30: 2659-65.
- Hamdy S, Rothwell JC. Gut feelings about recovery after stroke: the organization and reorganization of human swallowing motor cortex. *Trends Neurosci* 1998; 21: 278-82.
- He SQ, Dum RP, Strick PL. Topographic organization of corticospinal projections from the frontal lobe: motor areas on the lateral surface of the hemisphere. *J Neurosci* 1993; 13: 952-80.
- He SQ, Dum RP, Strick PL. Topographic organization of corticospinal projections from the frontal lobe: motor areas on the medial surface of the hemisphere. *J Neurosci* 1995; 15: 3284-306.
- Heald A, Bates D, Cartlidge NE, French JM, Miller S. Longitudinal study of central motor conduction time following stroke. 1. Natural history of central motor conduction. *Brain* 1993; 116 ( Pt 6): 1355-70.
- Hess CW, Mills KR, Murray NM. Responses in small hand muscles from magnetic stimulation of the human brain. *J Physiol* 1987; 388: 397-419.

- Honda M, Nagamine T, Fukuyama H, Yonekura Y, Kimura J, Shibasaki H. Movement-related cortical potentials and regional cerebral blood flow change in patients with stroke after motor recovery. *J Neurol Sci* 1997; 146: 117-26.
- Jankowska E, Hammar I, Slawinska U, Maleszak K, Edgley SA. Neuronal basis of crossed actions from the reticular formation on feline hindlimb motoneurons. *J Neurosci* 2003; 23: 1867-78.
- Jankowska E, Stecina K, Cabaj A, Pettersson LG, Edgley SA. Neuronal relays in double crossed pathways between feline motor cortex and ipsilateral hindlimb motoneurons. *J Physiol* 2006; 575: 527-41.
- Kamper DG, Rymer WZ. Impairment of voluntary control of finger motion following stroke: role of inappropriate muscle coactivation. *Muscle Nerve* 2001; 24: 673-81.
- Kernell D, Chien-Ping WU. Responses of the pyramidal tract to stimulation of the baboon's motor cortex. *J Physiol* 1967; 191: 653-72.
- Kimberley TJ, Khandekar G, Skraba LL, Spencer JA, Van Gorp EA, Walker SR. Neural substrates for motor imagery in severe hemiparesis. *Neurorehabil Neural Repair* 2006; 20: 268-77.
- Kopp B, Kunkel A, Muhlneckel W, Villringer K, Taub E, Flor H. Plasticity in the motor system related to therapy-induced improvement of movement after stroke. *Neuroreport* 1999; 10: 807-10.
- Kujirai T, Caramia MD, Rothwell JC, Day BL, Thompson PD, Ferbert A, et al. Corticocortical inhibition in human motor cortex. *J Physiol* 1993; 471: 501-19.
- Kuypers HG. Central cortical projections to motor and somato-sensory cell groups. An experimental study in the rhesus monkey. *Brain* 1960; 83: 161-84.
- Kuypers HG. The Descending Pathways to the Spinal Cord, Their Anatomy and Function. *Prog Brain Res* 1964; 11: 178-202.
- Kwan HC, Mackay WA, Murphy JT, Wong YC. An intracortical microstimulation study of output organization in precentral cortex of awake primates. *J Physiol (Paris)* 1978; 74: 231-3.
- Lance JW. The control of muscle tone, reflexes, and movement: Robert Wartenberg Lecture. *Neurology* 1980; 30: 1303-13.

- Landau WM, Sahrman SA. Preservation of directly stimulated muscle strength in hemiplegia due to stroke. *Arch Neurol* 2002; 59: 1453-7.
- Lemon RN. Variety of functional organization within the monkey motor cortex. *J Physiol* 1981; 311: 521-40.
- Lemon RN, Mantel GW, Muir RB. Corticospinal facilitation of hand muscles during voluntary movement in the conscious monkey. *J Physiol* 1986; 381: 497-527.
- Levin MF. Interjoint coordination during pointing movements is disrupted in spastic hemiparesis. *Brain* 1996; 119 ( Pt 1): 281-93.
- Liepert J. Motor cortex excitability in stroke before and after constraint-induced movement therapy. *Cogn Behav Neurol* 2006; 19: 41-7.
- Liepert J, Hamzei F, Weiller C. Lesion-induced and training-induced brain reorganization. *Restor Neurol Neurosci* 2004; 22: 269-77.
- Liepert J, Storch P, Fritsch A, Weiller C. Motor cortex disinhibition in acute stroke. *Clin Neurophysiol* 2000; 111: 671-6.
- Lum PS, Burgar CG, Shor PC. Evidence for strength imbalances as a significant contributor to abnormal synergies in hemiparetic subjects. *Muscle Nerve* 2003; 27: 211-21.
- Maccabee PJ, Amassian VE, Eberle LP, Cracco RQ. Magnetic coil stimulation of straight and bent amphibian and mammalian peripheral nerve in vitro: locus of excitation. *J Physiol* 1993; 460: 201-19.
- MacKinnon CD, Quartarone A, Rothwell JC. Inter-hemispheric asymmetry of ipsilateral corticofugal projections to proximal muscles in humans. *Exp Brain Res* 2004; 157: 225-33.
- Manganotti P, Patuzzo S, Cortese F, Palermo A, Smania N, Fiaschi A. Motor disinhibition in affected and unaffected hemisphere in the early period of recovery after stroke. *Clin Neurophysiol* 2002; 113: 936-43.
- Marinelli PV. The asymmetric tonic neck reflex. Its presence and significance in the newborn. *Clin Pediatr (Phila)* 1983; 22: 544-6.
- Marshall RS, Perera GM, Lazar RM, Krakauer JW, Constantine RC, DeLaPaz RL. Evolution of cortical activation during recovery from corticospinal tract infarction. *Stroke* 2000; 31: 656-61.

- Mazevet D, Meunier S, Pradat-Diehl P, Marchand-Pauvert V, Pierrot-Deseilligny E. Changes in propriospinally mediated excitation of upper limb motoneurons in stroke patients. *Brain* 2003; 126: 988-1000.
- Mercier C, Bourbonnais D. Relative shoulder flexor and handgrip strength is related to upper limb function after stroke. *Clin Rehabil* 2004; 18: 215-21.
- Meyer G. Forms and spatial arrangement of neurons in the primary motor cortex of man. *J Comp Neurol* 1987; 262: 402-28.
- Mills KR. Magnetic stimulation of the human nervous system. New York: Oxford University Press, 1999.
- Mills KR, Boniface SJ, Schubert M. Magnetic brain stimulation with a double coil: the importance of coil orientation. *Electroencephalogr Clin Neurophysiol* 1992; 85: 17-21.
- Muellbacher W, Artner C, Mamoli B. The role of the intact hemisphere in recovery of midline muscles after recent monohemispheric stroke. *J Neurol* 1999; 246: 250-6.
- Muller K, Kass-Iliyya F, Reitz M. Ontogeny of ipsilateral corticospinal projections: a developmental study with transcranial magnetic stimulation. *Ann Neurol* 1997; 42: 705-11.
- Murphy JT, Kwan HC, MacKay WA, Wong YC. Spatial organization of precentral cortex in awake primates. III. Input-output coupling. *J Neurophysiol* 1978; 41: 1132-9.
- Nakamura H, Kitagawa H, Kawaguchi Y, Tsuji H. Intracortical facilitation and inhibition after transcranial magnetic stimulation in conscious humans. *J Physiol* 1997; 498 ( Pt 3): 817-23.
- Nakamura H, Kitagawa H, Kawaguchi Y, Tsuji H, Takano H, Nakatoh S. Intracortical facilitation and inhibition after paired magnetic stimulation in humans under anesthesia. *Neurosci Lett* 1995; 199: 155-7.
- Nathan PW, Smith M, Deacon P. Vestibulospinal, reticulospinal and descending propriospinal nerve fibres in man. *Brain* 1996; 119 ( Pt 6): 1809-33.
- Nathan PW, Smith MC. The rubrospinal and central tegmental tracts in man. *Brain* 1982; 105: 223-69.
- Netz J, Lammers T, Homberg V. Reorganization of motor output in the non-affected hemisphere after stroke. *Brain* 1997; 120 ( Pt 9): 1579-86.

- Nirkko AC, Ozdoba C, Redmond SM, Burki M, Schroth G, Hess CW, et al. Different ipsilateral representations for distal and proximal movements in the sensorimotor cortex: activation and deactivation patterns. *Neuroimage* 2001; 13: 825-35.
- Nudo RJ, Milliken GW. Reorganization of movement representations in primary motor cortex following focal ischemic infarcts in adult squirrel monkeys. *J Neurophysiol* 1996; 75: 2144-9.
- Olivier E, Baker SN, Nakajima K, Brochier T, Lemon RN. Investigation into non-monosynaptic corticospinal excitation of macaque upper limb single motor units. *J Neurophysiol* 2001; 86: 1573-86.
- Palmer E, Ashby P. Corticospinal projections to upper limb motoneurons in humans. *J Physiol* 1992; 448: 397-412.
- Parmenter CL. The asymmetrical tonic neck reflex in normal first and third grade children. 1975.
- Pascual-Leone A, Cammarota A, Wassermann EM, Brasil-Neto JP, Cohen LG, Hallett M. Modulation of motor cortical outputs to the reading hand of braille readers. *Ann Neurol* 1993; 34: 33-7.
- Penfield W, Rasmussen T. *The cerebral cortex of man: a clinical study of localization of function*. New York: Macmillan, 1950.
- Rao SM, Binder JR, Hammeke TA, Bandettini PA, Bobholz JA, Frost JA, et al. Somatotopic mapping of the human primary motor cortex with functional magnetic resonance imaging. *Neurology* 1995; 45: 919-24.
- Rossini PM, Caltagirone C, Castriota-Scanderbeg A, Cicinelli P, Del Gratta C, Demartin M, et al. Hand motor cortical area reorganization in stroke: a study with fMRI, MEG and TCS maps. *Neuroreport* 1998; 9: 2141-6.
- Rothwell JC. Techniques and mechanisms of action of transcranial stimulation of the human motor cortex. *J Neurosci Methods* 1997; 74: 113-22.
- Ruohonen J, Ilmoniemi RJ. Modeling of the stimulating field generation in TMS. *Electroencephalogr Clin Neurophysiol Suppl* 1999; 51: 30-40.
- Schwerin SC, Dewald JPA. OPTIMAL INTERPULSE INTERVAL IN DUAL PULSE TMS FOR MAXIMAL FACILITATION OF PROXIMAL MUSCLES AFTER STROKE, 2003.

- Schwerin SC, Dewald JPA. IPSILATERAL HEMISPHERE CONTROL OF UPPER EXTREMITY MUSCLES FOLLOWING HEMIPARETIC STROKE USING TRANSCRANIAL MAGNETIC STIMULATION, 2004.
- Schwerin SC, Dewald JPA. NECK REFLEX-MEDIATED CHANGES IN ELBOW FLEXOR/EXTENSOR ACTIVITY POST STROKE: PRELIMINARY EVIDENCE FOR AN AUGMENTED ROLE OF CORTICOBULBOSPINAL PATHWAYS. Society for Neuroscience. Washington, DC, 2005.
- Serrien DJ, Strens LH, Cassidy MJ, Thompson AJ, Brown P. Functional significance of the ipsilateral hemisphere during movement of the affected hand after stroke. *Exp Neurol* 2004; 190: 425-32.
- Stepniewska I, Preuss TM, Kaas JH. Architectonics, somatotopic organization, and ipsilateral cortical connections of the primary motor area (M1) of owl monkeys. *J Comp Neurol* 1993; 330: 238-71.
- Strens LH, Fogelson N, Shanahan P, Rothwell JC, Brown P. The ipsilateral human motor cortex can functionally compensate for acute contralateral motor cortex dysfunction. *Curr Biol* 2003; 13: 1201-5.
- Talelli P, Greenwood RJ, Rothwell JC. Arm function after stroke: neurophysiological correlates and recovery mechanisms assessed by transcranial magnetic stimulation. *Clin Neurophysiol* 2006; 117: 1641-59.
- Thickbroom GW, Byrnes ML, Archer SA, Mastaglia FL. Motor outcome after subcortical stroke correlates with the degree of cortical reorganization. *Clin Neurophysiol* 2004; 115: 2144-50.
- Thickbroom GW, Sammut R, Mastaglia FL. Magnetic stimulation mapping of motor cortex: factors contributing to map area. *Electroencephalogr Clin Neurophysiol* 1998; 109: 79-84.
- Tombari D, Loubinoux I, Pariente J, Gerdelat A, Albucher JF, Tardy J, et al. A longitudinal fMRI study: in recovering and then in clinically stable sub-cortical stroke patients. *Neuroimage* 2004; 23: 827-39.
- Traversa R, Cicinelli P, Bassi A, Rossini PM, Bernardi G. Mapping of motor cortical reorganization after stroke. A brain stimulation study with focal magnetic pulses. *Stroke* 1997; 28: 110-7.

- Traversa R, Cicinelli P, Oliveri M, Giuseppina Palmieri M, Filippi MM, Pasqualetti P, et al. Neurophysiological follow-up of motor cortical output in stroke patients. *Clin Neurophysiol* 2000; 111: 1695-703.
- Turton A, Lemon RN. The contribution of fast corticospinal input to the voluntary activation of proximal muscles in normal subjects and in stroke patients. *Exp Brain Res* 1999; 129: 559-72.
- Turton A, Wroe S, Trepte N, Fraser C, Lemon RN. Contralateral and ipsilateral EMG responses to transcranial magnetic stimulation during recovery of arm and hand function after stroke. *Electroencephalogr Clin Neurophysiol* 1996; 101: 316-28.
- Twitchell TE. The restoration of motor function following hemiplegia in man. *Brain* 1951; 74: 443-80.
- Valls-Sole J, Pascual-Leone A, Wassermann EM, Hallett M. Human motor evoked responses to paired transcranial magnetic stimuli. *Electroencephalogr Clin Neurophysiol* 1992; 85: 355-64.
- van Kranen-Mastenbroek VH, Folmer KB, Caberg HB, Kingma H, Blanco CE, Troost J, et al. The influence of head position and head position change on spontaneous body posture and motility in full-term AGA and SGA newborn infants. *Brain Dev* 1997; 19: 104-10.
- Verleger R, Adam S, Rose M, Vollmer C, Wauschkuhn B, Kompf D. Control of hand movements after striatocapsular stroke: high-resolution temporal analysis of the function of ipsilateral activation. *Clin Neurophysiol* 2003; 114: 1468-76.
- Vles JS, van Oostenbrugge R, Kingma H, Caberg H, Casaer P. Influence of head position and head position-change on body posture in pre-term infants (A.T.N.R.). 1988.
- Ward NS, Brown MM, Thompson AJ, Frackowiak RS. Neural correlates of outcome after stroke: a cross-sectional fMRI study. *Brain* 2003; 126: 1430-48.
- Wassermann EM, McShane LM, Hallett M, Cohen LG. Noninvasive mapping of muscle representations in human motor cortex. *Electroencephalogr Clin Neurophysiol* 1992; 85: 1-8.
- Wassermann EM, Pascual-Leone A, Hallett M. Cortical motor representation of the ipsilateral hand and arm. *Exp Brain Res* 1994; 100: 121-32.

- Waters RS, Samulack DD, Dykes RW, McKinley PA. Topographic organization of baboon primary motor cortex: face, hand, forelimb, and shoulder representation. *Somatosens Mot Res* 1990; 7: 485-514.
- Weiller C, Ramsay SC, Wise RJ, Friston KJ, Frackowiak RS. Individual patterns of functional reorganization in the human cerebral cortex after capsular infarction. *Ann Neurol* 1993; 33: 181-9.
- Weiss T, Miltner WH, Dillmann J, Meissner W, Huonker R, Nowak H. Reorganization of the somatosensory cortex after amputation of the index finger. *Neuroreport* 1998; 9: 213-6.
- Werhahn KJ, Conforto AB, Kadom N, Hallett M, Cohen LG. Contribution of the ipsilateral motor cortex to recovery after chronic stroke. *Ann Neurol* 2003; 54: 464-72.
- Wilson V, Peterson B. Vestibulo and reticulospinal systems. In: Brooks V, editor. *Handbook of Physiology, Section I, Motor control. Vol II.* Bethesda, MD: American Phys Society, 1981: 667-702.
- Wolf SL, Butler AJ, Campana GI, Parris TA, Struys DM, Weinstein SR, et al. Intra-subject reliability of parameters contributing to maps generated by transcranial magnetic stimulation in able-bodied adults. *Clin Neurophysiol* 2004; 115: 1740-7.
- Woolsey CN, Settlage PH, Meyer DR, Sencer W, Pinto Hamuy T, Travis AM. Patterns of localization in precentral and "supplementary" motor areas and their relation to the concept of a premotor area. *Res Publ Assoc Res Nerv Ment Dis* 1952; 30: 238-64.
- Zemke R. Application of an ATNR rating scale to normal preschool children. 1985.
- Ziemann U. Intracortical inhibition and facilitation in the conventional paired TMS paradigm. *Electroencephalogr Clin Neurophysiol Suppl* 1999; 51: 127-36.
- Ziemann U, Ishii K, Borgheresi A, Yaseen Z, Battaglia F, Hallett M, et al. Dissociation of the pathways mediating ipsilateral and contralateral motor-evoked potentials in human hand and arm muscles. *J Physiol* 1999; 518 ( Pt 3): 895-906.



## **10 APPENDIX**

### ***10.1 Stimulation Grid Generation***

A stimulation grid is generated for each subject using that subject's anatomical MRI. The grid is 1 cm spaced on the scalp surface and is aligned with the anatomical sagittal, coronal, and axial planes as determined by the anatomical landmarks of nasion,inion and preauricular points.

#### ***10.1.1 MRI Utilization***

##### **10.1.1.1 Segmentation**

Each subject's MRI is uploaded into Curry. Segmentation is done for the cortex (see figure A.1) and the skin (see figure A.2). Cortex segmentation will be used much later to project the hotspots located on the scalp surface onto the cortical surface to investigate shifts in location. The skin segmentation will be used to generate the surface mesh used for stimulation grid generation.

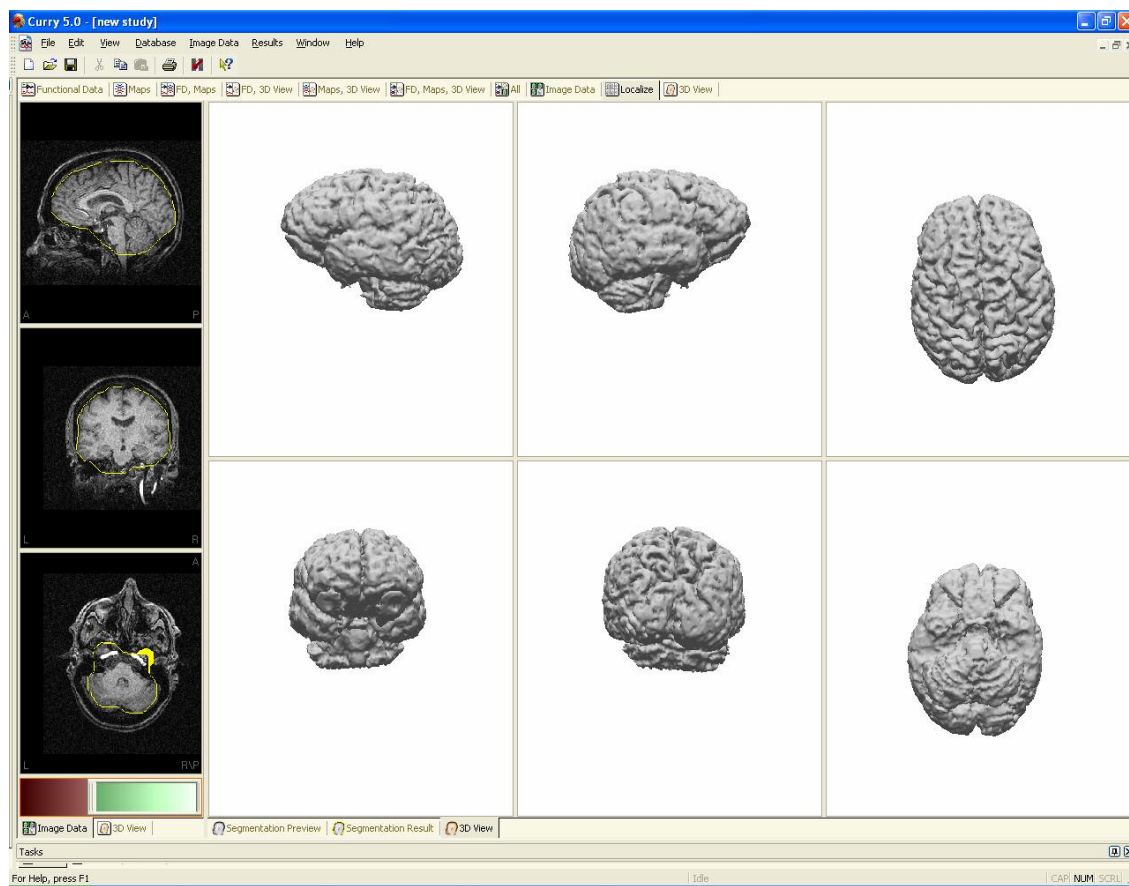


**Figure 10-1 Cortex Segmentation**

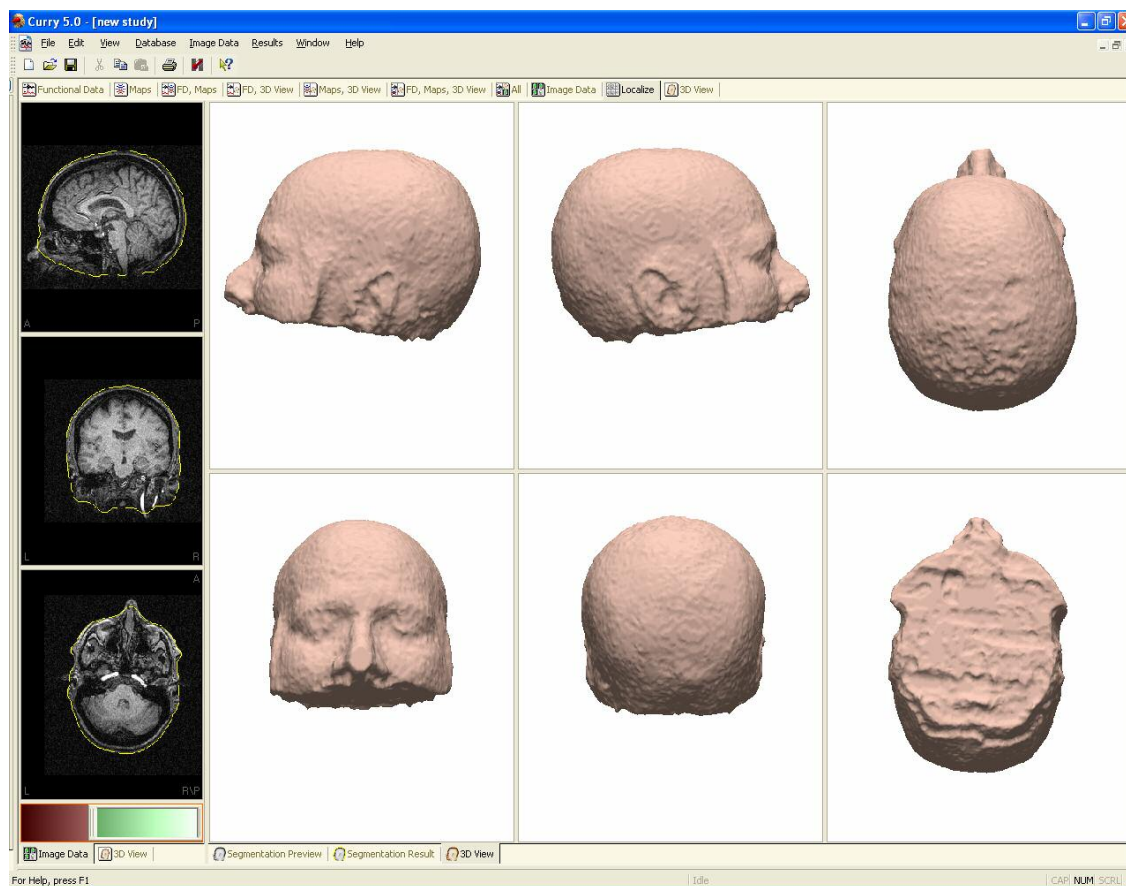


**Figure 10-2** Skin Segmentation.

### 10.1.1.2 Landmarks

The anatomical landmarks are chosen on the MRI: nasion,inion, preauricular points, and eye corners if the preauricular points are unidentifiable (see figure A.3). The anatomical landmarks will be used to determine the anatomical planes as well as for coregistration of actual stimulation points with the MRI.

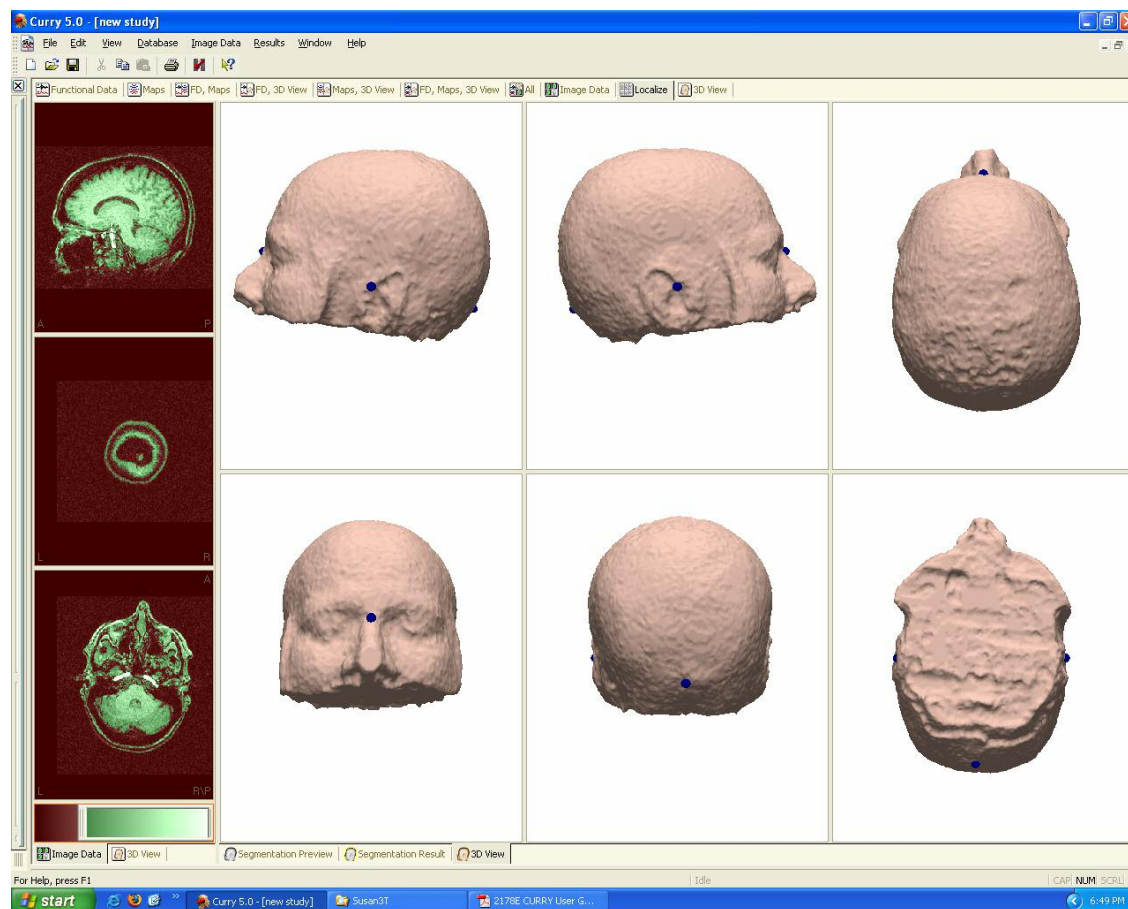


Figure 10-3 Anatomical Landmarks

### 10.1.1.3 Anatomical Plane Identification

Orthogonal axial, coronal and sagittal planes were generated using the surface landmarks (nasion,inion, left and right pre-auricular points): the sagittal plane was defined by the nasion and inion and the longitudinal fissure, the coronal plane by the pre-auricular points, and the axial plane was the plane perpendicular to the other two, positioned superior to the ears. (see figure A.4). The seedpoint as well as the normals to the planes were recorded. These planes will be used to generate the stimulation grid.

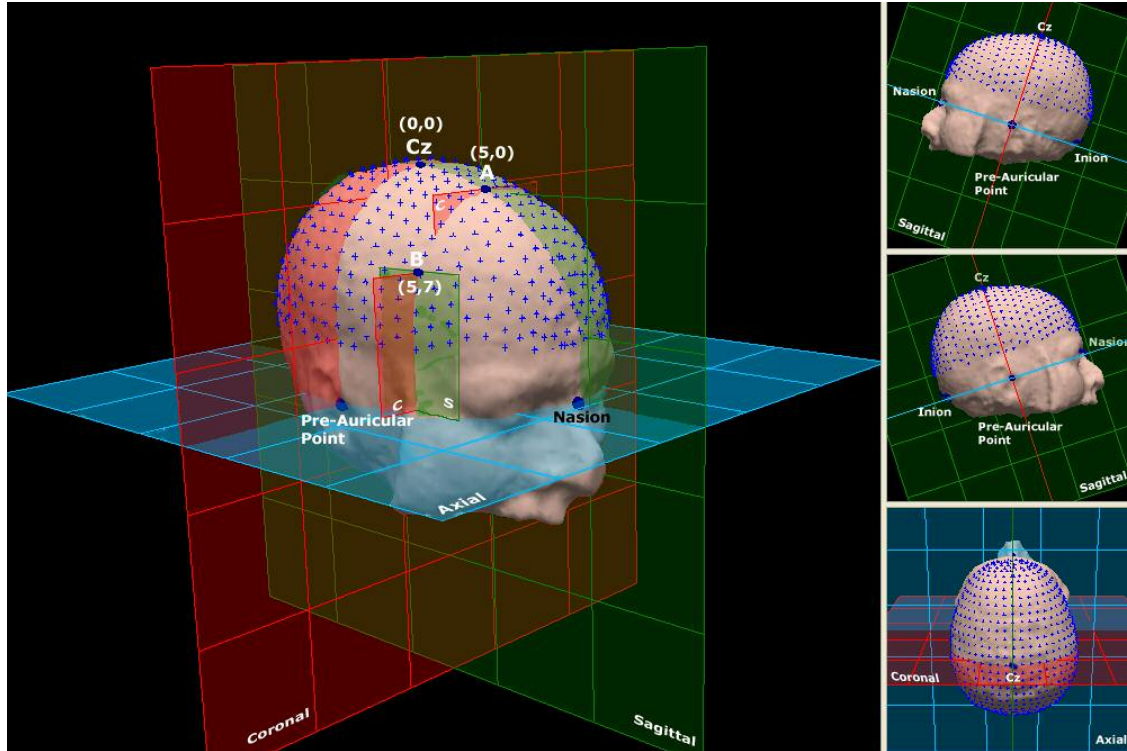
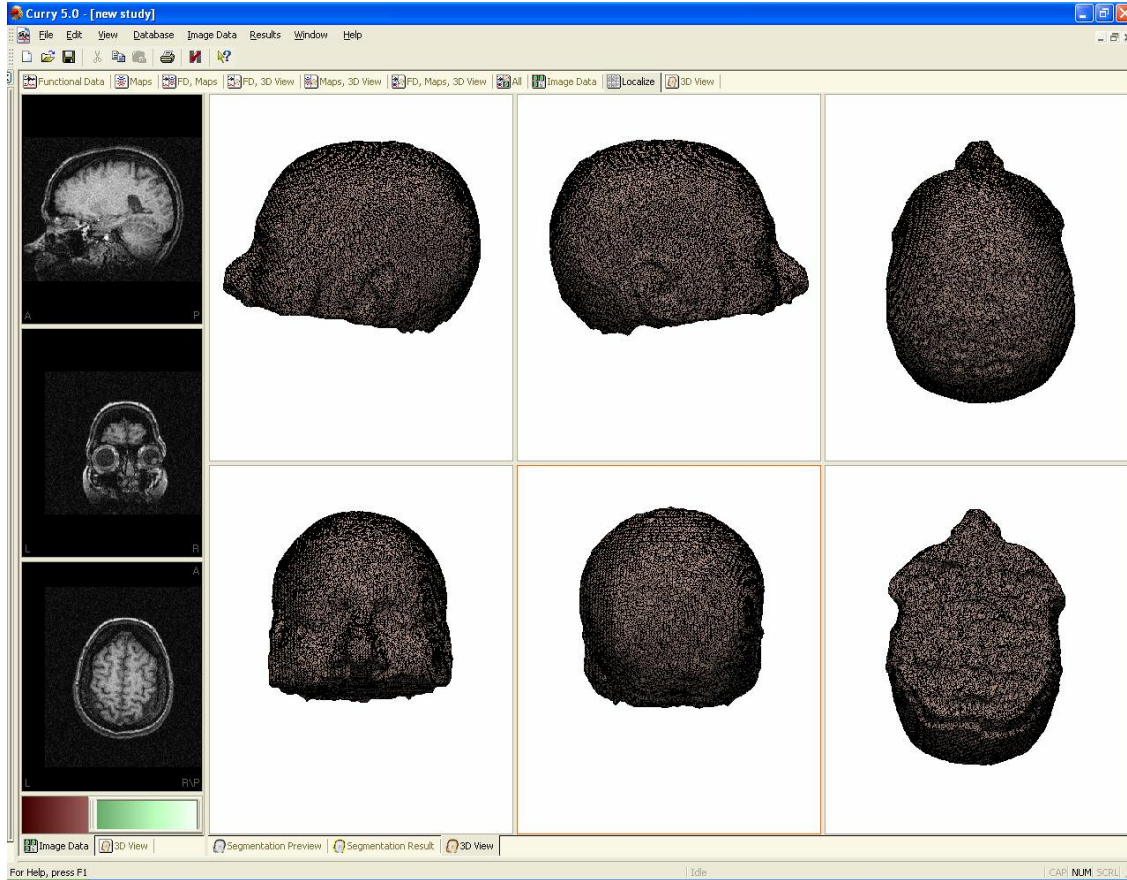


Figure 10-4 Anatomical Planes

#### 10.1.1.4 Triangulation of Head Surface

Using Curry we generated a surface mesh using 1 mm triangles. This will be used to generate the stimulation grid as well as to determine the closest point in the mesh to the current wand position to direct the wand to be held tangential to the head at that point. (see figure A.5).



**Figure 10-5** Triangulation Mesh.

### *10.1.2 Stimulation Grid Generation*

The stimulation grid was generated using Matlab. The main program is named Headsurfgrid.m. The seedpoints and normals to the anatomical planes determined above are used in addition to the surface mesh. The grid points were defined as the skin surface locations of the intersection of 1 cm spaced planes parallel to the coronal and sagittal planes (see figure A.4). The grid continued along the skin surface down to the axial plane. The following m-files are used and will be provided immediately after a short description of the program:

- **HeadsurfGrid.m**
- **read\_Curry\_file3.m**
- **selectPoint2.m**
- **find\_dis2plane.m**
- **proj\_curve.m**
- **GetEnvelope2.m**



- `find_subset.m`

### 10.1.2.1 Headsurfgrid.m

In matlab, run headsurfgrid. A window will open (see figure A.6)

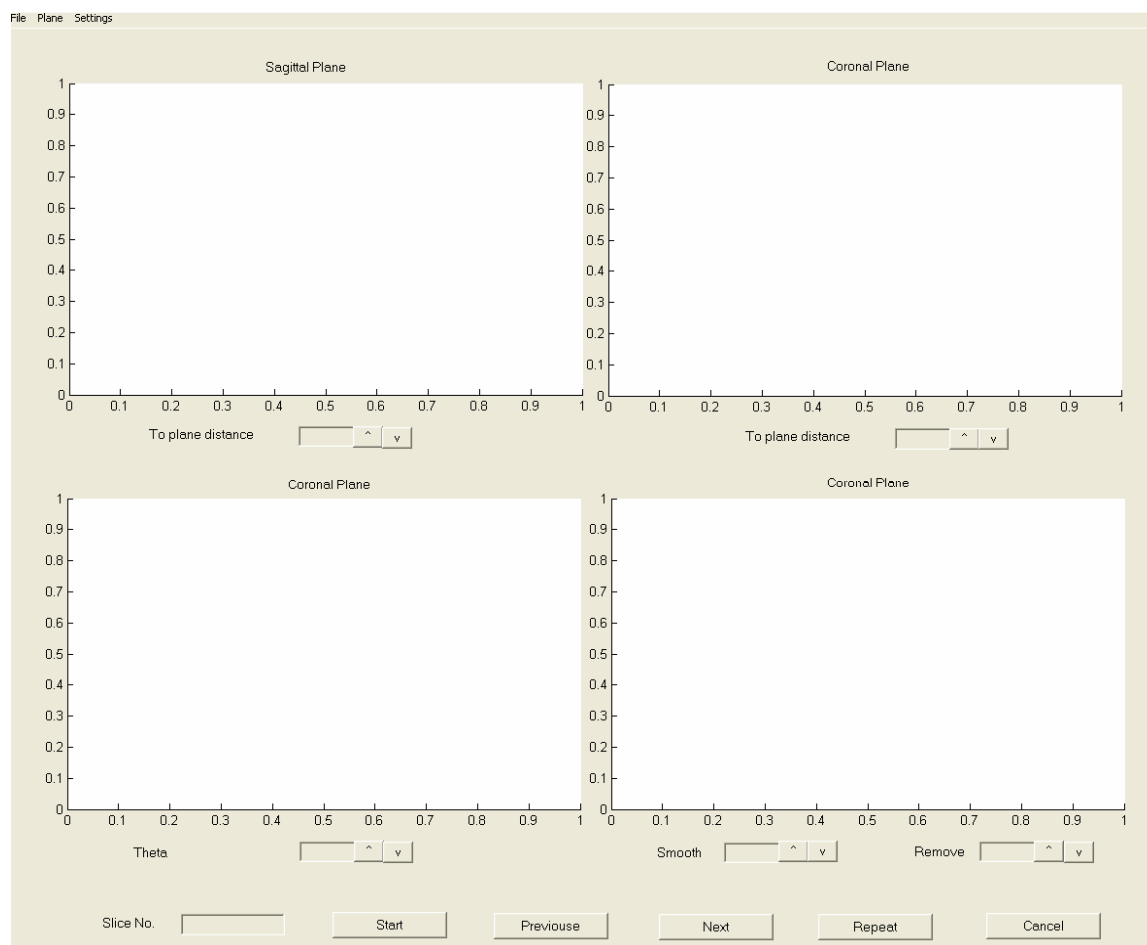


**Figure 10-6** Headsurfgrid Window

Click File, click open. The program will prompt for you to load a .bd0 file, however, you may have named the triangulation mesh as a .bd1-.bd9 file. If that is the case, simply change the preferences to any file type and choose your file.

Click Plane. Enter the plane seedpoint and the normal to each plane.

Example seedpoint:

-1.3 -7.0 25.1

Example normal to each plane:

Sagittal:     .990   .026   -.020  
 Coronal:     -.02   .965   .262  
 Axial:       .026   -.261   .965

Under settings, you can either choose a 1cm space grid, or normalize among different head sizes by choosing the number of points you desire between the Cz and the most lateral point of the grid.

Once everything has been entered hit the start button at the bottom of the screen. The window will look something like figure A.7.

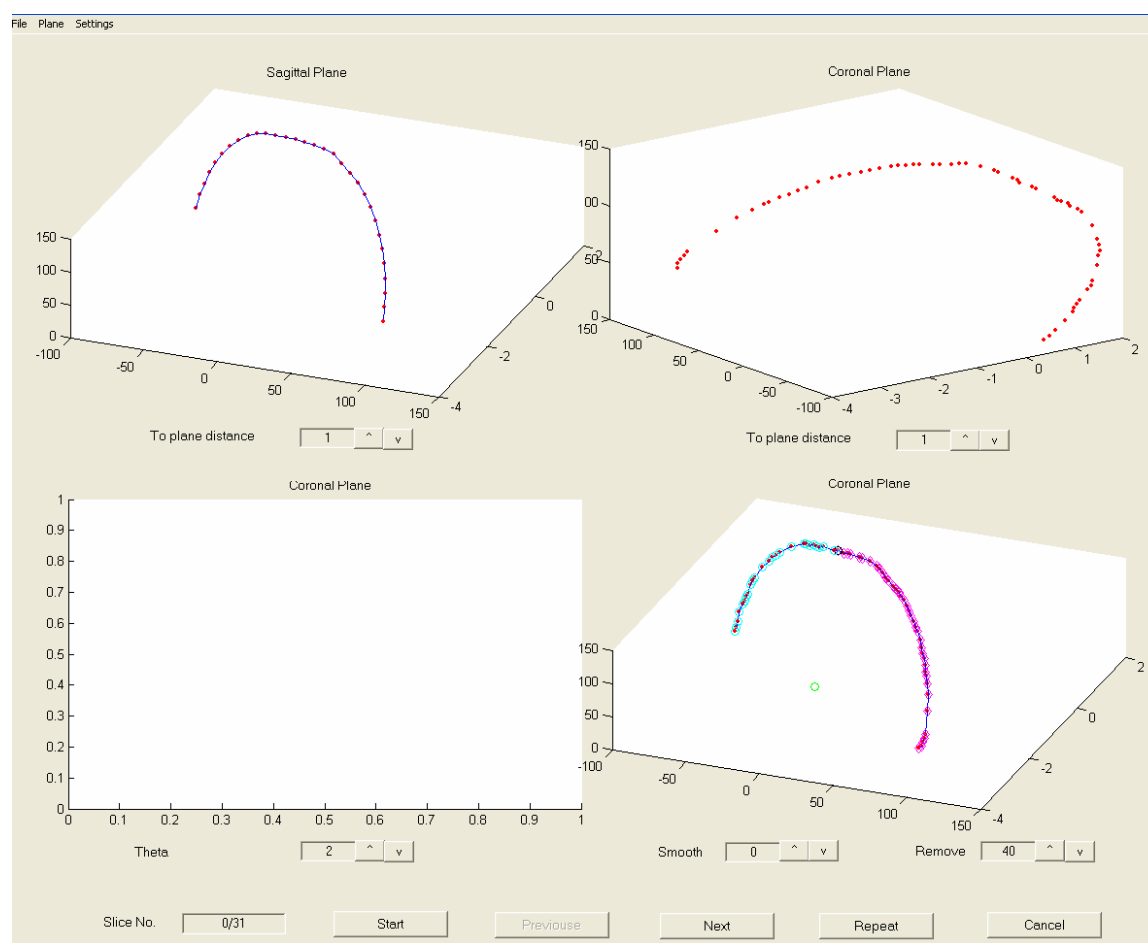


Figure 10-7 Headsurfgrid start results.



Continue clicking next until you reach the end of the head (see figure A.8 for midway through, and figure A.9 for completed). Using theta you can exclude points, using smooth you can smooth the curvefit.

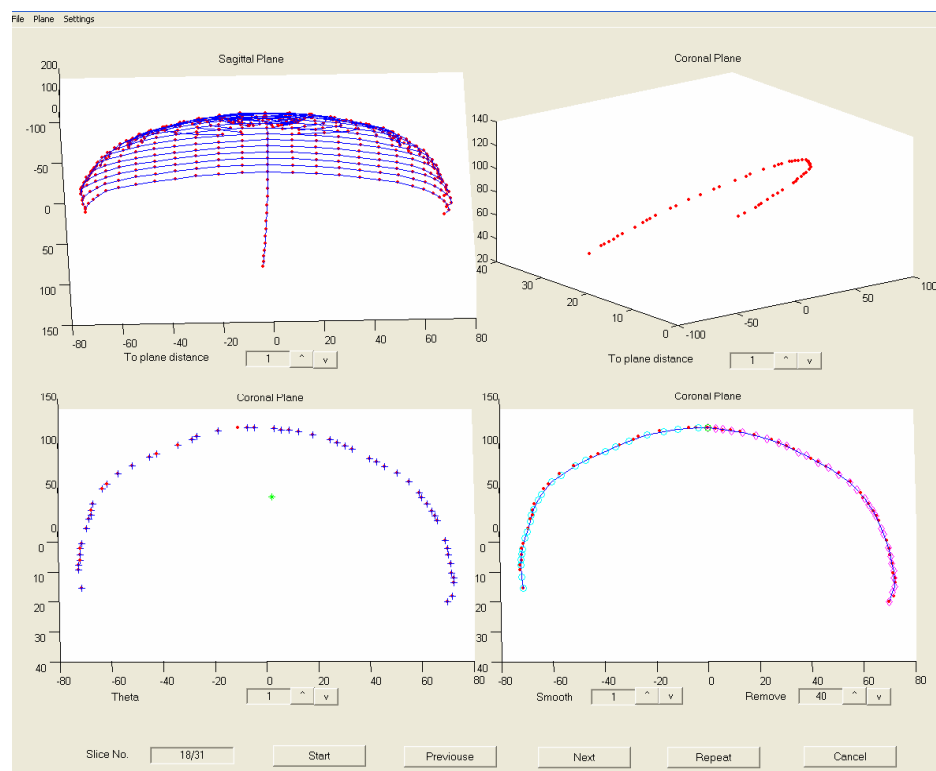
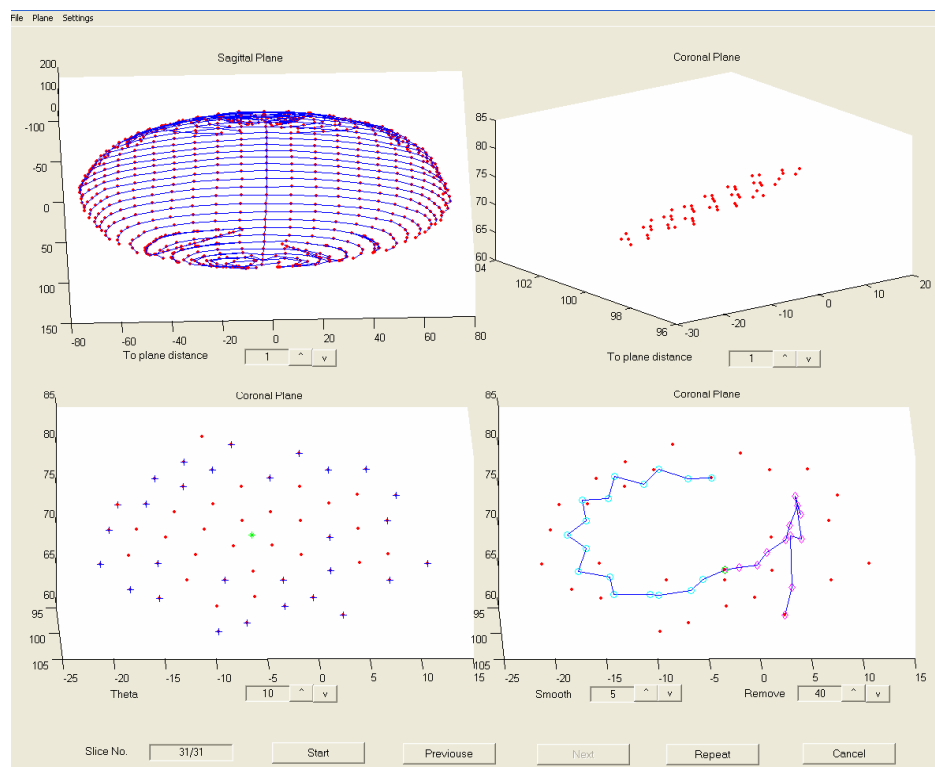


Figure 10-8 Headsurfgrid midway results.



**Figure 10-9** Headsurfgrid final results.

Under File, choose save. Output file has 5 columns, the first two are the x,y locations using Cz as the (0,0) point and each gridpoint anterior-posterior and medial-lateral as 1 cm away. The next 3 columns are the x, y, z, locations in the Curry coordinate frame.

Example output file (the ... represent unprinted data to keep the example short):

-12.000000	16.000000	-2.809900	-94.473742	26.868800
-11.000000	16.000000	-3.500137	-94.473742	35.181013
-10.000000	16.000000	-1.476504	-94.473742	44.851104
-9.000000	16.000000	-1.532234	-94.473742	47.295896
-8.000000	16.000000	-9.710777	-94.473742	42.320138
-7.000000	16.000000	-6.934229	-94.473742	42.896330
-6.000000	16.000000	-8.189467	-94.473742	38.466018
-5.000000	16.000000	-9.858433	-94.473742	34.151982
-4.000000	16.000000	-11.653804	-94.473742	30.467496
-3.000000	16.000000	-14.370932	-94.473742	24.546309
-2.000000	16.000000	-10.228068	-94.473742	19.949618
-1.000000	16.000000	-4.321355	-94.473742	18.169922
0.000000	16.000000	0.000000	-94.473742	25.925046
1.000000	16.000000	5.691800	-94.473742	21.294782
2.000000	16.000000	10.719136	-94.473742	21.890271
3.000000	16.000000	12.775250	-94.473742	30.135052
4.000000	16.000000	12.392021	-94.473742	25.931568

5.000000	16.000000	5.667934	-94.473742	27.375349
6.000000	16.000000	1.449842	-94.473742	31.800189
7.000000	16.000000	3.143402	-94.473742	41.189383
8.000000	16.000000	8.858876	-94.473742	36.090417
9.000000	16.000000	5.113148	-94.473742	35.446089
10.000000	16.000000	10.871718	-94.473742	38.626199
11.000000	16.000000	3.027146	-94.473742	41.811296
12.000000	16.000000	1.730231	-94.473742	48.475469
13.000000	16.000000	2.416209	-94.473742	38.499025
14.000000	16.000000	3.102187	-94.473742	28.522581
15.000000	16.000000	3.788165	-94.473742	18.546137
.				
.				
.				
-17.000000	0.000000	-61.832605	0.720297	7.631304
-16.000000	0.000000	-63.712141	0.720297	17.450613
-15.000000	0.000000	-68.404733	0.720297	25.815985
-14.000000	0.000000	-72.277347	0.720297	34.705451
-13.000000	0.000000	-73.214230	0.720297	44.649823
-12.000000	0.000000	-73.516329	0.720297	54.645200
-11.000000	0.000000	-72.687829	0.720297	64.495952
-10.000000	0.000000	-69.883261	0.720297	74.091883
-9.000000	0.000000	-67.214067	0.720297	83.689913
-8.000000	0.000000	-63.321291	0.720297	92.900036
-7.000000	0.000000	-58.428019	0.720297	101.546845
-6.000000	0.000000	-51.834159	0.720297	109.009237
-5.000000	0.000000	-44.191418	0.720297	115.456627
-4.000000	0.000000	-36.398819	0.720297	121.629407
-3.000000	0.000000	-28.150695	0.720297	127.273912
-2.000000	0.000000	-19.552526	0.720297	132.276660
-1.000000	0.000000	-9.977899	0.720297	134.787831
0.000000	0.000000	0.000000	0.720297	135.348000
1.000000	0.000000	9.967900	0.720297	134.547388
2.000000	0.000000	19.434463	0.720297	131.669185
3.000000	0.000000	28.091623	0.720297	126.663830
4.000000	0.000000	36.652422	0.720297	121.529447
5.000000	0.000000	43.909614	0.720297	114.649538
6.000000	0.000000	51.383866	0.720297	108.078402
7.000000	0.000000	57.371679	0.720297	100.142342
8.000000	0.000000	61.798724	0.720297	91.201413
9.000000	0.000000	65.986468	0.720297	82.201242
10.000000	0.000000	68.827368	0.720297	72.637333
11.000000	0.000000	70.446400	0.720297	62.803100
12.000000	0.000000	70.940600	0.720297	52.827973
13.000000	0.000000	71.787418	0.720297	42.877272
14.000000	0.000000	71.833592	0.720297	32.981909
15.000000	0.000000	70.511501	0.720297	23.069691
16.000000	0.000000	69.112843	0.720297	13.281145
17.000000	0.000000	66.089851	0.720297	4.167816
.				

.

.

-10.000000	-14.000000	-11.880368	100.888090	69.424364
-9.000000	-14.000000	-16.311875	100.888090	60.489750
-8.000000	-14.000000	-20.270888	100.888090	63.915728
-7.000000	-14.000000	-15.079546	100.888090	62.096010
-6.000000	-14.000000	-11.516336	100.888090	57.930575
-5.000000	-14.000000	-6.912835	100.888090	55.680739
-4.000000	-14.000000	-0.659051	100.888090	59.997677
-3.000000	-14.000000	-2.580287	100.888090	68.245291
-2.000000	-14.000000	-8.309819	100.888090	69.763789
-1.000000	-14.000000	-5.313480	100.888090	63.957101
0.000000	-14.000000	0.000000	100.888090	59.688659
1.000000	-14.000000	8.117483	100.888090	58.960364
2.000000	-14.000000	3.399811	100.888090	58.455047
3.000000	-14.000000	10.065424	100.888090	64.863889
4.000000	-14.000000	4.295080	100.888090	68.989924
5.000000	-14.000000	8.364382	100.888090	68.757349

## 10.1.2.2 The m-files used follow.

### 10.1.2.2.1 *HeadSurfGrid.m*

```

function varargout = HeadSurfGrid(varargin)
% HEADSURFGRID Application M-file for HeadSurfGrid.fig
% FIG = HEADSURFGRID launch HeadSurfGrid GUI.
% HEADSURFGRID('callback_name', ...) invoke the named callback.

% Last Modified by GUIDE v2.0 03-Jan-2003 14:21:07
if nargin <= 1 % LAUNCH GUI

    fig = openfig(mfilename,'reuse');
    % Use system color scheme for figure:
    set(fig,'Color',get(0,'defaultUicontrolBackgroundColor'));
    % Generate a structure of handles to pass to callbacks, and store it.
    handles = guihandles(fig);
    % Save handles structure
    if nargin == 1
        if exist(varargin(Darian-Smith et al.),'file')
            set(handles.curryFile,'String',varargin(Darian-Smith et al.));
            [head_points,count,NR]=read_Curry_file3(handles.curryFile,'LOCATION',0,0);
            handles.head_points=head_points;
            guidata(fig,handles)

        else
            errordlg('File Not Found','File Load Error')
            set(handles.curryFile,'String','')
        end
    end

    handles.Sagittal_seed=[0 0 0];
    handles.Sagittal_normal=[1 0 0];
    handles.Coronal_seed=[0 0 0];
    handles.Coronal_normal=[0 1 0];
    handles.Axial_seed=[0 0 0];
    handles.Axial_normal=[0 0 1];
    handles.ArcFix=1;
    handles.deltaArc=10; %in (mm)

```

```

handles.seedNum=10;
set(handles.dis2plane1,'String','1');
set(handles.dis2plane2,'String','1');
set(handles.Theta,'String','2');
set(handles.Smooth,'String','0');
set(handles.Remove_dis,'String','40');
set(handles.SliceNo,'String','0');
set(handles.goBackward,'enable','off');
set(handles.goForward,'enable','off');
set(handles.Repeat,'enable','off');
handles.head_points=[];
handles.temp_curve=[];
handles.plane_seeds=[];
handles.headgrid={};
handles.sliceIndex=0;
handles.Sag_Index=[];
handles.Co_Index=[];

guidata(fig, handles);

% If there is an output argument assigned,
% the first one is the figure handle
if nargout > 0
    varargout(Darian-Smith et al.) = fig;
end

elseif ischar(varargin(Darian-Smith et al.)) % INVOKE NAMED SUBFUNCTION OR
CALLBACK
    try
        if (nargout)
            [varargout{1:nargout}] = feval(varargin{:}); % FEVAL switchyard
        else
            feval(varargin{:}); % FEVAL switchyard
        end
    catch
        disp(lasterr);
    end
end

%| ABOUT CALLBACKS:
%| GUIDE automatically appends subfunction prototypes to this file, and

```

```

%| sets objects' callback properties to call them through the FEVAL
%| switchyard above. This comment describes that mechanism.
%|
%| Each callback subfunction declaration has the following form:
%| <SUBFUNCTION_NAME>(H, EVENTDATA, HANDLES, VARARGIN)
%|
%| The subfunction name is composed using the object's Tag and the
%| callback type separated by '_', e.g. 'slider2_Callback',
%| 'figure1_CloseRequestFcn', 'axis1_ButtondownFcn'.
%|
%| H is the callback object's handle (obtained using GCBO).
%|
%| EVENTDATA is empty, but reserved for future use.
%|
%| HANDLES is a structure containing handles of components in GUI using
%| tags as fieldnames, e.g. handles.figure1, handles.slider2. This
%| structure is created at GUI startup using GUIHANDLES and stored in
%| the figure's application data using GUIDATA. A copy of the structure
%| is passed to each callback. You can store additional information in
%| this structure at GUI startup, and you can change the structure
%| during callbacks. Call guidata(h, handles) after changing your
%| copy to replace the stored original so that subsequent callbacks see
%| the updates. Type "help guihandles" and "help guidata" for more
%| information.
%|
%| VARARGIN contains any extra arguments you have passed to the
%| callback. Specify the extra arguments by editing the callback
%| property in the inspector. By default, GUIDE sets the property to:
%| <MFILENAME>('<SUBFUNCTION_NAME>', gcbo, [], guidata(gcbo))
%| Add any extra arguments after the last argument, before the final
%| closing parenthesis.

% -----
function varargout = File_Callback(h, eventdata, handles, varargin)

% -----
function varargout = Open_file_Callback(h, eventdata, handles, varargin)

```

```

% Use UIGETFILE to allow for the selection of a custom address book.
[filename, pathname] = uigetfile( ...
    {'*.bd0', 'All MAT-Files (*.bd0)'; ...
    '*.*', 'All Files (*.*)'}, ...
    'Select curry file');
% If "Cancel" is selected then return
if isequal([filename,pathname],[0,0])
    return
% Otherwise construct the fullfilename and Check and load the file.
else
    File = fullfile(pathname,filename);
    handles.LastFile=File;
    [head_points,count,NR]=read_Curry_file3(File,'LOCATION',0,0);
    handles.head_points=head_points;
    guidata(h,handles)
end

```

```

% -----
function varargout = Save_file_Callback(h, eventdata, handles, varargin)

```

```

% Get the Tag of the menu selected
Tag = get(h,'Tag');
% Get the address array
plane_seeds = handles.plane_seeds;
headGrid = handles.headgrid;
% Based on the item selected, take the appropriate action
switch Tag
case 'Save_file'
    % Save to the default addrbook file
    File = handles.LastFile;
    FileExtInd = find(File==' ');
    File = [File(1:FileExtInd),'HG'];
    fid=fopen(File,'wt');
    for i=1:size(plane_seeds,1)
        y=handles.Sag_Index(i);
        %if (size(susan_Point{i},1)>3 & size(susan_Point{i},1)<50 )
        Point_remain=headGrid{i};
        %err_now=susan_err{i};
        Cor_ind=handles.Cor_Index{i};
    end
end

```



```

        for j=1:size(Point_remain,1)
            x=Cor_ind(j);
            fprintf(fid,'%f\t%f\t%f\t%f\t%f\t%f',x,-
1*y,Point_remain(j,1),Point_remain(j,2),Point_remain(j,3));
            fprintf(fid,'\n');
        end
    %end
end

fclose(fid);
case 'Save_as'
    % Allow the user to select the file name to save to
    [filename, pathname] = uiputfile( ...
        {'*.HG','*.*'}, ...
        'Save as');
    % If 'Cancel' was selected then return
    if isequal([filename,pathname],[0,0])
        return
    else
        % Construct the full path and save
        File = fullfile(pathname,filename);
        fid=fopen(File,'wt');
        for i=1:size(plane_seeds,1)
            y=handles.Sag_Index(i);
            %if (size(susan_Point{i},1)>3 & size(susan_Point{i},1)<50 )
            Point_remain=headGrid{i};
            %err_now=susan_err{i};
            Cor_ind=handles.Cor_Index{i};
            for j=1:size(Point_remain,1)
                x=Cor_ind(j);
                fprintf(fid,'%f\t%f\t%f\t%f\t%f\t%f',x,-
1*y,Point_remain(j,1),Point_remain(j,2),Point_remain(j,3));
                fprintf(fid,'\n');
            end
        %end
        end
        fclose(fid);
        handles.LastFile = File;
        guidata(h,handles)
    end
end
handles.deltaarc

```

```
% -----
function varargout = Plane_define_Callback(h, eventdata, handles, varargin)
```

```
handles=plane_def(handles);
guidata(h,handles);
```

```
% -----
function varargout = Setings_Callback(h, eventdata, handles, varargin)
```

```
handles=settings(handles);
guidata(h,handles)
```

```
% -----
function varargout = dis2plane1_Callback(h, eventdata, handles, varargin)
```

```
get(handles.dis2plane1,'String');
guidata(h,handles)
```

```
% -----
function varargout = dis2plane1add_Callback(h, eventdata, handles, varargin)
```

```
val = num2str(str2num(get(handles.dis2plane1,'String'))+0.5);
set (handles.dis2plane1,'String',val);
guidata(h,handles)
```

```
% -----
function varargout = dis2plane1Minu_Callback(h, eventdata, handles, varargin)
```

```
val = num2str(str2num(get(handles.dis2plane1,'String'))-0.5);
set (handles.dis2plane1,'String',val);
guidata(h,handles)
```

```
% -----
function varargout = dis2plane2_Callback(h, eventdata, handles, varargin)
```

```
get(handles.dis2plane2,'String');
guidata(h,handles)
```

```
% -----
function varargout = dis2plane2Add_Callback(h, eventdata, handles, varargin)
```

```
val = num2str(str2num(get(handles.dis2plane2,'String'))+0.5);
set (handles.dis2plane2,'String',val);
guidata(h,handles)
```

```
% -----
function varargout = dis2plane2Minu_Callback(h, eventdata, handles, varargin)
```

```
val = num2str(str2num(get(handles.dis2plane2,'String'))-0.5);
set (handles.dis2plane2,'String',val);
guidata(h,handles)
```

```
% -----
function varargout = Theta_Callback(h, eventdata, handles, varargin)
```

```
get(handles.Theta,'String');
guidata(h,handles)
```

```
% -----
function varargout = ThetaAdd_Callback(h, eventdata, handles, varargin)
```

```
val = num2str(str2num(get(handles.Theta,'String'))+1);
set (handles.Theta,'String',val);
guidata(h,handles)
```

```
% -----
function varargout = ThetaMinu_Callback(h, eventdata, handles, varargin)
```

```
val = num2str(str2num(get(handles.Theta,'String'))-1);
```

```
set(handles.Theta,'String',val);
guidata(h,handles)
```

```
% -----
function varargout = Smooth_Callback(h, eventdata, handles, varargin)
```

```
get(handles.Smooth,'String');
guidata(h,handles)
```

```
% -----
function varargout = smoothAdd_Callback(h, eventdata, handles, varargin)
```

```
val = num2str(str2num(get(handles.Smooth,'String'))+1);
set(handles.Smooth,'String',val);
guidata(h,handles)
```

```
% -----
function varargout = smoothMinu_Callback(h, eventdata, handles, varargin)
```

```
val = num2str(str2num(get(handles.Smooth,'String'))-1);
set(handles.Smooth,'String',val);
guidata(h,handles)
```

```
% -----
function varargout = Remove_dis_Callback(h, eventdata, handles, varargin)
```

```
get(handles.Remove_dis,'String');
guidata(h,handles)
```

```
% -----
function varargout = Remove_disAdd_Callback(h, eventdata, handles, varargin)
```

```
val = num2str(str2num(get(handles.Remove_dis,'String'))+0.5);
set(handles.Remove_dis,'String',val);
```

```

guidata(h,handles)

% -----
function varargout = Remove_disMinu_Callback(h, eventdata, handles, varargin)

val = num2str(str2num(get(handles.Remove_dis,'String'))-0.5);
set (handles.Remove_dis,'String',val);
guidata(h,handles)

% -----
function varargout = SliceNo_Callback(h, eventdata, handles, varargin)

% -----
function varargout = goBackward_Callback(h, eventdata, handles, varargin)
sliceNo=get(handles.SliceNo,'String');
index=find(sliceNo=='/');
sliceTotal=sliceNo(index:end);
totalNum=str2num(sliceTotal(2:end));
handles.sliceIndex=handles.sliceIndex-1;
set(handles.SliceNo,'String',[num2str(handles.sliceIndex),sliceTotal]);
guidata(h,handles)

Theta=get(handles.Theta,'String');
dis2plane=get(handles.dis2plane1,'String');
Smooth=get(handles.Smooth,'String');
remove_dis=get(handles.Remove_dis,'String');

[handles.headgrid{handles.sliceIndex},handles.deltaArc,Med(handles.sliceIndex),handles.Cor_I
ndex{handles.sliceIndex}]=...
selectPoint2(handles.plane_seeds(handles.sliceIndex,:), handles.Coronal_normal,
handles.Axial_seed, handles.Axial_normal, ...
handles.Sagittal_seed, handles.Sagittal_normal, 'Coronal', handles.head_points,
handles.deltaArc, handles.seedNum, ...
str2num(Theta), str2num(dis2plane), str2num(Smooth),
str2num(remove_dis), ...
0, handles.fig1, handles.fig2, handles.fig3, handles.fig4);

axes(handles.fig1)

```

```

point=handles.headgrid{handles.sliceIndex};
plot3(point(:,1),point(:,2),point(:,3),'r');
hold on
plot3(point(:,1),point(:,2),point(:,3));

if (handles.sliceIndex>0 & handles.sliceIndex<totalNum)
    set(handles.goBackward,'enable','on')
    set(handles.goForward,'enable','on')
elseif (handles.sliceIndex==totalNum)
    set(handles.goForward,'enable','off')
else
    set(handles.goBackward,'enable','off')
end

guidata(h,handles)
% %-----for debug-----
% point=handles.headgrid{i};
% axes(handles.fig1)
% hold on
% plot3(point(:,1),point(:,2),point(:,3),'r');
% plot3(point(:,1),point(:,2),point(:,3));

% -----
function varargout = goForward_Callback(h, eventdata, handles, varargin)
sliceNo=get(handles.SliceNo,'String');
index=find(sliceNo=='/');
sliceTotal=sliceNo(index:end);
totalNum=str2num(sliceTotal(2:end));
handles.sliceIndex=handles.sliceIndex+1;
set(handles.SliceNo,'String',[num2str(handles.sliceIndex),sliceTotal]);
guidata(h,handles)
Theta=get(handles.Theta,'String');
dis2plane=get(handles.dis2plane1,'String');
Smooth=get(handles.Smooth,'String');
remove_dis=get(handles.Remove_dis,'String');

[handles.headgrid{handles.sliceIndex},handles.deltaArc,Med(handles.sliceIndex),handles.Cor_I
ndex{handles.sliceIndex}] = ...
selectPoint2(handles.plane_seeds(handles.sliceIndex,:), handles.Coronal_normal,
handles.Axial_seed, handles.Axial_normal, ...

```

```

        handles.Sagittal_seed, handles.Sagittal_normal, 'Coronal', handles.head_points,
handles.deltaArc, handles.seedNum,...
                str2num(Theta), str2num(dis2plane), str2num(Smooth),
str2num(remove_dis), ...
                0, handles.fig1, handles.fig2, handles.fig3, handles.fig4);
axes(handles.fig1)
point=handles.headgrid{handles.sliceIndex};
plot3(point(:,1),point(:,2),point(:,3),'r. ');
hold on
plot3(point(:,1),point(:,2),point(:,3));

if (handles.sliceIndex>0 & handles.sliceIndex<totalNum)
    set(handles.goBackward,'enable','on')
    set(handles.goForward,'enable','on')
elseif (handles.sliceIndex==totalNum)
    set(handles.goForward,'enable','off')
else
    set(handles.goBackward,'enable','off')
end

guidata(h,handles)
% %-----for debug-----
% point=handles.headgrid{handles.sliceIndex};
% axes(handles.fig1)
% hold on
% plot3(point(:,1),point(:,2),point(:,3),'r. ');
% plot3(point(:,1),point(:,2),point(:,3));

% -----
function varargout = Cancel_Callback(h, eventdata, handles, varargin)

% -----
function varargout = Start_Callback(h, eventdata, handles, varargin)

if isempty(handles.head_points)
    error('Not a valid curry surface file','Read cury file Error')

```

else

```

axes(handles.fig1)
cla
axes(handles.fig2)
cla
axes(handles.fig3)
cla
axes(handles.fig4)
cla
handles.sliceIndex=0;
guidata(h,handles);

Theta=get(handles.Theta,'String');
dis2plane=get(handles.dis2plane1,'String');
Smooth=get(handles.Smooth,'String');
remove_dis=get(handles.Remove_dis,'String');
[S_Point,handles.deltaArc,CZ1,handles.Sag_Index]=selectPoint2(handles.Sagittal_seed,
handles.Sagittal_normal, ...,
handles.Axial_seed, handles.Axial_normal, ...
handles.Coronal_seed, handles.Coronal_normal, ...
'Sagittal', handles.head_points, handles.deltaArc,
handles.seedNum, ...
str2num(Theta), str2num(dis2plane),...
str2num(Smooth), str2num(remove_dis), ...
0, handles.fig1, handles.fig2, handles.fig3, handles.fig4);
plane_seeds=S_Point;
distance=find_dis2plane(handles.Coronal_seed, handles.Coronal_normal,plane_seeds);
distance=abs(distance);
dis_1stDef=distance(2:end)-distance(1:end-1);
%Index=find(dis_1stDef<0);
%delta_index=Index(2:end)-Index(1:end-1);
[max,Index]=max(dis_1stDef);
% if ~isempty(Index2)
%   if ( Index2(1)<0.3*size(plane_seeds,1) & Index2(end)>0.7*size(plane_seeds,1) )
%     handles.plane_seeds=plane_seeds(Index(Index2(1)+1):Index(Index2(end)-1),:);
%   elseif (Index2(1)>0.7*size(plane_seeds,1))
%     handles.plane_seeds=plane_seeds(1:Index(Index2(1)-1),:);
%   elseif (Index2(end)<0.3*size(plane_seeds,1))
%     handles.plane_seeds=plane_seeds(Index(Index2(end)+1):end,:);
%   else
%     handles.plane_seeds=plane_seeds(Index(Index2(1)+1):Index(Index2(end)-1),:);

```



```

% end
% end
[max,Index1]=max(distance(1:Index));
[max,Index2]=max(distance(Index+1:end));
handles.plane_seeds=plane_seeds(Index1:Index2+Index,:);
handles.Sag_Index=handles.Sag_Index(Index1:Index2+Index);
%handles.plane_seeds=S_Point;
%SliceNo=str2num(get(handles.SliceNo,'String'))+1;
SliceTotal=size(handles.plane_seeds,1);
set(handles.SliceNo,'String',['0/',num2str(SliceTotal)]);
set(handles.Repeat,'enable','on');
set(handles.goForward,'enable','on');
guidata(h,handles)

axes(handles.fig1)
hold on
plot3(handles.plane_seeds(:,1),handles.plane_seeds(:,2),handles.plane_seeds(:,3),'r');
plot3(handles.plane_seeds(:,1),handles.plane_seeds(:,2),handles.plane_seeds(:,3));
end

% -----
function varargout = Repeat_Callback(h, eventdata, handles, varargin)

sliceNo=get(handles.SliceNo,'String');
index=find(sliceNo=='/');
sliceTotal=sliceNo(index:end);
totalNum=str2num(sliceTotal(2:end));

Theta=get(handles.Theta,'String');
dis2plane=get(handles.dis2plane1,'String');
Smooth=get(handles.Smooth,'String');
remove_dis=get(handles.Remove_dis,'String');

[handles.headgrid{handles.sliceIndex},handles.deltaArc,Med(handles.sliceIndex),handles.Cor_I
ndex{handles.sliceIndex}] = ...
selectPoint2(handles.plane_seeds(handles.sliceIndex,:), handles.Coronal_normal,
handles.Axial_seed, handles.Axial_normal, ...
handles.Sagittal_seed, handles.Sagittal_normal, 'Coronal', handles.head_points,
handles.deltaArc, handles.seedNum, ...

```

```

                                str2num(Theta), str2num(dis2plane), str2num(Smooth),
str2num(remove_dis), ...      0, handles.fig1, handles.fig2, handles.fig3, handles.fig4);
axes(handles.fig1)
point=handles.headgrid{handles.sliceIndex};
plot3(point(:,1),point(:,2),point(:,3),'r');
hold on
plot3(point(:,1),point(:,2),point(:,3));

if (handles.sliceIndex>0 & handles.sliceIndex<totalNum)
    set(handles.goBackward,'enable','on')
    set(handles.goForward,'enable','on')
elseif (handles.sliceIndex==totalNum)
    set(handles.goForward,'enable','off')
else
    set(handles.goBackward,'enable','off')
end

guidata(h,handles)

% -----
function varargout = figure1_ResizeFcn(h, eventdata, handles, varargin)

```

### 10.1.2.2.2 *read\_Curry\_file3.m*

```

function [Matrix,count,NR]=read_Curry_file3(filename,type,needContinue,Continued)
% This function to read the curry file.
% Input: the curry file name and the information type you need to read from that file.
%       the Type can be: LOCATION, NORMALS, CONTRIB, STRENGTHS, ERRORS,
DEVIATIONS, and so on.
% Output: A is the matrix of data read from the file
%        count is the number of the data read from the file
if ~Continued
    begin=0;
    matched=0;
    found=0;
    located=0;
    A=[];
    count=0;
    line_num=0;
    got_info=0;
    already_jump=0;
    already_judged=0;
    fid=fopen(filename,'rt');
    now_read=1;
    start=1;
    timePoint=1;
    end_header=0;
else
    load workspace
    found=0;
    located=1;
    now_read=now_read-1;
    timePoint=timePoint+1;
    start=timenow+1;
end

keyNum=1;
NRnum=1;
while (~feof(fid) & ~found)
    TLine=fgets(fid);
    %disp(TLine);
    line_num=line_num+1;

```

```

if (line_num<250 & ~begin)
    if ~isempty( findstr(['POINT_KEYWORDS START'],TLine) )
        begin=1;
    end
elseif (line_num<250 & ~isempty( findstr(['POINT_KEY'],TLine) ) )
    key{keyNum}=TLine(strfind(TLine,'=')+2:end-1);
    keyNum=keyNum+1;
elseif (line_num<250 & ~isempty( findstr(['POINT_NR'],TLine) ) )
    NR(NRnum)=str2num(TLine(strfind(TLine,'=')+1:end));
    NRnum=NRnum+1;
elseif (~isempty( findstr(['POINT_TRAFO END_LIST'],TLine) ) )
    end_header=1;
elseif (~end_header & line_num>250)
    disp('May be a wrong file name')
    break
end
if (end_header)
    %Now judge whether the type is included
    if (~already_judged)
        for i=1:15
            if ( ~isempty(findstr([type,'_LIST'],key{i})))
                matched=1; match_line=i+1;break
            end
        end
        already_judged=1;
    end
    if (~matched)
        disp('May be a wrong type')

        break
    else
        %if (~already_jump)
        % fseek(fid,46*37,-1);
        already_jump=1;
        %end

        key_now=key{now_read};
        if ( ~((key_now(2)=='O') * (key_now(3)=='_')) )
            if (~isempty(findstr([key_now,' START_LIST'],TLine)) & length(TLine)>4)
                located=1; end
            end
        end
    end
end

```

```

if (located)
    row=NR(1);

    if (now_read==1 | now_read==2)
        col=3;
    elseif (now_read==3 | now_read==4)
        col=1;
    end
    if (now_read==2 | now_read==3 | now_read==4)
        time_rep=NR(2);
    else
        time_rep=1;
    end
    for timenow=start:time_rep
        if (strcmp(key_now,[type,'_LIST']) & timenow==timePoint)
            [Matrix,count]=fscanf(fid,'%f',[col,row]);
            Matrix=Matrix';
            found=1;
            disp([fgets(fid),num2str(timenow)])

            break
        else
            [temp,count_tmp]=fscanf(fid,'%f',[row,col]);
            disp([fgets(fid),num2str(timenow)])
            fgets(fid)
        end
    end
    line_num=line_num+time_rep*(row+2);
    now_read=now_read+1;
    located=0;
end
end
end
end
end
if ~needContinue
    fclose(fid)
    if (Continued)
        delete workspace
    end
else
    save workspace

```

end

### 10.1.2.2.3 *selectPoint2.m*

```

% selectPoint2.m
% This function detect the resolution/increasment of x and y in the axial plane, if we equally put
n point in hte coronal plane.
% plane2_seed is the CZ.
function [Point,deltaArc,Med,GridIndex]=selectPoint2(plane_seed, plane_normal, plane2_seed,
plane2_normal,plane3_seed, plane3_normal,...
           plane_direction, locations, deltaArc, seed_num, deltaTh, threshold,
smoothNum, remove_dis, ...
           debugOpt, axes1, axes2, axes3, axes4)
%-----Part1: controled by the dis2plane2-----
%find the curve of the locations which near the defined plane
curve=proj_curve(plane_seed, plane_normal,locations, threshold);

% only remain the curve above the axial plane
curve_abv=find_subset(plane2_seed, plane2_normal, curve);

axes(axes2)
plot3(curve_abv(:,1),curve_abv(:,2),curve_abv(:,3),'r.')

%-----
%-----Part2: Find the envelope of the curve: controled by delatTh-----
switch (plane_direction)
case('Sagittal')
    [tmp,Index]=sort(curve_abv(:,2));
    curve_abv=curve_abv(Index,:);
case('Coronal')
    curve_abv=GetEnvelope2(curve_abv,deltaTh,axes3);
    curve_abv=[curve_abv;plane_seed];
    [tmp,Index]=sort(curve_abv(:,1));
    curve_abv=curve_abv(Index,:);
end

distance=find_dis2plane(plane3_seed, plane3_normal,curve_abv);
[Min_dis,Index]=min(abs(distance));
Peak=curve_abv(Index,:);
%-----

```

```

%-----Part3: Sort the points according to the dis, smooth and remove some points

curve_1=curve_abv(Index:end,:); %Peak is included in the plane %curve_1 go from medial to
lateral.
curve_2=curve_abv(Index:-1:1,:); %peak is included in the plane %curve_2 go from lateral to
medial //?

%-----sort the points in the curve, the sorted curve goes from the CZ to lateral-----
switch (plane_direction)
case('Sagittal')
    base_direction=2;

case('Coronal')
    base_direction=1;
end

%-----debug: output the results before sort, smooth and remove-----
-----
axes(axes4)
cla
hold on
plot3(curve_1(:,1),curve_1(:,2),curve_1(:,3),'r.')
plot3(curve_2(:,1),curve_2(:,2),curve_2(:,3),'r.')

%-----

curve_1=sort_based_dis(curve_1,base_direction,0,smoothNum);
curve_1=point_rm(curve_1,remove_dis);
curve_2=sort_based_dis(curve_2,base_direction,0,smoothNum);
curve_2=point_rm(curve_2,remove_dis);
%-----debug: output the results after sort, smooth and remove-----
----
axes(axes4)
hold on
plot3(curve_1(:,1),curve_1(:,2),curve_1(:,3),'md')
plot3(curve_1(:,1),curve_1(:,2),curve_1(:,3))
plot3(curve_2(:,1),curve_2(:,2),curve_2(:,3),'co')
plot3(curve_2(:,1),curve_2(:,2),curve_2(:,3))
plot3(plane_seed(1,1),plane_seed(1,2),plane_seed(1,3),'go')
plot3(curve_abv(Index,1),curve_abv(Index,2),curve_abv(Index,3),'ko')

```



```

% xlabel('x')
% ylabel('y')

%-----

%-----
if(deltaArc==-1)
    % Calculate the total distance from the CZ to the PAL or PAR.
    curve_len=sum(sqrt(sum((curve_1(2:end,:)-curve_1(1:end-1,:)).^2,2)));

    % Calculate the increasement in the CZ~PAL if equally putting m seeds.
    deltaArc=curve_len/seed_num;
end

% [Point_in_arc_1,err_1]=find_point_in_acr(curve_1,'1',deltaArc,plane_direction);
% [Point_in_arc_2,err_2]=find_point_in_acr(curve_2,'2',deltaArc,plane_direction);
Point_in_arc_1=find_point_in_acr(curve_1,'1',deltaArc,plane_direction);
Point_in_arc_2=find_point_in_acr(curve_2,'2',deltaArc,plane_direction);

Point=[Point_in_arc_2;Peak;Point_in_arc_1];
GridIndex=[-length(Point_in_arc_2):length(Point_in_arc_1)];
%err=[err_2,0,err_1];
Med=(length(Point_in_arc_2)+1);

%-----

function Point_in_arc=find_point_in_acr(curve,direction,deltaArc,plane_direction)

arc_len_now(1)=0;
Point_in_acr=[];
j=1;
for i=2:(size(curve,1))
    arc_len_now(i)=arc_len_now(i-1)+sqrt(sum((curve(i,:)-curve(i-1,:)).^2));
end

while j*deltaArc<arc_len_now(end)
    Ind=find(arc_len_now<j*deltaArc);
    Index=Ind(end);
    L=arc_len_now(Index+1)-arc_len_now(Index);
    l=arc_len_now(Index+1)-j*deltaArc;
    Point_in_arc(j,:)=curve(Index+1,:)-l/L*(curve(Index+1,:)-curve(Index,:));
end

```

```

    j=j+1;

end

switch (direction)
case('2')
    Point_in_arc=flipud(Point_in_arc);
end

%-----

%-----
function sorted_curve=sort_based_dis(curve,base_direction,debugOpt,smoothNum)

if debugOpt
    %-----debug-----
    figure(3)
    hold on
    plot3(curve(1,1),curve(1,2),curve(1,3),'gd');
end
% [tmp,Index]=sort(abs(curve(:,base_direction)));
curve_pre_sort=curve;
Index_beg=1;
curve_link=Index_beg:length(curve);
%curve_new_link=curve_link;
for j=1:length(curve_link)-1
    min_dis=100;
    for i=j+1:length(curve_link)
        new_dis=sqrt(sum((curve_pre_sort(curve_link(j),:)-curve_pre_sort(curve_link(i),:)).^2,2));
        if new_dis<min_dis
            min_dis=new_dis;
            min_ind=curve_link(i);
            ind=i;
        end
    end
    curve_link(ind)=curve_link(j+1);
    curve_link(j+1)=min_ind;
    if debugOpt
        plot3(curve(curve_link(j+1),1),curve(curve_link(j+1),2),curve(curve_link(j+1),3),'gd');
        pause
    end
end
end

```

```

for i=1:length(curve_link)
    sorted_curve(i,:)=curve_pre_sort(curve_link(i,:));
end
%-----smooth the data-----
if (smoothNum)
    for k=1:smoothNum
        curve_new=sorted_curve;
        for i=2:size(sorted_curve,1)-1
            curve_new(i,:)=mean([sorted_curve(i-1,:);sorted_curve(i+1,:)]);
        end
        sorted_curve=curve_new;
        clear curve_new
    end
end

%-----
function clean_curve=point_rm(curve,remove_dis)

distance=sqrt(sum((curve(2:end,:)-curve(1:end-1,:)).^2,2));
Ind=find(distance>=remove_dis);
if (~isempty(Ind))
    Index=Ind(1);
else
    Index=size(curve,1);
end

clean_curve=curve(1:Index,:);

```

#### 10.1.2.2.4 *find\_dis2plane.m*

```

% find_dis2plane.m
% This function calculate the distanc of locations to the plane defined by the plane_seed and
plane_normal.
function distance=find_subset(plane_seed, plane_normal,locations)
% define the coefficinets of the coronal plane Ax+By+Cz+D=0
plane=[plane_normal,-(plane_normal*plane_seed)]; % in th ecurry coordinary

% Find the distance of the locations in the skin to the coronal plan

distance=locations*plane_normal';

if plane(4)~=0
    distance=distance+repmat(plane(4),size(locations,1),1);
end

```

### 10.1.2.2.5 *proj\_curve.m*

```

function curve=proj_curve(plane_seed, plane_normal,locations,threshold)
%define the coefficients of the coronal plane Ax+By+Cz+D=0
plane=[plane_normal,-(plane_normal*plane_seed)]; % in the ordinary coordinate system

% Find the distance of the locations in the skin to the coronal plane
distance=locations*plane_normal';

if plane(4)~=0
    distance=distance+repmat(plane(4),size(locations,1),1);
end

% Find the subset locations in the skin which satisfies distance is less than the threshold
% flag=0;
% while(~flag)
%threshold=2; %in the unit of mm
% threshold=input('Please input the threshold (mm):');
    Index=find(abs(distance)<threshold);
    subset=locations(Index,:);

    curve=subset-repmat(distance(Index),1,3).*repmat(plane_normal,length(distance(Index)),1);
% plot3(curve(:,1),curve(:,2),curve(:,3),'r')
% flag=input('Accept? (0: No, 1: Yes):');
% end

```

### 10.1.2.2.6 *GetEnvelope2.m*

```

function Env_curve=GetEnvelope2(curve,deltaTh,yjaxes)
% Function to get the outer torque envelope on a plane.
% Usage: SEMag=GetEnvelope(FMs)
%   Input: FMs: torques on x and y axis (x - 1st column, y - 2nd column)
%   Output: SEMag: magnitude of the spline fitted envelope at 1 degree intervals
% Compute the center of the curve
axes(yjaxes)
hold on
cla
plot3(curve(:,1),curve(:,2),curve(:,3),'r.')

hold on
center=mean(curve,1);
%plot3(center(1,1),center(1,2),center(1,3),'go');
% Transfer all the data in the curve to the center
% curve=curve-repmat(center,size(curve,1),1);

% Compute the length of the curve
Len=sqrt(sum(curve'.^2));
[Mlen,Ind]=max(Len);

ox=curve(Ind,:)-center;
ox=ox/norm(ox);
if Ind~=1 oy=curve(1,:)-center; else oy=curve(end,:)-center; end
oy=oy/norm(oy);
oz=cross(ox,oy);
oy=cross(oz,ox);
Tran=[ox',oy',oz',center'];
Tran=[Tran; 0 0 0 1];
Ones1=ones(size(curve,1),1);
curve=[curve,Ones1];

curve1=(inv(Tran)*curve)';
% figure(4)
% plot3(curve1(:,1),curve1(:,2),curve1(:,3),'r.')
% hold on
% plot3(0,0,0,'go')
% Exclude torques smaller than 1 Nm to minimize computations and avoid errors that
% may arise with torques close to 0 Nm.

```

```

% eidx=find(Len > 1);
% EMag=EMag(eidx);
EAng=atan2(curve1(:,2),curve1(:,1))*180/pi; % -pi<=EAng<=pi
Len=sqrt(sum(curve1'.^2));

% figure(2)
% subplot(411),plot(EMag)
% subplot(412),plot((atan2(FMs(eidx,2),FMs(eidx,1)))*180/pi)
% subplot(413),plot(EAng)

%
uidx=find(EAng<0); EAng(uidx)=EAng(uidx)+360; % 0<=EAng<=2*pi
% subplot(414),plot(EAng)

th=0:deltaTh:360;
cnt=0;
% Find the maximum torque within 2 degree bins
for i=1:length(th)-1
    idx=find(EAng >= th(i) & EAng < th(i+1));
    if ~isempty(idx) % more than one point in bin
        cnt=cnt+1;
        [NLen(cnt),midx]=max(Len(idx)); % Maximum torque magnitude for each bin
        %NEAng(cnt)=EAng(idx(midx)); % Corresponding angle
        Ncurve(cnt,:)=curve1(idx(midx),:);
    end
end

%-----Merge the data which are very close to each other-----
%distance=abs(sorted_curve(2:end,[base_direction,3])-sorted_curve(1:end-
1,[base_direction,3]));
%plot(theta)
%delete_list=[];
% smooth=0;
% while(~smooth)
%     %points=sorted_curve(1:end,[base_direction,3]);
%     for i=1:length(points)-1
%         theta(i)=acos( dot(points(i,:),points(i+1,:))/norm(points(i,:))/norm(points(i+1,:)) );
%     end
%     smooth=1;
%     i=1;
%     while (i<size(sorted_curve,1))

```

```

%
% %-----if the distance(1) or distance(2) is too close, then replace the first point by the
median of the two, and delete the second one
% if (theta(i)<0.005)
%     sorted_curve(i,:)=mean([sorted_curve(i,:);sorted_curve(i+1,:)]);
%     curve_new=[sorted_curve(1:i,:);sorted_curve(i+2:size(sorted_curve,1),:)];
%     sorted_curve=curve_new;
%     smooth=0;
%     clear curve_new;
% end
% i=i+1;
% end
% end
%
% Transfer the curve back to the original coordinate
Env_curve=(Tran*Ncurve)';
Env_curve=Env_curve(:,1:3);
axes(yjaxes)
hold on
plot3(Env_curve(:,1),Env_curve(:,2),Env_curve(:,3),'b+')
plot3(center(1,1),center(1,2),center(1,3),'g*')

% Fit a spline to the outermost points and get the fitted envelope at 1 degree intervals
% th=1:360;
% SEMag=spline(NEAng,NEMag,th);

% Compute the cartesian coordinates for the fitted envelope
% [x,y]=pol2cart(th*pi/180,SEMag);
% FMe=[x' y'];

% figure(1)
% subplot(211),plot(EAng,EMag,'o',NEAng,NEMag,'r.',th,SEMag,'g*')
% subplot(212),plot(NEAng,NEMag, '.')
% figure(2)
% plot(FMs(:,1),FMs(:,2),'b',FMe(:,1),FMe(:,2),'c.')
% plot(FMe)

```





### 10.1.2.2.7 *find\_subset.m*

```

function subset=find_subset(plane_seed, plane_normal,locations)
% define the coefficients of the coronal plane Ax+By+Cz+D=0
plane=[plane_normal,-(plane_normal*plane_seed)]; % in the ordinary coordinate system

% Find the distance of the locations in the skin to the coronal plane

distance=locations*plane_normal';

if plane(4)~=0
    distance=distance+repmat(plane(4),size(locations,1),1);
end

% Find the subset locations in the skin which satisfies distance is less than the threshold
threshold=0; %in the unit of mm
Index=find(distance>threshold);
subset=locations(Index,:);

```

### 10.1.3 Coregistration of Stimulation Grid with MRI

The output file from Headsurfgrid.m is modified to fit a .sp points file for Curry.

Example .sp file, the ... indicates data excluded to keep the file reasonably short.

```

POINT_KEYWORDS   START #           Do   not   edit!
  POINT_KEY_LOCATIONS =      LOCATION_LIST
  POINT_KEY_NORMALS =      NORMALS_LIST
  POINT_KEY_CONTRIB =      NO_LIST
  POINT_KEY_STRENGTHS =    NO_LIST
  POINT_KEY_ERRORS =      NO_LIST
  POINT_KEY_DEVIATIONS =  NO_LIST
  POINT_KEY_FIELDS =      NO_LIST
  POINT_KEY_PCA =         NO_LIST
  POINT_KEY_COLORIND =    NO_LIST
  POINT_KEY_CHARTRAFO =   NO_LIST
  POINT_KEY_NUMBERS =     NO_LIST
  POINT_KEY_NEIGHBORS =   NO_LIST
  POINT_KEY_TRIANGLES =   NO_LIST
  POINT_KEY_REMARKS =     REMARK_LIST
  POINT_KEY_COMPRESSED =  NO_LIST
  POINT_NR_LOCATIONS =    608
  POINT_NR_TIMEPTS =      1
  POINT_NR_TIMEPT_ACT =   0
  POINT_TYPE =            1
  POINT_COORD_SYSTEM =    1
  POINT_PLOT_FLAGS =      0
  POINT_PLOT_COLOR =      1
  POINT_PLOT_COLOR_N =    1
  POINT_PLOT_PLANE =      -1
  POINT_PLOT_SHAPE =      4
  POINT_PLOT_TRANSPA =    100
  POINT_PLOT_CLIPPING =   0
  POINT_PLOT_BORDER =     50
  POINT_PLOT_ADJACENT =   0
  POINT_PLOT_CLOSED =     0
  POINT_T_FIRST =         0
  POINT_T_DELTA =         0
  POINT_DISTANCE =        0
  POINT_AREA =            0
  POINT_VOLUME =          0
  POINT_SCALE =           1
  POINT_LOGSCALE =        1
POINT_KEYWORDS   END

POINT_DESCRIPTION START_LIST #       Do   not   edit!
FRGstimpts pts
608 points      from Localize window
POINT_DESCRIPTION END_LIST

```

```

POINT_TRAFO START_LIST #    Do    not    edit!
      1      0      0      0
      0      1      0      0
      0      0      1      0
      0      0      0      1
POINT_TRAFO END_LIST

```

```

LOCATION_LIST      START #    Do    not    edit!
LIST_DESCRIPTION =    points
LIST_UNITS      =    mm
LIST_NR_ROWS    =    608
LIST_NR_COLUMNS =    3
LIST_NR_TIMEPTS =    1
LIST_VALID      =    1
LIST_BINARY     =    0
LIST_TYPE       =    1
LIST_TRAFO_TYPE =    1
LIST_FIRST_COLUMN =    1
LIST_INDEX_MIN  =    -1
LIST_INDEX_MAX  =    -1
LIST_INDEX_ABS_MAX =    -1
LOCATION_LIST      END

```

```

LOCATION_LIST      START_LIST #    Do    not    edit!
-14.344001  -104.517039  17.97055
-7.474681   -104.137977  16.843152
-1.277928   -103.934554  16.280077
5.433844    -103.896496  16.269471
-10.062053  -105.38664   29.380508
-18.94411   -104.092568  24.972058
-27.826167  -102.798495  20.563607
-25.031672  -102.163799  18.525605
-23.368858  -104.044698  24.738132
-16.383521  -104.427935  26.118749
-7.98964    -104.596786  26.819034
0.740107    -104.754139  27.484976
5.789577    -104.68773   27.353427
13.355829   -102.928501  21.697922
17.180353   -101.328993  16.504028
7.529413    -102.136662  18.995419
-2.121527   -102.94433   21.48681
...
-2.362572   -27.6228     127.219397
7.572775    -27.39648    126.644711
17.320165   -26.766761   124.742075
26.336425   -25.540947   120.866266
35.488485   -24.325219   117.024157
44.146677   -22.844497   112.304316
52.229304   -21.093749   106.685389
59.886219   -19.193645   100.570249

```

```

66.532886  -16.991603  93.441101
72.014546  -14.543969  85.486226
76.617797  -11.941427  77.007245
81.121931  -9.32394    68.475873
82.357781  -6.5133     59.252334
-93.098332  3.255193   58.429269
-90.746133  0.439348   67.730537
-88.130609  -2.354081  76.959988
-84.866924  -5.073839  85.962331
-79.6536    -7.528622  94.124204
-73.437738  -9.704916  101.387547
-66.201887  -11.677989 108.001326
-58.238614  -13.38095  113.7394
-49.875407  -14.860688 118.747675
-40.993723  -16.143069 123.11713
-31.949114  -17.311507 127.115244
-22.29253   -17.931646 129.323152

```

...

```

-21.894755  82.567461  73.174861
-17.602299  81.013556  78.358463
-8.713528   81.329782  77.470455
-2.56107    79.258343  84.388236
5.915943    79.058992  85.190419
14.40791    80.495255  80.612506
15.9577     82.273602  74.790469
6.437917    82.408378  74.183923
-1.943653   82.120525  74.986383
2.973061    79.616212  83.307916
10.378762   77.809606  89.376648
10.291958   78.127519  88.329613
2.327703    77.58384   89.981083
-6.901661   76.561366  93.184783

```

LOCATION\_LIST            END\_LIST

```

NORMALS_LIST            START #        Do    not    edit!
      LIST_DESCRIPTION =        points
      LIST_UNITS        =        mm
      LIST_NR_ROWS      =        608
      LIST_NR_COLUMNS   =        3
      LIST_NR_TIMEPTS   =        1
      LIST_VALID        =        1
      LIST_BINARY       =        0
      LIST_TYPE         =        1
      LIST_TRAFO_TYPE   =        3
      LIST_FIRST_COLUMN =        1
      LIST_INDEX_MIN    =       -1
      LIST_INDEX_MAX    =       -1
      LIST_INDEX_ABS_MAX =       -1
NORMALS_LIST            END

```

NORMALS\_LIST            START\_LIST #        Do    not    edit!



```

0      0      1
0      0      1
0      0      1
0      0      1
0      0      1
0      0      1
0      0      1
0      0      1
0      0      1
0      0      1

```

```

NORMALS_LIST      END_LIST

```

```

REMARK_LIST START #      Do      not      edit!
      LIST_DESCRIPTION =      remarks
      LIST_UNITS      =
      LIST_NR_ROWS    =      608
      LIST_NR_COLUMNS =      40
      LIST_NR_TIMEPTS =      1
      LIST_VALID      =      1
      LIST_BINARY     =      0
      LIST_TYPE       =      5
      LIST_TRAFO_TYPE =      0
      LIST_FIRST_COLUMN =      1
      LIST_INDEX_MIN  =      -1
      LIST_INDEX_MAX  =      -1
      LIST_INDEX_ABS_MAX =      -1

```

```

REMARK_LIST END

```

```

REMARK_LIST START_LIST #      Do      not      edit!
"-3  15"
"-2  15"
"-1  15"
"0   15"
"-6  14"
"-5  14"
"-4  14"
"-3  14"
"-2  14"
"-1  14"
"0   14"
"1   14"
"2   14"
"3   14"
"4   14"
"5   14"
"6   14"
...
"-13 0"
"-12 0"
"-11 0"
"-10 0"
"-9  0"

```

```
"-8  0"  
"-7  0"  
"-6  0"  
"-5  0"  
"-4  0"  
"-3  0"  
"-2  0"  
"-1  0"  
"0   0"  
"1   0"  
"2   0"  
"3   0"  
"4   0"  
"5   0"  
"6   0"  
"7   0"  
"8   0"  
"9   0"  
"10  0"  
"11  0"  
"12  0"  
"13  0"  
...  
"-3  -14"  
"-2  -14"  
"-1  -14"  
"0   -14"  
"1   -14"  
"2   -14"  
"3   -14"  
"4   -14"  
"5   -14"  
"6   -14"  
"7   -14"  
"8   -14"  
"9   -14"  
"10  -14"  
REMARK_LIST END_LIST
```



Then the stimulation points are shown on the MRI skin segmentation (see figure A.10). The points overlying the sensorimotor cortices are chosen for investigation within the experiment (see figure A.11).

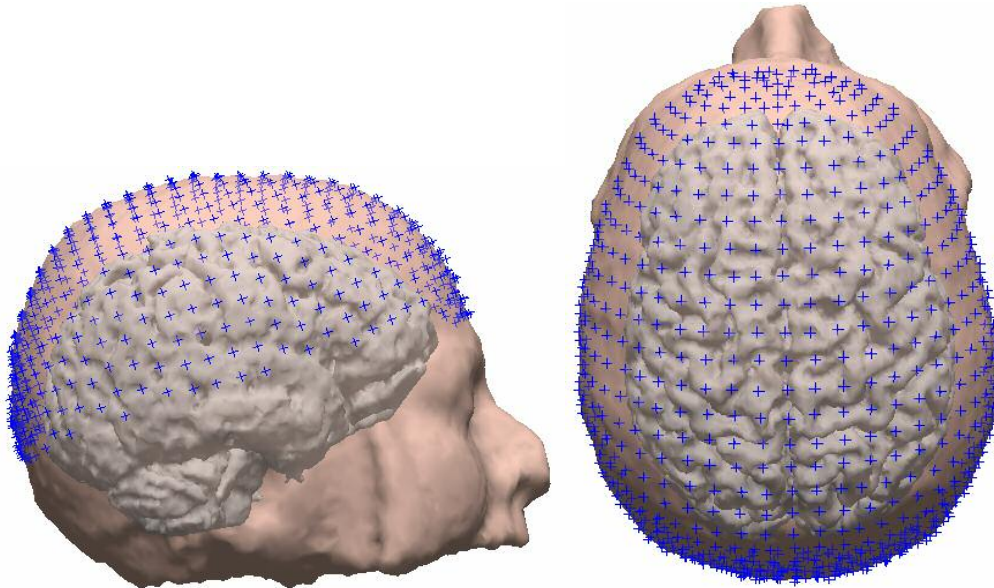


**Figure 10-10** Stimulation Sites on Skin Segmentation of MRI.

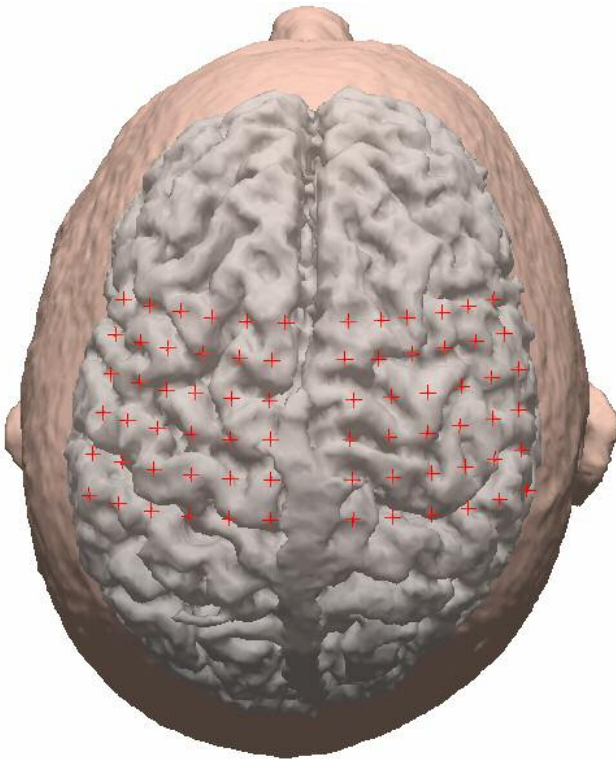


**Figure 10-11** Stimulation Sites above Sensorimotor Cortices.

### ***A.2 TMS\_dialog Program***

The TMS\_dialog program was developed in-house using C++. The goal was to take the subject's head in space, coregister it with the MRI, including the stimulation grid, and also to take the stimulating wand in space and direct the stimulation point on the wand to a specific stimulation point on the subject's head. This involved a number of coordinate transformations (see figure x). . To do this, an Optotrak camera system was used with infrared markers on a rigid body on the subject's head, and also on a rigid body on the stimulating wand. The other inputs to the TMS\_dialog will be reviewed. The TMS\_dialog program also reported the tangential angle of the stimulating wand to the head, and the degree of the wand handle from the mid-sagittal plane. Once a the stimulation wand was put into place at a stimulation site, a multi-joint arm held it in place during the stimulation trials. The output of the program will also be reviewed. An example of the accuracy will be shown using a mannequin.

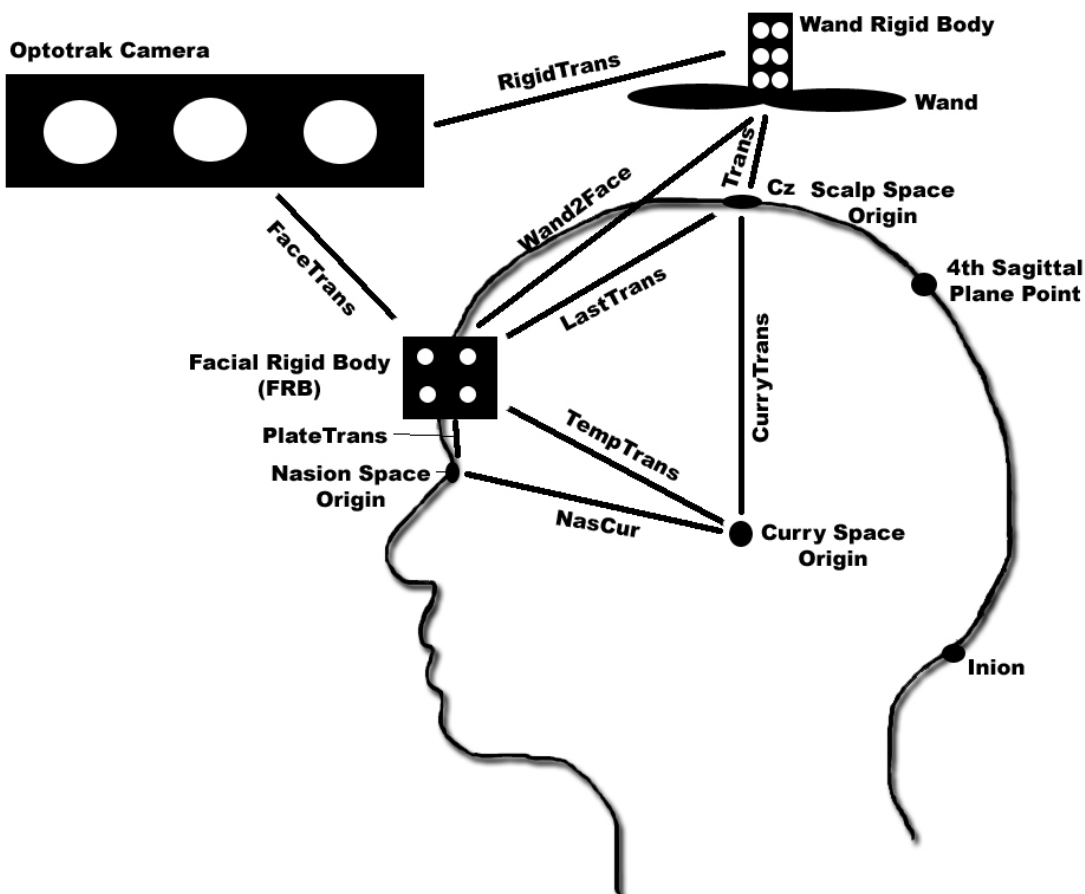


Figure 10-12 TMS\_dialog Coordinate Transformations Performed

### A.2.1 Rigid Bodies

Several rigid bodies were used in the program. The wand rigid body had the origin at the stimulation point on the inferior surface of the wand. The facial rigid body was a plastic plate held onto the forehead with adhesive. The dig rigid body was determined by digitizing the facial landmarks in the facial rigid body coordinate frame.

#### A.2.1.1 Wand Rigid Body – wand.rig

Wand has a plate with 6 ireds securely fastened to it (see figure A.x). We created a rigid body that has the origin at the stimulation point of the wand (3cm posterior to the anterior bifurcation of the wings (see figure A.x)). In the ired rigid body coordinate frame, digitize the wand

stimulation point, a point on the handle of the wand, and the farthest lateral point on the wand. These points have permanent marks on the wand.

Throughout the experiment, the Optotrak camera only needs to “see” 3 of 6 ireds to be able to report the location of the stimulation point.

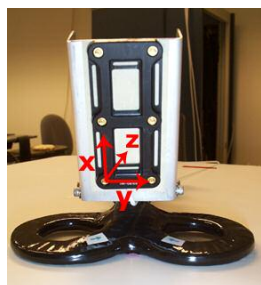


Figure 10-13 Ired plate on the wand.



Figure 10-14 Stimulation point on the wand.

Example wand.rig file:

```

Marker Description File

Imaginary 3D
3      ;Number of markers
Marker      X      Y      Z
Point1     -0.2663  35.0636  -68.3370
Point2     30.4925  22.9274  -62.4772
Point3     1.2651  -27.5932  -7.5446

```

### A.2.1.2 Facial Rigid Body – frb.rig

The facial rigid body is a hard plastic plate with 4 ireds stuck to it with double-sided stickers (see figure A.x). The coordinate frame of the facial rigid body has the origin at the lower left ired (when facing the plastic plate), the x direction is toward the bottom ired on the right. The temporary y direction is toward the top left ired. The z direction is the dot product of the two

vectors. The final y vector is the result of the dot product of the x and the z and is in a similar direction as the temporary y.

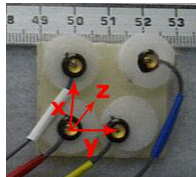


**Figure 10-15** Facial rigid body.

Example Frb.rig file:

```

Marker Description File

Real 3D
4           ;Number of markers
1           ;Number of different views
Front
Marker      X           Y           Z           Views
1           0.0000      -0.0000      -0.2885      1
2           19.0171     -0.0000      0.2167      1
3           -1.3657     13.8679     0.2274      1
4           24.4962     20.2646     -0.1556     1

MaxSensorError
0.20

Max3dError
0.50

MarkerAngle
60

3dRmsError
0.50

SensorRmsError
0.10

MinimumMarkers
3

```

### A.2.1.3 Nasion Rigid Body - dig.rig

Digitize the location of the facial landmarks with respect to the facial rigid body-using a probe with infrared markers: Nasion, right eye (ear), left eye (ear). Use optotrak software to create the rigid body. The nasion is the origin, the x direction is toward the right eye, the temporary y is toward the left eye, the z vector is the result of the dot product of the x and temporary y. The

final y vector is the result of the dot product of the x and the z and is in a similar direction as the temporary y (see figure A.x).

Example dig.rig file:

```

Marker Description File

Imaginary 3D
3      ;Number of markers
Marker      X      Y      Z
Point1      13.5840  -27.9873  -21.1943
Point2      -69.0593 -18.6453  -116.4226
Point3      92.5541   3.9432   -99.9465

```

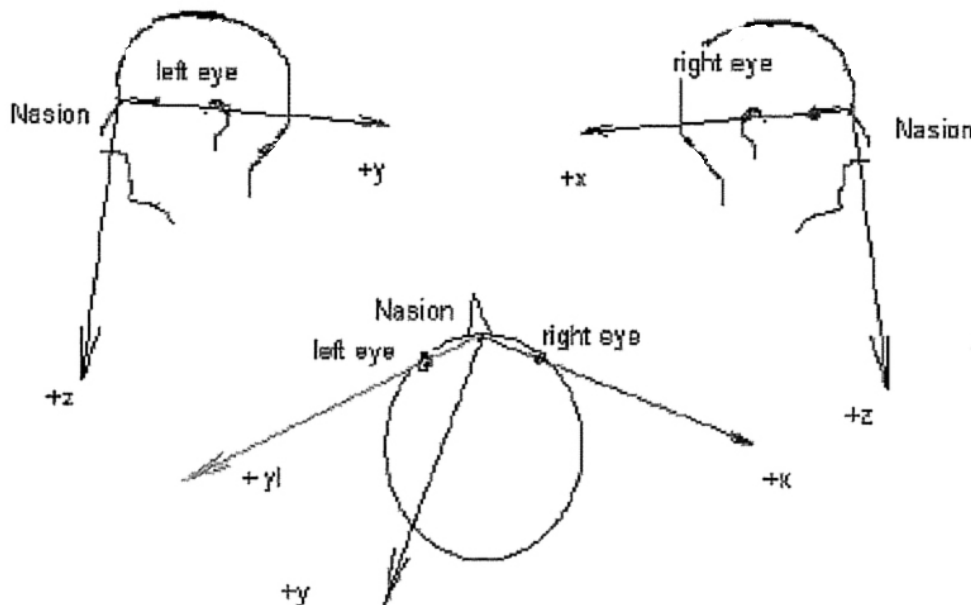


**Figure 10-16** Nasion coordinate frame using landmarks digitized on the subject's head.

### *A.2.1 TMS\_dialog Input Files*

All files must have the same base name, except for the .rig files which must have the names shown here:

- .pln
- .tfm
- curry.pts
- .stm

- .cur
- dig.rig
- wand.rig
- frb.rig

### A.2.1.1 .pln file

Digitize 4 points that lie along the midsagittal plane: Cz, Nasion, Inion, a fourth point lying anywhere between the Cz and the Inion (see figure A.x).

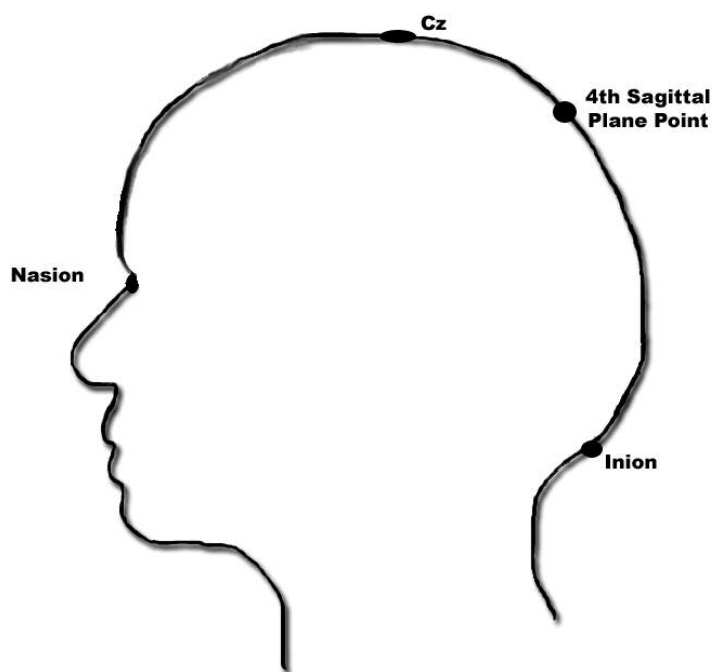


Figure 10-17 Four midsagittal plane points for .pln file

Example .pln file:

```

Marker Description File

Imaginary 3D
4 ;Number of markers
Marker      X          Y          Z
Point1     -7.1526     101.6700     -86.9808
Point2      12.0518     -37.4511     -19.3876
Point3      10.5847      -7.1020     -199.2692
Point4       8.2110      36.6412     -194.6221

```

### A.2.1.1 .tfm & curry.pts files

These files are exactly the same, just with different names. Once the facial landmarks are digitized on the subject, up to 60 scalp sites are also digitized. Typically, we digitized points along the interaural and nasion-inion lines. These points are then coregistered with the MRI using Curry. The points are evaluated as to whether they lie on the scalp surface (do not hover above or dive below (see figure A.x)) and whether the points lie on the interaural and nasion-inion lines (see figure A.x). If they do not, the landmarks on the MRI are re-chosen and the fit is checked again. Once a good fit is made, the MRI landmarks are named as the .tfm and curry.pts files.

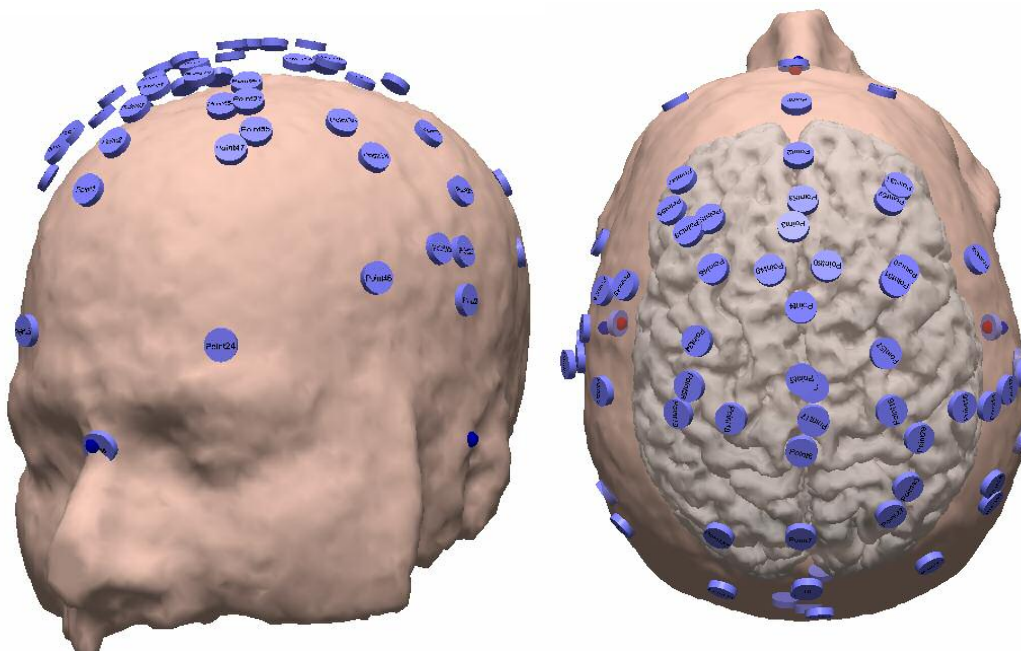


**Figure 10-18** Scalp points coregistered with MRI

Example .tfm or curry.pts file:

```
0.9      -99.8     -0.9
-90.3    -1.1     18.8
81.3     -1.6     21.9
```

#### **A.2.1.1 .stm file**

This can either include all the gridpoints created with Headsurfgrid, or just the gridpoints that lie above the sensorimotor cortices. If all the gridpoints are included, the first 2 columns are the x,y coordinates from the Cz. If it is the subset of points, then typically the first column counts from 1-30 or so and the second column is all zeroes. This is so you can label the gridpoints 1-30 and refer to them in that way. The last 3 columns are the x, y, z locations.

An example .stm file of just stimulation points above the sensorimotor cortices:



1	0	60.91422	-27.8612	121.5891
2	0	52.6955	-29.5822	127.0196
3	0	43.94517	-30.9656	131.5725
4	0	34.96761	-32.2062	135.7529
5	0	25.4783	-33.0112	138.787
6	0	61.56455	-19.2739	126.5416
7	0	53.64241	-21.1264	132.3066
8	0	44.62972	-22.3489	136.4411
9	0	35.24283	-23.2613	139.7603
10	0	25.81917	-24.1395	142.9886
11	0	62.11405	-10.2633	130.9811
12	0	53.46653	-11.7382	135.7747
13	0	44.56039	-13.0034	140.0181
14	0	35.13864	-13.8835	143.2514
15	0	26.00396	-14.7383	146.3903
16	0	-14.1973	-41.0506	135.6298
17	0	-23.8574	-39.9013	133.3279
18	0	-33.4115	-38.6241	130.6674
19	0	-42.6751	-37.092	127.2831
20	0	-51.8816	-35.5083	123.7531
21	0	-13.8457	-32.1819	139.956
22	0	-23.4974	-31.0292	137.6447
23	0	-32.9215	-29.6201	134.6114
24	0	-42.3612	-28.2277	131.6256
25	0	-51.0853	-26.3548	127.261
26	0	-13.4694	-23.1735	143.7801
27	0	-23.1174	-22.0051	141.4257
28	0	-32.7796	-20.9644	139.4216
29	0	-41.666	-19.3048	135.6557
30	0	-49.7328	-17.1106	130.354

#### A.2.1.1 .cur file

This file is based on the triangular mesh created from the skin segmentation. Using NormalsR.m, the triangular mesh is loaded, and the normals determined and the output is the .cur file.

1<sup>st</sup> cell = number of vertices

1<sup>st</sup> three columns = vertice location: x, y, z – not ordered by triangle, just a list of vertices

next 3 columns = associated normal: x, y, z

A.2.1.1.1 NormalsR.m

```
function NormalsR(fname)
```

```

disp('did you change the file location within NormalsR?');
%%%%%%%%%%%%%%%%%%%%%%%%%%%%%%%%%%%%%%%%% Read in the DATA
%%%%%%%%%%%%%%%%%%%%%%%%%%%%%%%%%%%%%%%%%
disp(['File = ' fname]);
fid=fopen(['C:\SUSAN\FRGR081304\' fname '.txt'],'r')
i=0;
error=1;
%reads in 1 line at a time to look for the number of vertices and the number of triangles.
while 1
    line = fgetl(fid);

    if ~isstr(line), break, end

    %Find the number of vertices (nodes)
    if strcmp(line,' NUMNODESTOTAL    = ',27)
        numpts=str2num(line(28:end));
    end

    %Find the number of triangles
    if strcmp(line,' NUMTRIANGLESTOTAL  = ',27)
        numtri=str2num(line(28:end));
    end

    %Get the list of vertices
    if strcmp(line,'LOCATION_LIST START_LIST # Do not edit!',39)
        vertices=fscanf(fid,'%e',numpts*3);

    end

    %We think that the normals output by Curry are not geometric normals but instead intensity
    values used by Curry
    %Therefore, we will not use the Normals provided, but calculate our own
    if strcmp(line,'NORMALS_LIST START_LIST # Do not edit!',38)
        normlist=fscanf(fid,'%e',numpts*3);
    end
end

```

```

% %Get the triangle list which is an index to the vertice list
% if strcmp(line,'TRIANGLE_LIST START_LIST # Do not edit!',39)
%   trilst=fscanf(fid,'%e',numtri*3);
% end
end
%%%%%%%%%% Finished Reading in the Data
%%%%%%%%%%

%%%%%%%%%% Reorder the Data
%%%%%%%%%%
%Reorder the data such that the vertice and triangle lists are in 3 columns
%Vertice list=x,y,z coordinates
%Triangle list=vertice1index, vertice2index, vertice3index
k=1;
for j=1:numpts
    j %Displays the counter in the command window so you know where the program is
    vert3(j,1:3)=[vertices(k,1), vertices(k+1,1), vertices(k+2,1)];
    k=k+3;
end
%plot3(vert3(:,1), vert3(:,2), vert3(:,3),'r. ');
save vert3 vert3

% k=1;
% for p=1:numtri
%   p
%   trilst3(p,1:3)=[trilst(k,1), trilst(k+1,1), trilst(k+2,1)];
%   k=k+3;
% end
% save trilst3 trilst3

%%Added 10/24 by SCS for testing of Curry Normals
k=1
for y=1:numpts
    y
    normlist3(y,1:3)=[normlist(k,1), normlist(k+1,1), normlist(k+2,1)];
    k=k+3;
end
save normlist3 normlist3
%end of 10/24 addition
%%%%%%%%%% Finished Reordering the Data
%%%%%%%%%%

```

```

%%%%%%%%%% Determine the averaged normal of all triangles which
use each vertice%%%%%%%%%%
% for g=1:numpts %Do for one vertice at a time
%   g
%   %find all the triangles which use this vertice
%   k=find(trilist3(:,1)==g);
%   l=find(trilist3(:,2)==g);
%   m=find(trilist3(:,3)==g);
%   trigroup=[k' l' m'];
%
%   p=length(trigroup);
%   for i=1:p %find the normal of each triangle which uses this vertice
%       %Create vectors in each triangle that use this vertice
%       vector1(1,1)=vert3(trilist3(trigroup(i),2)+1,1)-vert3(trilist3(trigroup(i),1)+1,1);
%       vector1(1,2)=vert3(trilist3(trigroup(i),2)+1,2)-vert3(trilist3(trigroup(i),1)+1,2);
%       vector1(1,3)=vert3(trilist3(trigroup(i),2)+1,3)-vert3(trilist3(trigroup(i),1)+1,3);
%       vector2(1,1)=vert3(trilist3(trigroup(i),3)+1,1)-vert3(trilist3(trigroup(i),1)+1,1);
%       vector2(1,2)=vert3(trilist3(trigroup(i),3)+1,2)-vert3(trilist3(trigroup(i),1)+1,2);
%       vector2(1,3)=vert3(trilist3(trigroup(i),3)+1,3)-vert3(trilist3(trigroup(i),1)+1,3);
%       %cross product to compute the normal to each triangle
%       normal=CROSS(vector1,vector2);
%       %normalize result
%       mag=sqrt(normal(1,1)^2+normal(1,2)^2+normal(1,3)^2);
%       Nnormal=normal./mag;
%       %Make sure it is the outward normal, not the inward normal
%       vector3(1:3)=vert3(trilist3(trigroup(i),1)+1,1:3);
%       test=DOT(Nnormal,vector3);
%       if test>=0
%           Gnormal(i,:)=Nnormal;
%       else
%           normal=CROSS(vector2,vector1);
%           mag=sqrt(normal(1,1)^2+normal(1,2)^2+normal(1,3)^2);
%           Nnormal=normal./mag;
%           Gnormal(i,:)=Nnormal;
%       end
%       clear Nnormal normal mag test vector1 vector2
%       %Repeat finding the normal for the next triangle
%   end
%   %average all normals across all triangles with this vertex

```

```

%   Gnormal;
%   VertNorm(g,:)=mean(Gnormal);
%   VertNormSTD(g,:)=std(Gnormal);
%   %Repeat for the next vertex
% end
%save AveNormals VertNorm -ascii
%save STDNormals VertNormSTD -ascii
%%%%%%%%%% Normal list is now created
%%%%%%%%%%
%%%%%%%%%%

%VertNorm; %Display Normal List if you want to
%VertNormA(1,1)=numpts; %first line is the number of points
%VertNormA(2:numpts+1,1:3)=vert3(:,:);%the first 3 columns are the vertice x,y,z
%VertNormA(2:numpts+1,4:6)=VertNorm(:,:);%the next 3 columns are the normal x,y,z
%save VertNormA VertNormA -ascii %Save Normal list

%Create output file such that the first row just has the number of vertices
%the second row is the 1st triangle, 1st vertice x y z, associated normal x y z
%the third row is the 1st triangle, 2nd vertice x y z, associated normal x y z
%the 4th row is the 1st triangle, 3rd vertice x y z, associated normal x y z
%the 5th row is the 2nd triangle, 1st vertice x y z, associated normal x y z
%etc
load vert3.mat
% VertNormA(1,1:6)=ones;
% VertNormA(1,1)=numpts; %first line is the number of points
% VertNormA(2:size(vert3,1)+1,1:3)=vert3(:,1:3);
% VertNormA(2:size(vert3,1)+1,4:6)=VertNorm;
%   % k=1;
%   % for m=1:numtri
%   %   m
%   % VertNormA(k+1,1:3)=vert3(trilist3(m,1)+1,:);
%   % VertNormA(k+1,4:6)=VertNorm(trilist3(m,1)+1,:);
%   %
%   % VertNormA(k+2,1:3)=vert3(trilist3(m,2)+1,:);
%   % VertNormA(k+2,4:6)=VertNorm(trilist3(m,2)+1,:);
%   %
%   % VertNormA(k+3,1:3)=vert3(trilist3(m,3)+1,:);
%   % VertNormA(k+3,4:6)=VertNorm(trilist3(m,3)+1,:);
%   % k=k+3;
%   % end

```

```
% %Add the unit normals to the vertices to create a shell around the head
% UnitNormShell=vert3+VertNorm;
% figure
% plot3(vert3(:,1), vert3(:,2), vert3(:,3),'r.')
% hold on
% plot3(UnitNormShell(:,1), UnitNormShell(:,2), UnitNormShell(:,3),'g.')

VertNormB(1,1:6)=ones;
VertNormB(1,1)=numpts; %first line is the number of points
VertNormB(2:size(vert3,1)+1,1:3)=vert3(:,1:3);
VertNormB(2:size(vert3,1)+1,4:6)=normlist3;

% save MatlabNormList VertNormA -ascii
% save MatlabNormList VertNormA
save CurryList VertNormB -ascii
% save CurryNormList normlist3 -ascii
% save UnitNormShell UnitNormShell
```

### *A.2.2 Angle Reporting*

#### **A.2.2.1 Tangential angle:**

We wanted the stimulation point on the coil to be touching the head with the wand wings tangential to the head. At the head surface mesh point closest to the wand stimulation point, the program gets the normal to that point (stored in the .cur file). On the display screen, there are two vectors-one showing the normal to the point, the other that changes which is the normal to the wand plane (plane includes all 3 points digitized on the wand inferior surface). As the wand is rotated and the normal changes the screen updates. Once the 2 vectors align, the wand is tangential to the head at the stimulation point.

#### **A.2.2.2 45° angle from midsagittal plane.**

Most TMS experiments are performed with the handle of the wand either pointing straight backward, thus in-line or parallel to the midsagittal plane or at a 45° degree angle from the midsagittal plane. The 4 midsagittal plane points (.pln file) are used to reconstruct the midsagittal plane. Two points on the inferior surface of the wand, the stimulation point and the point on the handle posterior to the stimulation point, create a vector which will describe the angle of the wand from the midsagittal plane. This vector and the midsagittal plane are both projected onto a horizontal plane that lies at the highest point of the head, and the angle between them is calculated. A chosen angle is displayed as the straight vertical vector on the display screen. The actual wand angle is a moving vector. If the 2 vectors line up, the wand is being held at the preferred angle.

### *A.2.3 Mannequin Test*

A mannequin was used to test the accuracy of choosing stimulation points from the MRI, using the TMS\_dialog program to guide the wand to stimulation points, recording the ACTUAL stimulation points and coregistering them back onto the MRI. For the mannequin, small vitamin E capsules were pushed into the head surface. In addition, a small water balloon filled with water was inserted in the mannequin neck. This assured us that enough signal would be in the MRI to be recorded as well as offered an orientation landmark. The vitamin E capsules were also visible with MRI. The MRI scan was opened in Curry and the locations of the vitamin E capsules were recorded. These became the stimulation sites. The TMS\_dialog guided the wand to each vitamin E capsule (the mannequin head was covered by a black elastic cap) and the TMS\_dialog program recorded the stimulation site. These points were uploaded in Curry and coregistered with the MRI and resulted in an excellent fit (see figure x).

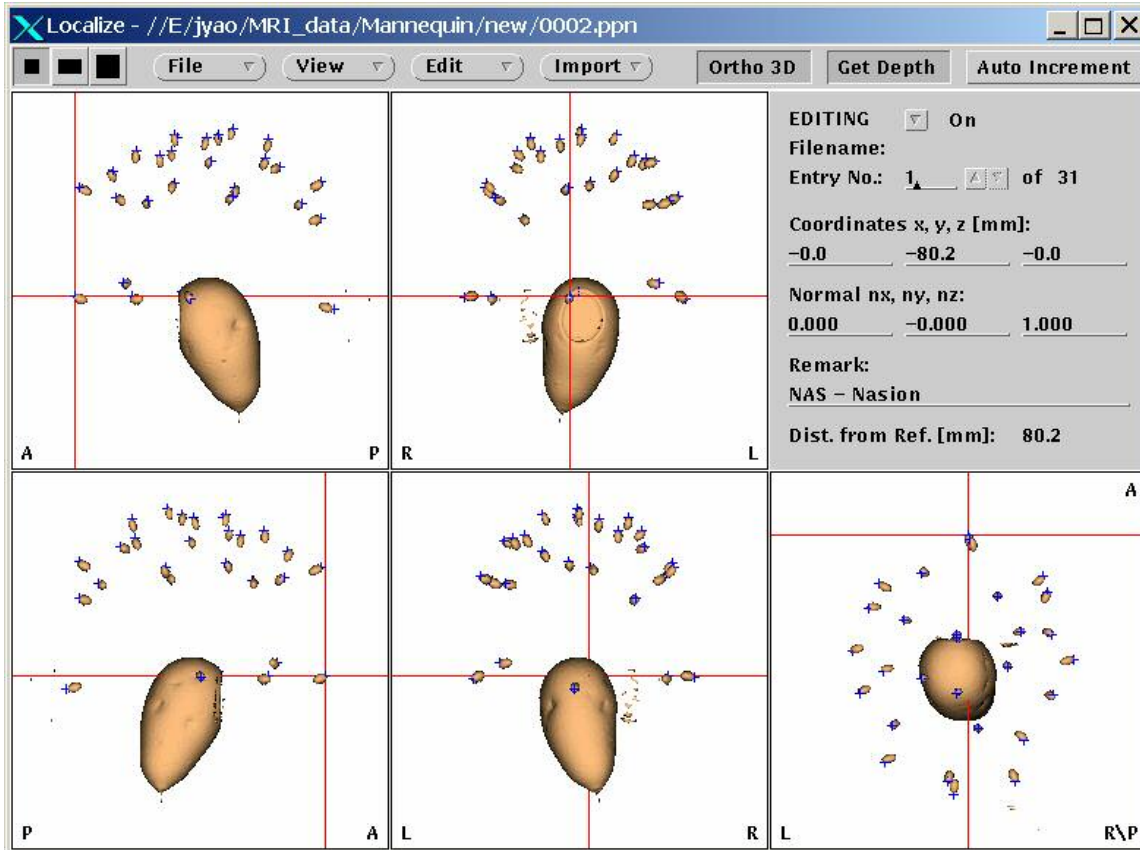


**Figure 10-19** Mannequin actual stimulation sites. Sites in blue and vitamin E capsules in tan. The water balloon is the big tan region.

#### A.2.4 TMS\_dialog Output Files

- .tms
- .tms.stm

#### A.2.5 Project Points onto Cortex

Using Curry, a points file can be projected onto the cortex (see figure A.x).



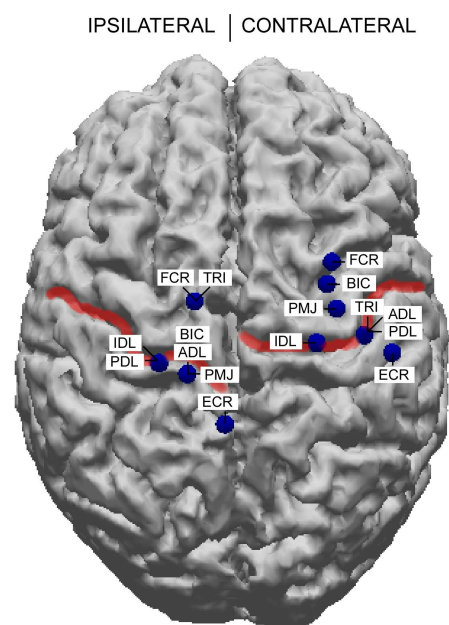


**Figure 10-20** Hotspots found at the scalp surface projected onto the cortical surface.